U.S. ARMY RDECOM

TECHNICAL REPORT RDMR-WS-12-03

DROP TOWER CHARACTERIZATION OF ARMY RESEARCH LAB (ARL)-FABRICATED THIN-FILM LEAD ZIRCONATE TITANATE (PZT) TRANSDUCERS

Tracy D. Hudson and Stephen Glenn Cruit
Weapons Sciences Directorate
Aviation and Missile Research, Development, and Engineering Center

And

Michael Allen
Miltec Corporation
678 Discovery Drive NW
Huntsville, AL 35806-2802

April 2012

AMRDEC

DESTRUCTION NOTICE

FOR CLASSIFIED DOCUMENTS, FOLLOW THE PROCEDURES IN DoD 5200.22-M, INDUSTRIAL SECURITY MANUAL, SECTION II-19 OR DoD 5200.1-R, INFORMATION SECURITY PROGRAM REGULATION, CHAPTER IX. FOR UNCLASSIFIED, LIMITED DOCUMENTS, DESTROY BY ANY METHOD THAT WILL PREVENT DISCLOSURE OF CONTENTS OR RECONSTRUCTION OF THE DOCUMENT.

DISCLAIMER

THE FINDINGS IN THIS REPORT ARE NOT TO BE CONSTRUED AS AN OFFICIAL DEPARTMENT OF THE ARMY POSITION UNLESS SO DESIGNATED BY OTHER AUTHORIZED DOCUMENTS. THE VIEWS EXPRESSED HEREIN ARE THOSE OF THE AUTHOR AND DO NOT REFLECT THE OFFICIAL POLICY OR POSITION OF THE DEPARTMENT OF THE ARMY, DEPARTMENT OF DEFENSE OR THE U.S. GOVERNMENT. REFERENCE HEREIN TO ANY SPECIFIC COMMERCIAL, PRIVATE, OR PUBLIC PRODUCTS, PROCESS, OR SERVICE BY TRADE NAME, TRADEMARK, MANUFACTURER, OR OTHERWISE, DOES NOT CONSTITUTE OR IMPLY ITS ENDORSEMENT, RECOMMENDATION, OR FAVORING BY THE U.S. GOVERNMENT.

TRADE NAMES

USE OF TRADE NAMES OR MANUFACTURERS IN THIS REPORT DOES NOT CONSTITUTE AN OFFICIAL ENDORSEMENT OR APPROVAL OF THE USE OF SUCH COMMERCIAL HARDWARE OR SOFTWARE.

REPORT DOCUMENTATION PAGE

Form Approved
OMB No. 074-0188

1. AGENCY USE ONLY	2. REPORT DATE	3. REPORT TYPE AND DATES COVERED
	April 2012	Final

4. TITLE AND SUBTITLE
Drop Tower Characterization of Army Research Lab (ARL)-Fabricated Thin-Film Lead Zirconate Titanate (PZT) Transducers

5. FUNDING NUMBERS

6. **AUTHOR**(S)

Tracy D. Hudson, Stephen Glenn Cruit, and Michael Allen

7. PERFORMING ORGANIZATION NAME(S) AND ADDRESS(ES)
Commander, U.S. Army Research, Development, and Engineering Command
ATTN: RDMR-WSI
Redstone Arsenal, AL 35898-5000

8. PERFORMING ORGANIZATION REPORT NUMBER
TR-RDMR-WS-12-03

9. SPONSORING / MONITORING AGENCY NAME(S) AND ADDRESS(ES)

10. SPONSORING / MONITORING AGENCY REPORT NUMBER

11. SUPPLEMENTARY NOTES

12a. DISTRIBUTION / AVAILABILITY STATEMENT
Approved for public release; distribution is unlimited.

12b. DISTRIBUTION CODE
A

13. ABSTRACT ***(Maximum 200 Words)***

The report documents the characterization of the impulse response of piezoelectric thin-film transducers to low-impacts provided by a "ball-drop" apparatus and the effects of device size and annealing process on the impulse response. The specific piezoelectric thin-film transducers are 1-micron thick Lead Zirconate Titanate (PZT) films, as deposited by Army Research Laboratory's (ARL's) Sensors and Electronics Devices Directorate in support of Army Technology Objective Sensor, Warhead, and Fuzing Technology Integrated for Combined Effects (SWFTICE) during Fiscal Year (FY) 2011. Summary results are of low-yield for these specific lot fabrications, but iterative designs/fabrications are forthcoming from laboratory fabrication for further testing.

14. SUBJECT TERMS
Lead Zirconate Titanate (PZT), transducers, impact sensors, ferroelectrics

15. NUMBER OF PAGES
96

16. PRICE CODE

17. SECURITY CLASSIFICATION OF REPORT	18. SECURITY CLASSIFICATION OF THIS PAGE	19. SECURITY CLASSIFICATION OF ABSTRACT	20. LIMITATION OF ABSTRACT
UNCLASSIFIED	UNCLASSIFIED	UNCLASSIFIED	SAR

NSN 7540-**01**-280-5500

Standard Form 298 (Rev. 2-89)
Prescribed by ANSI Std. Z39-18
298-102

TABLE OF CONTENTS

LIST OF ILLUSTRATIONS

LIST OF TABLES

I. INTRODUCTION

This report discusses the characterization of thin-film transducers made from Lead Zirconate Titanate (PZT) piezoelectric films for use in the Sensor, Warhead, and Fuse Technology Integrated for Combined Effects (SWFTICE) program. The devices received from Army Research Laboratory (ARL), in June 2011, were attempts at changing the annealing process for thin-film, post-deposition processing used on the transducers and at using a smaller area of PZT film than used in past devices. The shipment received from ARL was comprised of devices of seven different sized areas of PZT film and made by using three different annealing processes. Characterization was completed by means of a vertical drop tower apparatus (shown in Section IX.) which allowed a weight to be dropped from a set height onto the chosen transducer. The transducer was electrically connected to an oscilloscope through a buffer-amplifier circuit to allow the amplitude of the change in voltage to be measured upon impact. Prior to characterization using the drop tower, each device had its capacitance measured using a Fluke 289 Multimeter and was examined optically. Other testing (as documented in Sections VII. and VIII.) was performed on select devices prior to characterization by means of a drop tower. These tests included hysteresis (Polarization Versus Voltage (P-V)) testing (as explained in Section VII.), capacitance testing post-noodle wire attachment, and post-noodle wire hysteresis testing.

II. NAMING OF ARL DEVICES

The devices were shipped from ARL in seven Gel-Paks [1]. The first four cases contained devices produced using the standard annealing process, the fifth case contained devices produced using an experimental rapid-ramp annealing process, and the last two cases contained devices produced using a second experimental annealing process, double ramp. Devices were named as depicted in Figure 1.

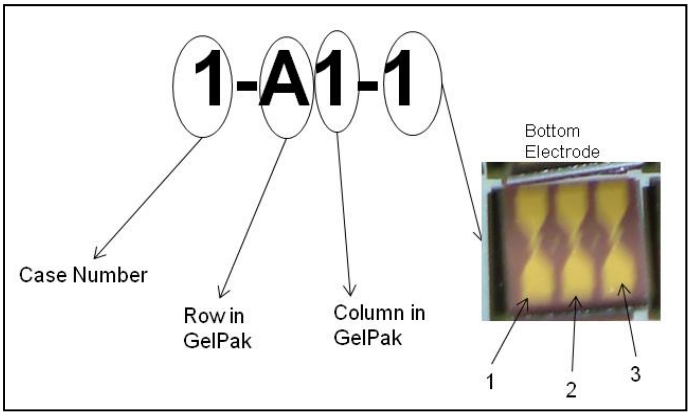

Figure 1. Naming Nomenclature for PZT Transducers

III. DESCRIPTION OF ANNEALING PROCESSES

ARL's standard annealing process, used on Cases 1 through 4 (Wafer 5721) and shown in Figure 2, called for the initial thin-film PZT wafer to be heated at a rate of 4 °C per second until a temperature of 700 °C was reached. This temperature was held for 60 seconds, and then the wafer was cooled to 300 °C at a rate of 4 °C per second. Based on the preliminary testing

performed at the Aviation and Missile Research, Development, and Engineering Center (AMRDEC), this process appears to produce the largest percentage of functional devices.

Figure 2. Standard Annealing Process Devices

ARL's rapid-ramp annealing process, used on Case 5 (Wafer 5713) and shown in Figure 3, called for the wafer to be heated at a rapid rate of 199 °C per second until a temperature of 700 °C was reached. This temperature was held for 60 seconds, and then the wafer was cooled to 300 °C at a rate of 199 °C per second. Based on the preliminary testing preformed by AMRDEC, this process appears to produce the smallest percentage of functional devices. A plausible explanation for this low-yield involves movement within shipping package that damaged the devices in Case 5.

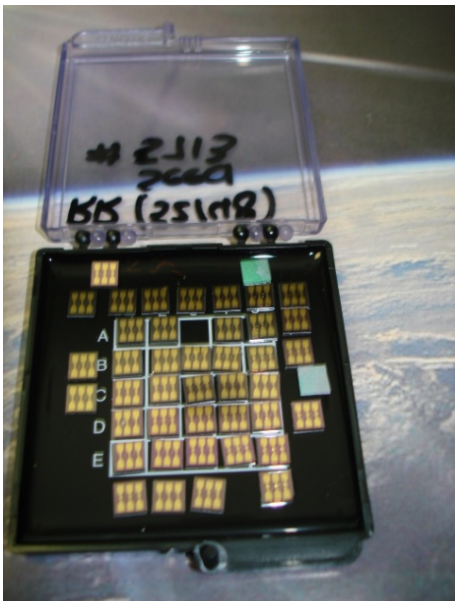

Figure 3. Rapid-Ramp Annealing Process Devices

ARL's double-ramp annealing process, used on Cases 6 and 7 (Wafer 5711) and shown in Figure 4, called for the wafer to be heated at a rate of 199 °C per second until a temperature of 120 °C was reached. This temperature was held for 120 seconds, and then the wafer was heated again at the same rate until a temperature of 700 °C was reached. The wafer was held at this final temperature for 30 seconds prior to being cooled to 300 °C at a rate of 199°C per second.

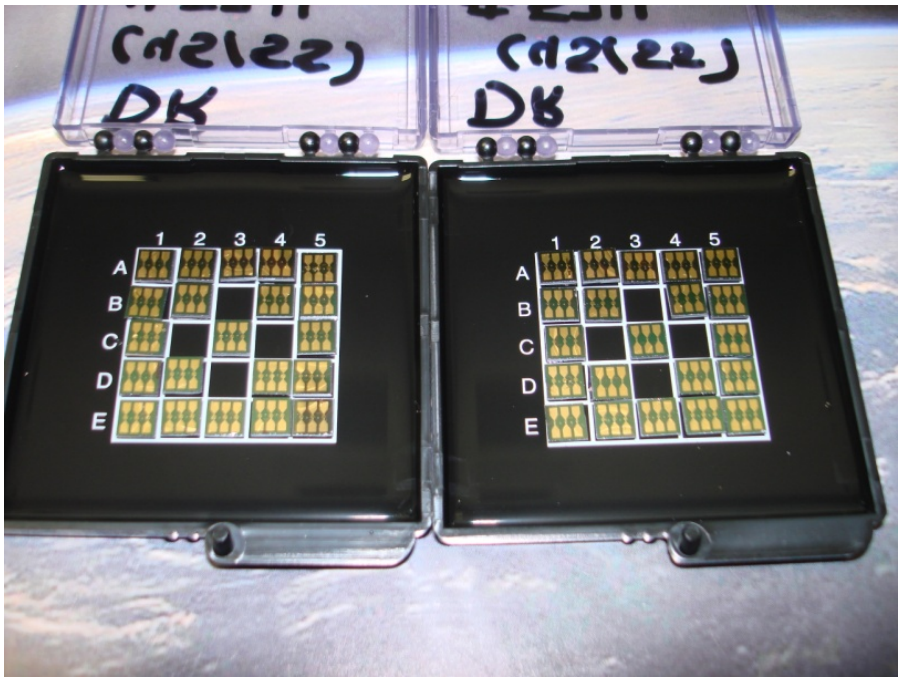

Figure 4. Double-Ramp Annealing Process Devices

IV. CAPACITANCE MEASURMENTS OF STANDARD ANNEALING PROCESS DEVICES

Before being shipped by ARL, a spot check was done on an unspecified number of devices from each of the seven sizes contained in the shipment using their standard 10-kilohertz, 10-millivolt amplitude sinusoidal waveform. Once at AMRDEC, the average capacitance values were measured using the setup shown in Figure 5 and tabulated in Table 1. Prior analysis of the Fluke multimeter using Agilent MS0654A determined that the Fluke 289 multimeter measured the capacitance value of the die-level devices using a nominal 6-hertz, 862.5-millivolt peak amplitude waveform [2]. As capacitance is a frequency-dependent value, this difference in waveforms explains the difference in capacitance as measured by ARL and the capacitance as measure by AMRDEC. The capacitance values measured by AMRDEC are detailed in Appendix A. Based on these capacitance measurements, the number of functioning die from this group can be determined. The data shown in Table 2 is based on the diameter of the PZT transducer devices.

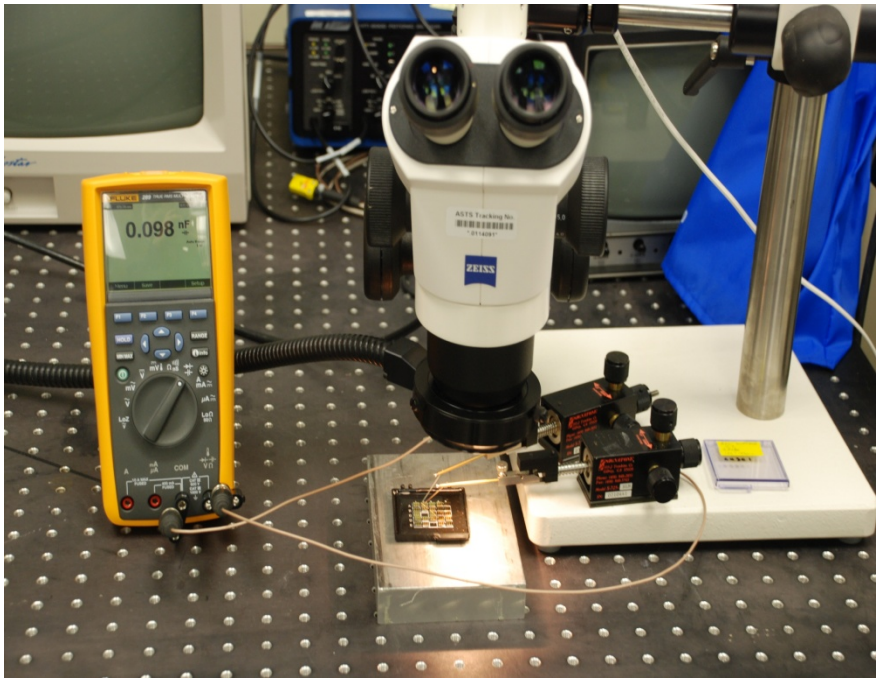

Figure 5. AMRDEC Experimental Setup for Capacitance Measurement

Table 1. Average Capacitance Measurements of Standard Annealing Process Devices

Device Diameter	Average Capacitance (ARL)	Average Capacitance (AMRDEC)	Standard Deviation (AMRDEC)
120µm	528pF	792 pF	33.87
150µm	800pF	1.2 nF	0.43
180µm	1.09nF	1.51 nF	0.05
210µm	1.48nF	1.98 nF	0.09
240µm	1.86nF	2.44nF	0.30
270µm	2.35nF	3.13 nF	0.15
300µm	2.88nF	3.63 nF	0.44

Table 2. Summary Yield of Standard Annealing Process Devices Based on Capacitance Measurements

Diameter	Number Good	Number Shorted	Percent Good
120µm	33	0	100
150µm	37	2	94.9
180µm	30	1	96.8
210µm	27	3	90.0
240µm	31	2	93.9
270µm	25	5	83.3
300µm	28	2	93.3
Total:	208	17	92.4

V. CAPACITANCE MEASURMENT OF RAPID-RAMP ANNEALING PROCESS DEVICES

Devices from the annealing process did not have their capacitance checked by ARL prior to being shipping to AMRDEC; however, these devices were tested by AMRDEC in the same manner as the standard annealing process devices. The average capacitance values of these devices are shown in Table 3. The group of devices yielded a much lower percentage of functioning devices than either the standard or double-ramp annealing processes. The initial indication of this came during capacitance measurement. Nearly all of the devices were found to have a capacitance value much higher than the average established by the other two lots. Over 40 percent of these devices were found to be electrically shorted and therefore unusable. Furthermore, the abnormal capacitance values caused concern regarding the level of functionality of these devices. Table 4 shows the number of devices known to be bad at this point in testing and assumes those devices, which give an abnormally high capacitance reading, are functioning. The actual number of functioning devices, determined through hysteresis loop checks, is much lower than indicated by capacitance values. The detailed capacitance values measured by AMRDEC for these rapid ramp annealed PZT devices are shown in Appendix B.

Table 3. Average Capacitance Measurements of Rapid-Ramp Annealing Process Devices

Device Diameter	Average Capacitance (AMRDEC)	Standard Deviation (AMRDEC)
120μm	1.28nF	0.28
150μm	2.05 nF	0.31
180μm	2.84 nF	0.04
210μm	3.70 nF	0.31
240μm	4.72nF	0.50
270μm	6.13 nF	0.68
300μm	6.98 nF	1.60

Table 4. Summary Yield of Rapid-Ramp Annealing Process Devices Based on Capacitance Measurements

Diameter	Number Good	Number Shorted	Percent Good
120μm	11	4	73.3
150μm	18	6	75.0
180μm	3	21	14.3
210μm	9	0	100
240μm	12	9	57.1
270μm	8	7	53.3
300μm	14	7	66.7
Total:	75	54	58.1

VI. CAPACITANCE MEASUREMENT OF DOUBLE-RAMP ANNEALING PROCESS DEVICES

Devices from the annealing process did not have their capacitance checked by ARL prior to being shipped to AMRDEC; however, these devices were tested by AMRDEC in the same manner as the standard and rapid-ramp annealing process devices. The capacitance values of these devices much more closely resembled the standard anneal process than the rapid ramp process, as reflected by the average values shown in Table 5. The testing revealed that, while not as destructive to devices as the rapid ramp process, this method of annealing did not produce as large a percentage of functional devices as the standard anneal process. Table 6 shows the number of functioning devices, as determined by capacitance values alone. The detailed capacitance values measured by AMRDEC are shown in Appendix C.

Table 5. Average Capacitance Measurements of Double-Ramp Annealing Process Devices

Device Diameter	Average Capacitance (AMRDEC)	Standard Deviation (AMRDEC)
120µm	0.76nF	0.15
150µm	1.15 nF	0.13
180µm	1.53 nF	0.13
210µm	1.80 nF	0.43
240µm	2.50nF	0.14
270µm	3.14 nF	0.28
300µm	3.42 nF	0.73

Table 6. Summary Yield of Double-Ramp Annealing Process Devices Based on Capacitance Measurements

Diameter	Number Good	Number Shorted	Percent Good
120µm	16	5	76.2
150µm	12	6	66.7
180µm	11	7	61.1
210µm	16	5	76.2
240µm	12	6	66.7
270µm	11	10	52.4
300µm	6	3	66.7
Total:	84	42	66.7

VII. HYSTERESIS MEASUREMENT ON ALL ARL DEVICES

A small number of devices (exact figures are documented in Section VIII.) was set aside from the standard annealing process lot for ball-drop testing without a hysteresis test being performed on them. Three devices of each diameter from the double-ramp annealing process lot were sent to Radiant Technologies, Inc. [3] to confirm the accuracy of AMRDEC's hysteresis testing setup and process. This testing produced hysteresis plots nearly identical to those collected by AMRDEC on comparable devices. A hysteresis plot was collected from the remaining devices using the setup described in Figures 6 through 8. Appendix D contains the report summary of Radiant Technologies, Inc. measurements.

Figure 6. Radiant Technologies, Inc. Precision Premier II Ferroelectrics Tester

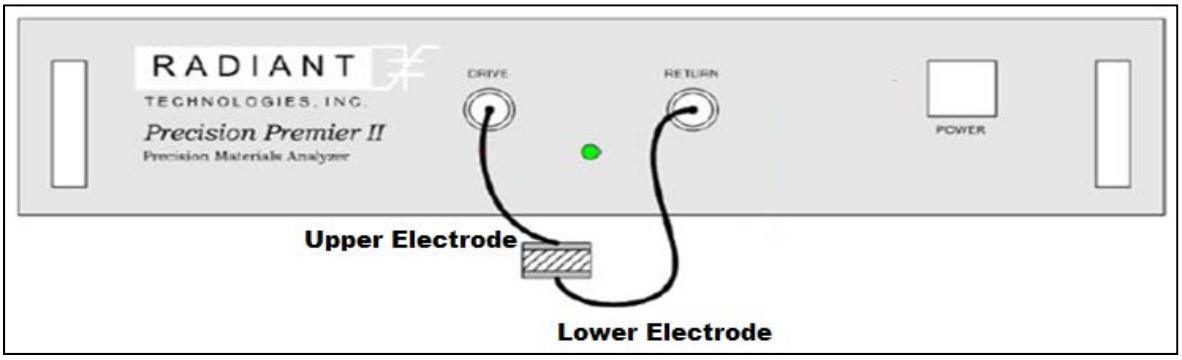

Figure 7. Hysteresis Testing Setup Diagram for PZT Transducers

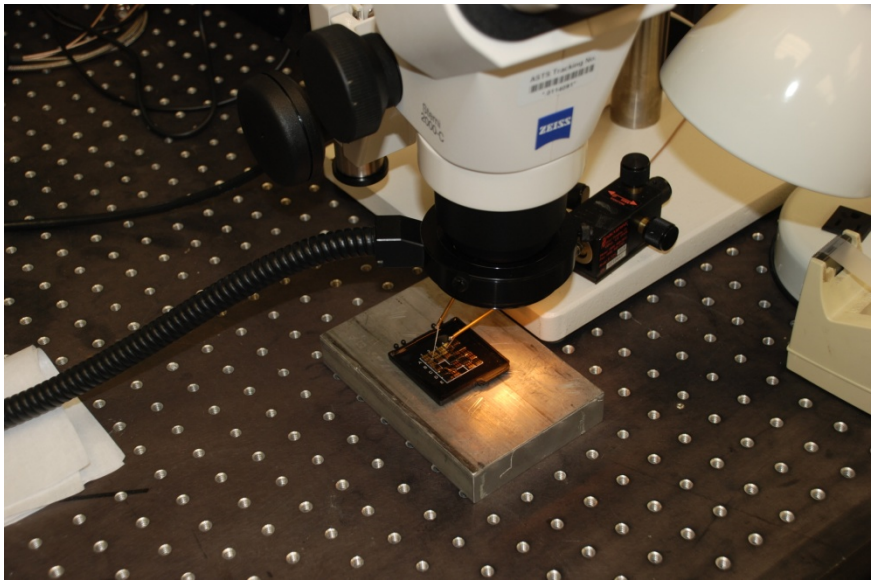

Figure 8. Photograph of Hysteresis Testbed

Devices remained in their original Gel-Paks during hysteresis testing. The Gel-Paks were placed under a microscope to allow for easier positioning of probes on the devices. Each device was connected to AMRDEC's Radiant Precision Premier II ferroelectric tester by means of two probes connected to the gold contacts on each device. The probe connected to the drive terminal of the Radiant Technologies, Inc. tester (shown in Figure 6) was placed on the upper electrode of each device. The probe connected to the return terminal on the Radiant Technologies, Inc. tester was placed on the lower electrode of each device. This setup is shown in Figures 7 and 8.

Devices were tested using the following parameters—maximum voltage (15 volts), period (50 milliseconds), delay (500 milliseconds), thickness (1 micrometer), and area (based on device diameter). The area of each size device, as well as the area of devices from AMRDEC's Lester 1 wafer (1-micron Niobium-doped Lead Zirconate Titanate (PNZT)), is shown in Table 7. Typical good, bad, and electrically shorted device plots are shown in Figures 9 through 11, respectively. Many devices which produced abnormal hysteresis plots (bad devices) would produce normal plots if reconditioned (a typical step for AMRDEC's devices); however, reconditioning was not completed due to time constraints.

Table 7. Calculated Device Areas Based on PZT Transducer Diameters

Device Type	Area (cm^2)
ARL 120	0.000113097
ARL 150	0.000176715
ARL 180	0.000254469
ARL 210	0.000346361
ARL 240	0.000452389
ARL 270	0.000572555
ARL 300	0.000706858
Lester 1	0.0201

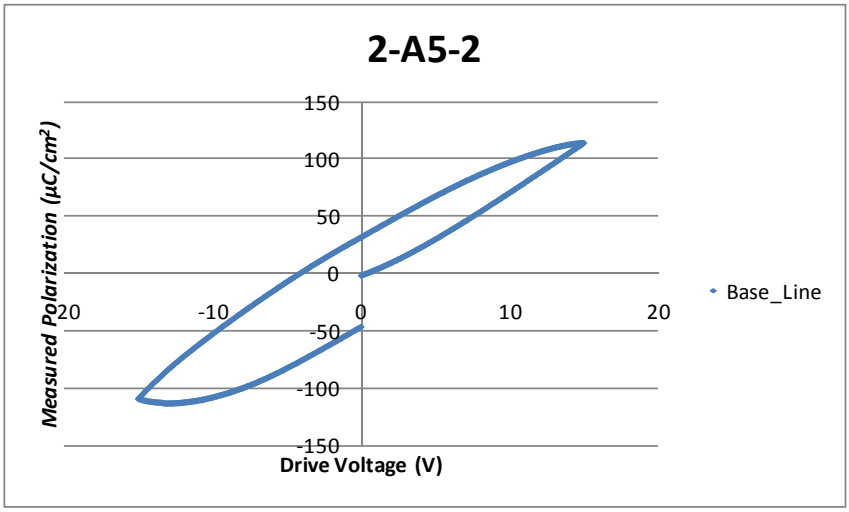

Figure 9. Good Device Example of Hysteresis Measurement

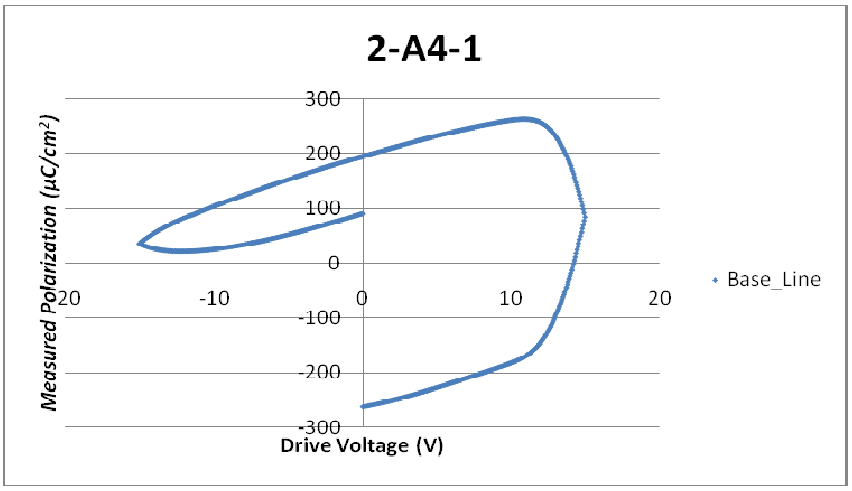

Figure 10. Bad Device Example of Hysteresis Measurement

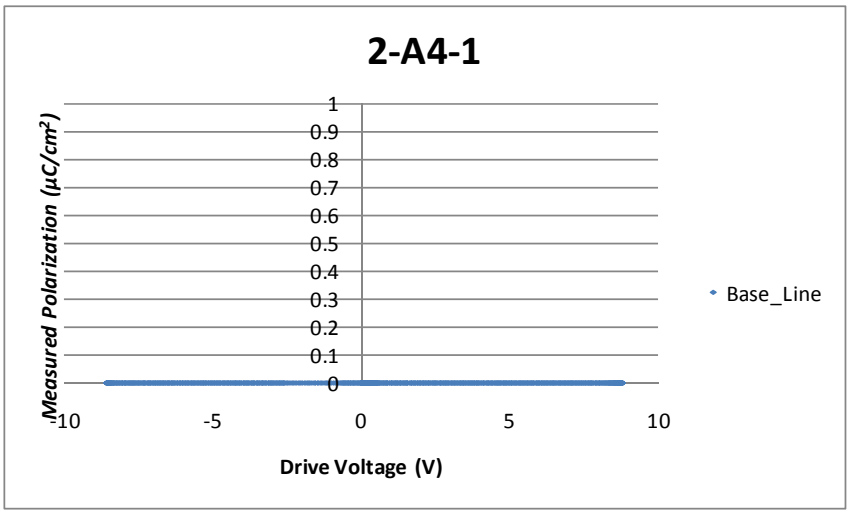

Figure 11. Electrically Shorted Device Example of Hysteresis Measurement

Reconditioning is a process by which the device is electrically reset to its original state. This is done using a 1-hertz square wave at the maximum voltage the device can withstand for a 100-second duration. Reconditioning and another set of hysteresis tests should be completed at a later date. Hysteresis plots were obtained from several devices after noodle wire attachment; these plots closely resembled the initial hysteresis test plots from the same devices.

Additional follow-up conversations with ARL suggest that the low-yield and irregular hysteresis plots are the result of excessive hydrogen damage during fabrication. Unfortunately, the metallization Titanium/Gold (Ti/Au) and passivation layer for the air bridge (photoresist) does not enable the ability of a high temperature anneal for recovery.

VIII. DEVICE ASSEMBLY

To facilitate ball drops, 6-inch long noodle wire leads (Number 32 American Wire Gauge (AWG)) were bonded to the electrodes of each device to be tested. In the past, on larger devices, noodle wires were soldered to the electrodes using lead-based solder; however, due to the delicate nature and small size of these devices, all devices on which soldering was attempted were destroyed. This meant noodle wires had to be bonded to devices using CW2400 silver-based, two-part conductive epoxy from CircuitWorks [4].

To facilitate the attachment of noodle wires, die were placed on individual Gel-Paks, and leads were taped in place (Figure 12). When epoxy was cured (24 to 72 hours), the adhesive on the tape was chemically degraded using isopropanol. The Gel-Pak was then placed on a vacuum release station where the tape and die were removed. The structural properties of this epoxy led to leads being pulled off of the devices during handling and testing. Several devices were shorted as a result of epoxy flowing over the ferroelectric material. Because of this issue, a capacitance reading was collected from several devices post-wire attachment. These measurements can be found in Table 8. A waveshaper (Figure 13) was then bonded to the back of each die to be tested using a cyanoacrylate-based adhesive. Final assemblies are shown in Figure 14 for center-mounted and edge-mounted sensor assemblies.

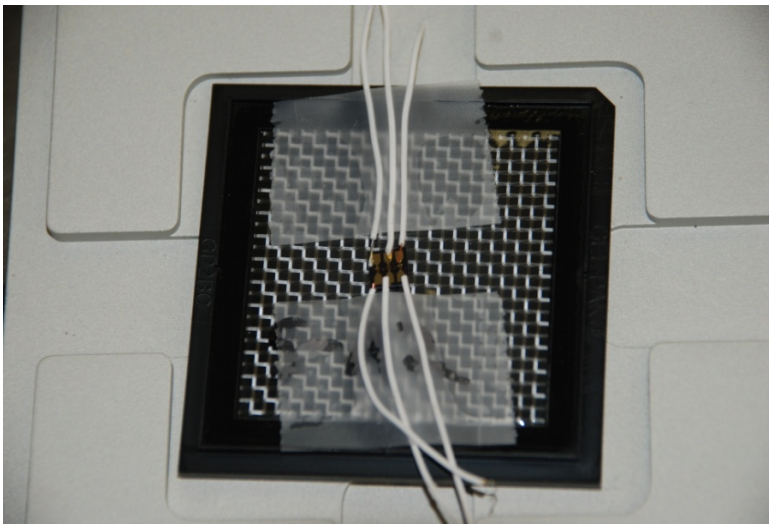

Figure 12. Device Mounted on Gel-Pak Ready for Noodle Wire Attachment

Table 8. Capacitance Measurements Before and After Noodle Wire Attachment

Device	Pre-Noodle Wire (nF)	Post-Noodle Wire (nF)
2-B5-1	1.55	1.77
2-B5-2	1.56	0.425
2-B5-3	1.55	0.397
2-E1-1	1.92	1.93
2-E1-2	1.93	Short
2-E1-3	2.03	0.115
3-A1-1	2.49	0.112
3-A1-2	2.61	0.112

Table 8. Capacitance Measurements Before and After Noodle Wire Attachment (Concluded)

Device	Pre-Noodle Wire (nF)	Post-Noodle Wire (nF)
3-A1-3	2.67	0.115
3-E3-1	3.08	0.335
3-E3-2	3.33	Short
3-E3-3	3.09	0.341
4-A2-1	3.56	3.68
4-A2-2	3.91	3.97
4-A2-3	4.05	0.120
2-A2-1	1.48	1.47
2-A2-2	1.49	2.05
2-A2-3	1.49	1.55
2-D1-1	1.92	0.122
2-D1-3	2.08	2.02
3-C1-1	2.51	0.122
3-C1-2	2.53	0.118
3-C1-3	2.87	0.123
3-E1-1	3.08	3.17
3-E1-2	3.04	Short
3-E1-3	3.03	3.02
4-A5-1	3.78	3.78
4-A5-2	3.81	3.77
4-A5-3	3.94	0.120

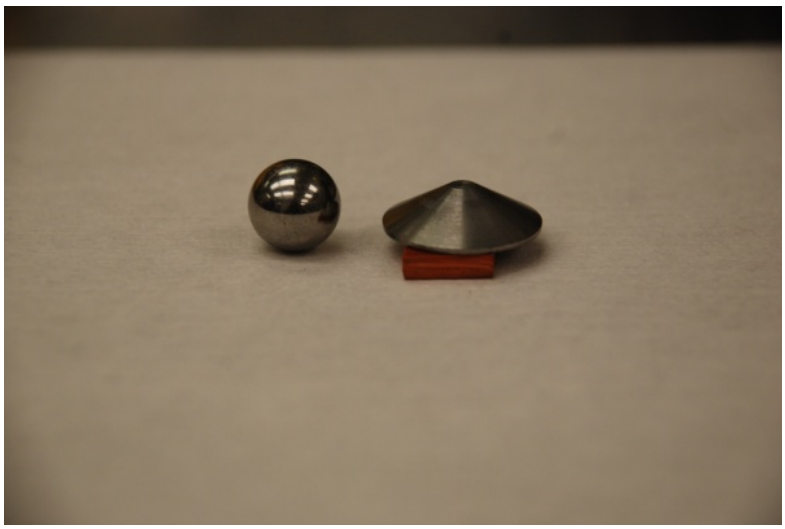

Figure 13. Waveshaper (on Right) Beside a 0.5-Inch Steel Ball

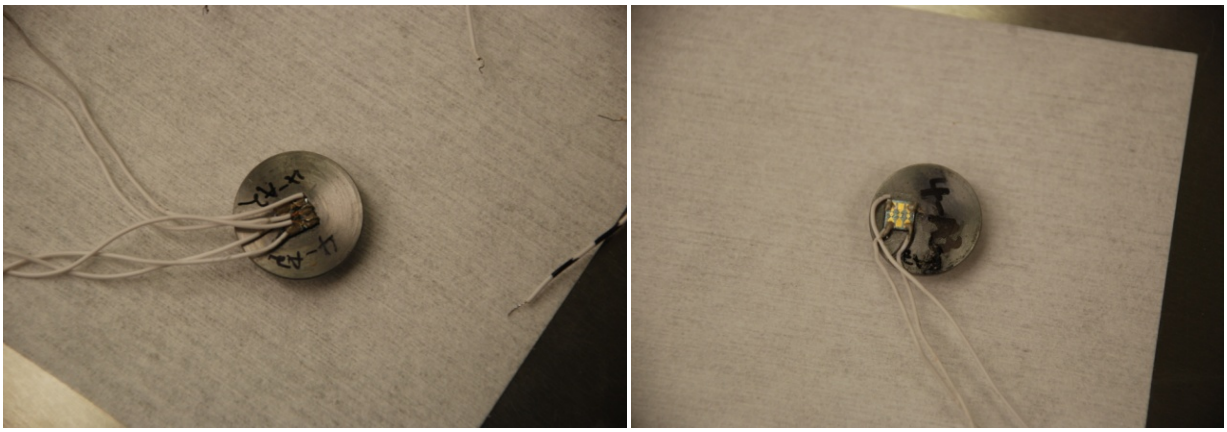

(a) Center Mounted *(b) Edge Mounted*

Figure 14. Sensor Assemblies

A total of 16 standard process die (shown in Figure 15) were bonded to waveshapers—13 die were bonded to the center of the waveshaper (as is customary), and 3 die were offset from the center. The offset attachment was done due to the result of an abnormal ball-drop test (described in detail in Section IX.) in which the weight impacted the waveshaper on its edge. This positioning of the die yielded no usable drop test results.

Figure 15. Final Device Assembly at AMRDEC Prior to Drop Tower Characterization

IX. DROP TOWER CHARACTERIZATION

A representation of the drop tower used by AMRDEC, located at the Charles M. Bowden Laboratory (building 7804), is shown in Figure 16, and a photograph of the same drop tower apparatus is shown in Figure 17. This tower uses an approximately 3-foot long tube to guide a weight to impact the backside (opposite the device) of a waveshaper. In previous testing [2], a 0.5-inch diameter steel ball was used as a weight, but due to a lack of device sensitivity, a larger 3-ounce steel cylinder was used as a drop weight. Upon impact, the devices produced an

electrical signal which was then measured on an oscilloscope by means of a buffer amplifier circuit. An example of this signal can be seen in Figure 18.

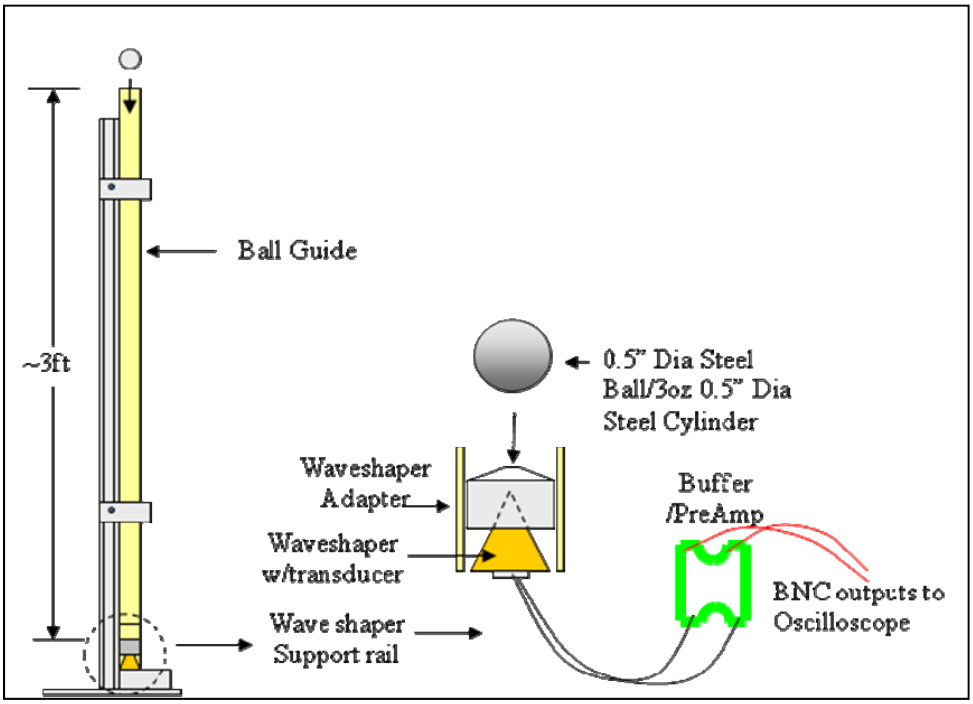

Figure 16. Diagram of Drop Tower Setup

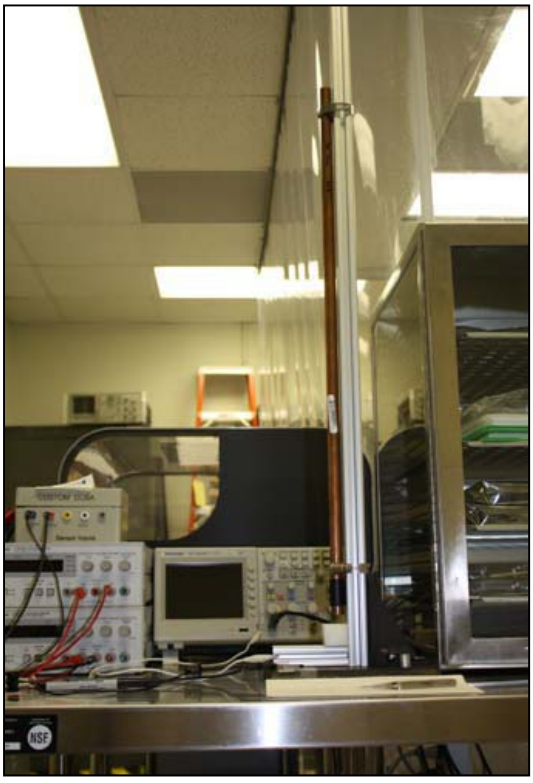

Figure 17. Photograph of Drop Tower Experiment

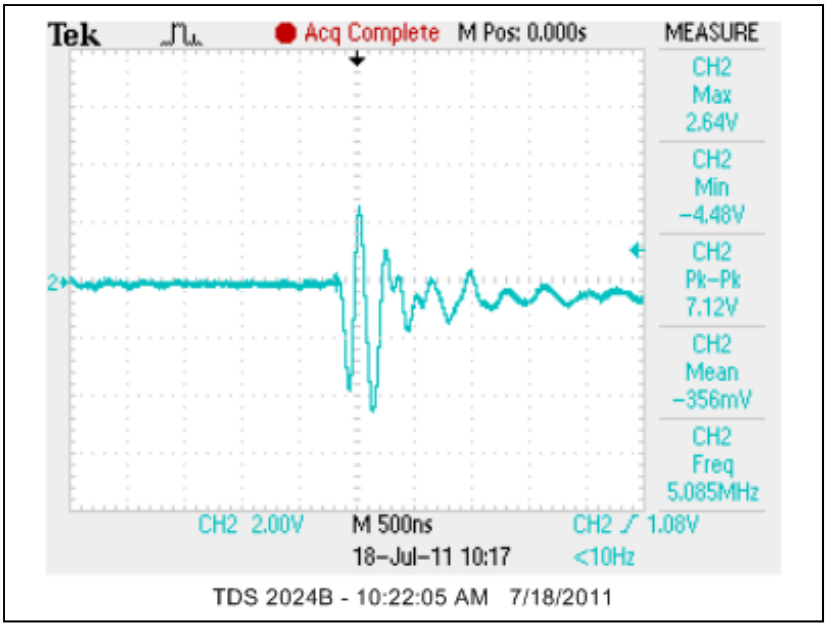

Figure 18. Oscilloscope Trace of Normal Ball-Drop Signal

During drop tower testing of these devices, interference caused by Radio Frequency (RF) signals became a major setback. The RF signals shown in Figure 19 masked the signals given by the devices upon impact. Unsuccessful efforts were made to shield the tower from this interference. Instead, the signal from the device was enlarged by removing the steel ball and replacing it with a 3-ounce steel cylinder.

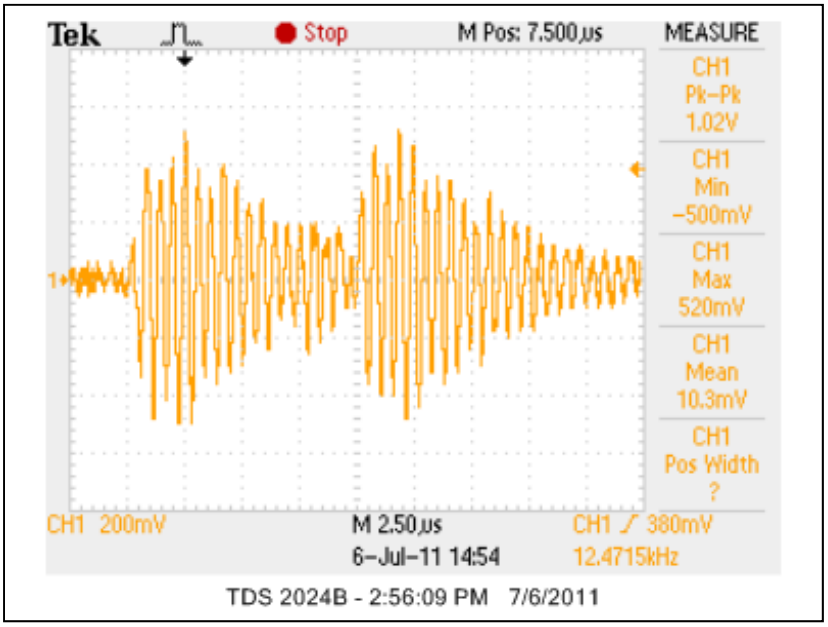

Figure 19. Example of Laboratory RF Interference Waveform

A happenstance occurrence during testing caused the weight to be dropped near the edge of the waveshaper. This drop produced a remarkable signal nearly 10 times in amplitude over that of a normally centered drop. Later testing showed that while this type of signal was possible, the devices did not function reliably when impacted off-center, and some devices produced inconsistent signals, while others did not produce a signal at all. To investigate this effect further, three die were mounted off-center on the waveshaper. No signals were observed from these device impacts.

Detailed drop tower tests for centered and off-centered devices are detailed in Appendixes E and F, respectively.

X. CONCLUSION

It appeared that the smaller device size produced a signal with a much lower pulsewidth than that of larger devices; however, the voltage produced was comparable to that of some types of larger devices. The standard annealing process appeared to be less destructive to the devices, but an argument can be made that devices from the rapid ramp process were damaged during shipping, as evident from several devices being flipped and observing scratches on several devices under a microscope. Drop tower testing has not been performed on these devices due to time constraints which caused a lack of data to determine the effectiveness of each annealing process. Subsequent testing should include ball drops of these devices, as well as reconditioning of all devices.

REFERENCES

1. "Gel-Pak: Home Page," GelPak, 22 July 2011, <http://gelpak.com/>

2. Hudson, Tracy D.; Kranz, Michael; Allen, Michael S.; and Sanchez, Sharon, "Drop Tower Characterization Op Custom Thin-Film Lead Zirconate Titanate (PZT) Transducers Fabricated by Army Research Laboratory," TR-RDMR-WS-11-04, Aviation and Missile Research, Development, and Engineering Center (AMRDEC), Redstone Arsenal, AL, 2011.

3. "Ferroelectric Materials Testing & Integrated Ferroelectric Devices," Radiant Technologies, Inc., 22 July 2011, <http://www.ferrodevices.com/1/297/index.asp>

4. "ITW Chemtronics," CircuitWorks Conductive Epoxy CW2400, Kennesaw, GA, July 2011, <http://www.chemtronics.com>

LIST OF ACRONYMS AND ABBREVIATIONS

AMRDEC	Aviation and Missile Research, Development, and Engineering Center
ARL	Army Research Laboratory
AWG	American Wire Gauge
FY	Fiscal Year
P-V	Polarization Versus Voltage
PNZT	Niobium-doped Lead Zirconate Titanate
PZT	Lead Zirconate Titanate
RF	Radio Frequency
SWFTICE	Sensor, Warhead, and Fuse Technology Integrated for Combined Effects
Ti/Au	Titanium/Gold

APPENDIX A
CAPACITANCE MEASUREMENTS OF STANDARD ANNEALING PROCESS DEVICES

Capacitance Measurements of Standard Annealing Process Devices

Device	Capacitance	Diameter
1-A1-1	766pF	120 μm
1-A1-2	748pF	120 μm
1-A1-3	746pF	120 μm
1-A2-1	776pF	120 μm
1-A2-2	790pF	120 μm
1-A2-3	879pF	120 μm
1-A3-1	772pF	120 μm
1-A3-2	836pF	120 μm
1-A3-3	772pF	120 μm
1-A4-1	836pF	120 μm
1-A4-2	777pF	120 μm
1-A4-3	757pF	120 μm
1-A5-1	778pF	120 μm
1-A5-2	773pF	120 μm
1-A5-3	774pF	120 μm
1-B1-1	792pF	120 μm
1-B1-2	812pF	120 μm
1-B1-3	811pF	120 μm
1-B2-1	805pF	120 μm
1-B2-2	832pF	120 μm
1-B2-3	812pF	120 μm
1-B3-1	808pF	120 μm
1-B3-2	819pF	120 μm
1-B3-3	888pF	120 μm
1-B4-1	757pF	120 μm
1-B4-2	762pF	120 μm
1-B4-3	755pF	120 μm
1-B5-1	780pF	120 μm
1-B5-2	790pF	120 μm
1-B5-3	783pF	120 μm
1-C1-1	776pF	120 μm
1-C1-2	787pF	120 μm
1-C1-3	788pF	120 μm
1-C3-1	1.15nF	150 μm
1-C3-2	1.14nF	150 μm
1-C3-3	1.25nF	150 μm
1-C4-1	1.14nF	150 μm
1-C4-2	1.14nF	150 μm
1-C4-3	41.4nF	150 μm
1-C5-1	1.16nF	150 μm

Device	Capacitance	Diameter
1-C5-2	1.15nF	150 μm
1-C5-3	1.13nF	150 μm
1-D1-1	1.14nF	150 μm
1-D1-2	1.14nF	150 μm
1-D1-3	1.15nF	150 μm
1-D2-1	1.08nF	150 μm
1-D2-2	1.07nF	150 μm
1-D2-3	1.08nF	150 μm
1-D3-1	1.09nF	150 μm
1-D3-2	1.09nF	150 μm
1-D3-3	1.09nF	150 μm
1-D4-1	1.11nF	150 μm
1-D4-2	1.12nF	150 μm
1-D4-3	1.12nF	150 μm
1-D5-1	1.14nF	150 μm
1-D5-2	1.12nF	150 μm
1-D5-3	1.12nF	150 μm
1-E1-1	1.13nF	150 μm
1-E1-2	3.71nF	150 μm
1-E1-3	1.25nF	150 μm
1-E2-1	Short	150 μm
1-E2-2	1.14nF	150 μm
1-E2-3	1.10nF	150 μm
1-E3-1	1.13nF	150 μm
1-E3-2	1.12nF	150 μm
1-E3-3	1.12nF	150 μm
1-E4-1	1.16nF	150 μm
1-E4-2	1.15nF	150 μm
1-E4-3	1.15nF	150 μm
1-E5-1	1.09nF	150 μm
1-E5-2	Short	150 μm
1-E5-3	1.09nF	150 μm
2-A1-1	1.50nF	180 μm
2-A1-2	1.52nF	180 μm
2-A1-3	1.52nF	180 μm
2-A2-1	1.48nF	180 μm
2-A2-2	1.49nF	180 μm
2-A2-3	1.49nF	180 μm
2-A3-1	1.49nF	180 μm
2-A3-2	1.50nF	180 μm

Capacitance Measurements of Standard Annealing Process Devices (Continued)

Device	Capacitance	Diameter
2-A3-3	1.49nF	180 µm
2-A4-1	Short	180 µm
2-A4-2	1.51nF	180 µm
2-A4-3	1.51nF	180 µm
2-A5-1	1.49nF	180 µm
2-A5-2	1.48nF	180 µm
2-A5-3	1.48nF	180 µm
2-B1-1	1.47nF	180 µm
2-B1-2	1.46nF	180 µm
2-B1-3	1.38nF	180 µm
2-B2-1	1.54nF	180 µm
2-B2-2	1.53nF	180 µm
2-B2-3	1.51nF	180 µm
2-B3-1	1.52nF	180 µm
2-B3-2	1.72nF	180 µm
2-B3-3	1.51nF	180 µm
2-B4-1	1.55nF	180 µm
2-B4-2	1.50nF	180 µm
2-B4-3	1.56nF	180 µm
2-B5-1	1.55nF	180 µm
2-B5-2	1.56nF	180 µm
2-B5-3	1.55nF	180 µm
2-D1-1	1.92nF	210 µm
2-D1-2	1.94nF	210 µm
2-D1-3	2.08nF	210 µm
2-D2-1	1.89nF	210 µm
2-D2-2	1.96nF	210 µm
2-D2-3	2.00nF	210 µm
2-D3-1	1.93nF	210 µm
2-D3-2	1.92nF	210 µm
2-D3-3	1.80nF	210 µm
2-D4-1	1.98nF	210 µm
2-D4-2	877pF	210 µm
2-D4-3	1.90nF	210 µm
2-D5-1	Short	210 µm
2-D5-2	Short	210 µm
2-D5-3	2.07nF	210 µm
2-E1-1	1.92nF	210 µm
2-E1-2	1.93nF	210 µm
2-E1-3	2.03nF	210 µm

Device	Capacitance	Diameter
2-E2-1	2.08nF	210 µm
2-E2-2	1.84nF	210 µm
2-E2-3	2.06nF	210 µm
2-E3-1	1.95nF	210 µm
2-E3-2	1.97nF	210 µm
2-E3-3	1.99nF	210 µm
2-E4-1	2.01nF	210 µm
2-E4-2	2.04nF	210 µm
2-E4-3	2.03nF	210 µm
2-E5-1	1.99nF	210 µm
2-E5-2	Short	210 µm
2-E5-3	2.22nF	210 µm
3-A1-1	2.49nF	240 µm
3-A1-2	2.61nF	240 µm
3-A1-3	2.67nF	240 µm
3-A2-1	2.60nF	240 µm
3-A2-2	1.85nF	240 µm
3-A2-3	1.23nF	240 µm
3-A3-1	2.17nF	240 µm
3-A3-2	2.25nF	240 µm
3-A3-3	2.39nF	240 µm
3-A4-1	2.41nF	240 µm
3-A4-2	2.40nF	240 µm
3-A4-3	2.41nF	240 µm
3-A5-1	2.68nF	240 µm
3-A5-2	2.49nF	240 µm
3-A5-3	2.48nF	240 µm
3-B1-1	Short	240 µm
3-B1-2	2.33nF	240 µm
3-B1-3	2.34nF	240 µm
3-B2-1	2.49nF	240 µm
3-B2-2	Short	240 µm
3-B2-3	2.45nF	240 µm
3-B3-1	2.55nF	240 µm
3-B3-2	2.31nF	240 µm
3-B3-3	2.51nF	240 µm
3-B4-1	2.42nF	240 µm
3-B4-2	2.43nF	240 µm
3-B4-3	2.44nF	240 µm
3-B5-1	2.56nF	240 µm

Capacitance Measurements of Standard Annealing Process Devices (Concluded)

Device	Capacitance	Diameter
3-B5-2	2.88nF	240 μm
3-B5-3	2.76nF	240 μm
3-C1-1	2.51nF	240 μm
3-C1-2	2.53nF	240 μm
3-C1-3	2.87nF	240 μm
3-D1-1	3.05nF	270 μm
3-D1-2	2.94nF	270 μm
3-D1-3	3.09nF	270 μm
3-D2-1	3.06nF	270 μm
3-D2-2	3.02nF	270 μm
3-D2-3	3.08nF	270 μm
3-D3-1	261nF	270 μm
3-D3-2	3.12nF	270 μm
3-D3-3	3.08nF	270 μm
3-D4-1	Short	270 μm
3-D4-2	3.02nF	270 μm
3-D4-3	3.08nF	270 μm
3-D5-1	3.02nF	270 μm
3-D5-2	Short	270 μm
3-D5-3	Short	270 μm
3-E1-1	3.08nF	270 μm
3-E1-2	3.04nF	270 μm
3-E1-3	3.03nF	270 μm
3-E2-1	3.15nF	270 μm
3-E2-2	3.14nF	270 μm
3-E2-3	3.13nF	270 μm
3-E3-1	3.08nF	270 μm
3-E3-2	3.33nF	270 μm
3-E3-3	3.09nF	270 μm
3-E4-1	Short	270 μm
3-E4-2	3.57nF	270 μm
3-E4-3	3.55nF	270 μm
3-E5-1	3.16nF	270 μm
3-E5-2	3.23nF	270 μm
3-E5-3	3.22nF	270 μm
4-A1-1	3.65nF	300 μm
4-A1-2	3.67nF	300 μm
4-A1-3	3.71nF	300 μm
4-A2-1	3.56nF	300 μm
4-A2-2	3.91nF	300 μm
4-A2-3	4.05nF	300 μm
4-A3-1	3.72nF	300 μm
4-A3-2	3.70nF	300 μm
4-A3-3	3.70nF	300 μm
4-A4-1	3.68nF	300 μm
4-A4-2	3.44nF	300 μm
4-A4-3	3.71nF	300 μm
4-A5-1	3.78nF	300 μm
4-A5-2	3.81nF	300 μm
4-A5-3	3.94nF	300 μm
4-B1-1	3.71nF	300 μm
4-B1-2	3.60nF	300 μm
4-B1-3	3.58nF	300 μm
4-B2-1	3.70nF	300 μm
4-B2-2	1.60nF	300 μm
4-B2-3	3.58nF	300 μm
4-B3-1	Short	300 μm
4-B3-2	3.78nF	300 μm
4-B3-3	4.22nF	300 μm
4-B4-1	3.60nF	300 μm
4-B4-2	3.14nF	300 μm
4-B4-3	3.65nF	300 μm
4-B5-1	Short	300 μm
4-B5-2	3.67nF	300 μm
4-B5-3	3.69nF	300 μm

APPENDIX B
CAPACITANCE MEASUREMENTS OF RAPID-RAMP ANNEALING PROCESS DEVICES

Capacitance Measurements of Rapid-Ramp Annealing Process Devices

Device	Capacitance	Diameter
5-A1-1	*	180
5-A1-2	*	180
5-A1-3	*	180
5-A2-1	*	270
5-A2-2	*	270
5-A2-3	*	270
5-A3-1	*	120
5-A3-2	*	120
5-A3-3	*	120
5-A4-1	*	180
5-A4-2	*	180
5-A4-3	*	180
5-A5-1	2.33 nF	150
5-A5-2	2.00 nF	150
5-A5-3	2.30 nF	150
5-A6-1	0.65 nF	120
5-A6-2	0.89 nF	120
5-A6-3	*	120
5-A7-1	*	300
5-A7-2	8.10 nF	300
5-A7-3	8.45 nF	300
5-B1-1	1.30 nF	300
5-B1-2	1.66 nF	300
5-B1-3	2.45 nF	300
5-B2-1	3.63 nF	210
5-B2-2	4.43 nF	210
5-B2-3	3.83 nF	210
5-B3-1	1.37 nF	120
5-B3-2	1.37 nF	120
5-B3-3	1.35 nF	120
5-B5-1	4.64 nF	240
5-B5-2	4.47 nF	240
5-B5-3	5.01 nF	240
5-B6-1	1.76 nF	150
5-B6-2	1.80 nF	150
5-B6-3	1.70 nF	150
5-B7-1	0.34 nF	150
5-B7-2	0.34 nF	150
5-B7-3	0.35 nF	150
5-C1-1	*	180

Device	Capacitance	Diameter
5-C1-2	**	180
5-C1-3	**	180
5-C2-1	**	180
5-C2-2	**	180
5-C2-3	2.81 nF	180
5-C3-1	1.43 nF	120
5-C3-2	1.32 nF	120
5-C3-3	1.71 nF	120
5-C4-1	3.56 nF	210
5-C4-2	3.72 nF	210
5-C4-3	3.42 nF	210
5-C5-1	4.14 nF	240
5-C5-2	4.13 nF	240
5-C5-3	4.20 nF	240
5-C6-1	5.65 nF	270
5-C6-2	5.60 nF	270
5-C6-3	5.65 nF	270
5-C7-1	9.00 nF	300
5-C7-2	8.09 nF	300
5-C7-3	7.33 nF	300
5-D2-1	**	240
5-D2-2	**	240
5-D2-3	4.12 nF	240
5-D3-1	3.60 nF	210
5-D3-2	3.78 nF	210
5-D3-3	3.36 nF	210
5-D4-1	5.78 nF	270
5-D4-2	5.72 nF	270
5-D4-3	6.25 nF	270
5-D5-1	*	180
5-D5-2	2.84 nF	180
5-D5-3	2.88 nF	180
5-D6-1	1.29 nF	120
5-D6-2	1.41 nF	120
5-D6-3	1.24 nF	120
5-D7-1	6.78 nF	300
5-D7-2	6.36 nF	300
5-D7-3	6.35 nF	300
5-E2-1	1.89 nF	150
5-E2-2	1.85 nF	150

Capacitance Measurements of Rapid-Ramp Annealing Process Devices (Concluded)

Device	Capacitance	Diameter
5-E2-3	1.77 nF	150
5-E3-1	0.70 nF	270
5-E3-2	*	270
5-E3-3	7.16 nF	270
5-E4-1	**	180
5-E4-2	**	180
5-E4-3	**	180
5-E5-1	*	270
5-E5-2	7.20 nF	270
5-E5-3	**	270
5-E6-1	**	180
5-E6-2	**	180
5-E6-3	**	180
5-E7-1	5.62 nF	300
5-E7-2	7.84 nF	300
5-E7-3	7.52 nF	300
5-F2-1	2.46 nF	150
5-F2-2	2.25 nF	150
5-F2-3	**	150
5-F3-1	2.41 nF	150
5-F3-2	2.46 nF	150
5-F3-3	2.32 nF	150
5-F4-1	**	240
5-F4-2	**	240

Device	Capacitance	Diameter
5-F4-3	5.41 nF	240
5-F5-1	2.06 nF	240
5-F5-2	***	240
5-F5-3	5.38 nF	240
5-F6-1	**	300
5-F6-2	0.94 nF	300
5-F6-3	1.04 nF	300
5-F7-1	0.54 nF	180
5-F7-2	0.55 nF	180
5-F7-3	0.71 nF	180
5-G2-1	5.02 nF	240
5-G2-2	5.03 nF	240
5-G2-3	5.08 nF	240
5-G3-1	*	150
5-G3-2	2.42 nF	150
5-G3-3	*	150
5-G4-1	**	240
5-G4-2	**	240
5-G4-3	**	240
5-G5-1	1.67 nF	150
5-G5-2	1.67 nF	150
5-G5-3	1.76 nF	150
5-G6-1	7.01 nF	300
5-G6-2	*	300
5-G6-3	6.87 nF	300

Gold trace connects these devices shorting one of the two. Possible mask defect?

Bad Device

Possible Bad Device

* Shorted device

** unstable device

*** device shorted by possible mask defect

APPENDIX C
CAPACITANCE MEASUREMENTS OF DOUBLE-RAMP ANNEALING PROCESS DEVICES

Capacitance Measurements of Double-Ramp Annealing Process Devices

Device	Capacitance	Diameter
6-A1-1	*	180µm
6-A1-2	1.43 nF	180µm
6-A1-3	*	180µm
6-A2-1	1.64 nF	180µm
6-A2-2	1.48 nF	180µm
6-A2-3	1.71 nF	180µm
6-A3-1	2.88 nF	270µm
6-A3-2	*	270µm
6-A3-3	2.85 nF	270µm
6-A4-1	*	150µm
6-A4-2	1.16 nF	150µm
6-A4-3	1.30 nF	150µm
6-A5-1	*	180µm
6-A5-2	1.36 nF	180µm
6-A5-3	1.36 nF	180µm
6-B1-1	1.69 nF	180µm
6-B1-2	1.53 nF	180µm
6-B1-3	1.64 nF	180µm
6-B2-1	*	270µm
6-B2-2	*	270µm
6-B2-3	*	270µm
6-B4-1	2.63 nF	240µm
6-B4-2	2.40 nF	240µm
6-B4-3	2.20 nF	240µm
6-B5-1	*	150µm
6-B5-2	1.26 nF	150µm
6-B5-3	1.07 nF	150µm
6-C1-1	1.86 nF	210µm
6-C1-2	*	210µm
6-C1-3	*	210µm
6-C3-1	0.73 nF	120µm
6-C3-2	0.85 nF	120µm
6-C3-3	*	120µm
6-C5-1	1.86 nF	210µm
6-C5-2	1.87 nF	210µm
6-C5-3	2.21 nF	210µm
6-D1-1	3.24 nF	270µm
6-D1-2	*	270µm
6-D1-3	3.18 nF	270µm
6-D2-1	0.75 nF	120µm

Device	Capacitance	Diameter
6-D2-2	0.78 nF	120µm
6-D2-3	0.75 nF	120µm
6-D4-1	0.86 nF	120µm
6-D4-2	2.53 nF	120µm
6-D4-3	0.92 nF	120µm
6-D5-1	0.59 nF	210µm
6-D5-2	0.90 nF	210µm
6-D5-3	17.10 nF	210µm
6-E1-1	0.37 nF	150µm
6-E1-2	0.44 nF	150µm
6-E1-3	0.41 nF	150µm
6-E2-1	2.03 nF	210µm
6-E2-2	*	210µm
6-E2-3	2.00 nF	210µm
6-E3-1	0.53 nF	180µm
6-E3-2	0.55 nF	180µm
6-E3-3	0.55 nF	180µm
6-E4-1	2.66 nF	240µm
6-E4-2	2.63 nF	240µm
6-E4-3	2.61 nF	240µm
6-E5-1	2.09 nF	210µm
6-E5-2	2.09 nF	210µm
6-E5-3	2.03 nF	210µm
7-A1-1	0.77 nF	120µm
7-A1-2	*	120µm
7-A1-3	0.24 nF	120µm
7-A2-1	1.04 nF	150µm
7-A2-2	*	150µm
7-A2-3	1.18 nF	150µm
7-A3-1	*	120µm
7-A3-2	0.83 nF	120µm
7-A3-3	0.82 nF	120µm
7-A4-1	*	120µm
7-A4-2	0.77 nF	120µm
7-A4-3	0.71 nF	120µm
7-A5-1	3.84 nF	300µm
7-A5-2	3.34 nF	300µm
7-A5-3	**	300µm
7-B1-1	1.88 nF	210µm
7-B1-2	1.82 nF	210µm

Capacitance Measurements of Double-Ramp Annealing Process Devices (Concluded)

Device	Capacitance	Diameter
7-B1-3	1.87 nF	210µm
7-B2-1	1.05 nF	150µm
7-B2-2	1.03 nF	150µm
7-B2-3	1.45 nF	150µm
7-B4-1	1.49 nF	180µm
7-B4-2	1.46 nF	180µm
7-B4-3	**	180µm
7-B5-1	1.04 nF	150µm
7-B5-2	1.03 nF	150µm
7-B5-3	1.13 nF	150µm
7-C1-1	*	300µm
7-C1-2	3.72 nF	300µm
7-C1-3	2.00 nF	300µm
7-C3-1	7.67 nF	240µm
7-C3-2	2.53 nF	240µm
7-C3-3	5.63 nF	240µm
7-C5-1	*	240µm
7-C5-2	*	240µm
7-C5-3	2.38 nF	240µm
7-D1-1	0.78 nF	120µm
7-D1-2	0.81 nF	120µm
7-D1-3	0.72 nF	120µm
7-D2-1	3.22 nF	270µm
7-D2-2	2.99 nF	270µm

Device	Capacitance	Diameter
7-D2-3	0.70 nF	270µm
7-D4-1	4.01 nF	300µm
7-D4-2	0.72 nF	300µm
7-D4-3	3.63 nF	300µm
7-D5-1	1.88 nF	210µm
7-D5-2	*	210µm
7-D5-3	1.85 nF	210µm
7-E1-1	2.89 nF	270µm
7-E1-2	2.92 nF	270µm
7-E1-3	*	270µm
7-E2-1	3.55 nF	270µm
7-E2-2	*	270µm
7-E2-3	3.69 nF	270µm
7-E3-1	3.12 nF	270µm
7-E3-2	0.86 nF	270µm
7-E3-3	*	270µm
7-E4-1	*	240µm
7-E4-2	2.38 nF	240µm
7-E4-3	2.48 nF	240µm
7-E5-1	2.64 nF	240µm
7-E5-2	2.51 nF	240µm
7-E5-3	3.08 nF	240µm

* Device was shorted
** Button was detached from device
Bad Device
Questionable Device

APPENDIX D
RADIANT TECHNOLOGIES, INC. CHARACTERIZATION OF SIMILAR ARL-FABRICATED DEVICES

RADIANT TECHNOLOGIES, INC.

Radiant Technologies, Inc.
2835D Pan American Freeway NE
Albuquerque, NM 87107
Tel: 505-842-8007
Fax: 505-842-0366
e-mail: radiant@ferrodevices.com
www.ferrodevices.com

Hysteresis Loops of ARL Samples

Date: July 16, 2011
Author: Joe Evans

Discussion:
Dr. Tracy Hudson of Army AMRDEC sent me nine substrates with three capacitors each to test for recovery. The capacitors all had 1μ-thick PZT and had circular top electrodes that ranged in diameters from 120μ to 300μ. The capacitors were prepared by Dr. Polcawich's team at the Army Research Laboratory in Maryland.

All of the capacitors were integrated with etched PZT and gold bond pads contacting the top and bottom electrodes. I suspect the electrodes themselves are platinum. I found that the capacitors all had collapsed hysteresis loops, most likely from the effects of photolithography and processing. I tested all substrates for their initial hysteresis loops at 15V with a 1 millisecond period. I subjected substrate 6-B1 to more extensive testing to determine if it could withstand a recovery process and at what voltage. I ended up blowing up all three capacitors on that substrate with either 1 second 15 volt hysteresis loops or a 10Hz (10ms) 15 volt sine wave recovery. I stopped executing recovery procedures on the capacitors at that point because I might have destroyed every capacitor in the sample set.

Properly crystallized PZT always recovers when exposed to 650ºC oxygen above 0.1 Torr. I recommend that Dr. Hudson execute a 15 minute 650C oxygen anneal on one of the substrates to see if the gold on the substrate can withstand the temperature exposure. If so, then he should subject all of the substrates to that anneal and re-test them.

Results:
I executed 1 millisecond 15 volt hysteresis loops on all capacitors. I executed Hysteresis vs Volts and Hysteresis vs Period specifically on the capacitors of substrate 6-B1. I then executed a 15 volt 10Hz sine wave recovery on capacitors 2 and 3 of 6-B1, blowing both capacitors. Below I plot the results of the tests from 6-B1 plus the virgin capacitor loops for all caps. In all cases, the measurements were made with the microscope light off, the room lights on, and DRIVE on the bottom electrode.

All of the virgin plots below use the same scale on the Y-axis to allow visual comparison. Finally, I tested all caps whether they were marked as bad or if they looked bad. Those capacitors with less than the proscribed area generated loops with lower Pmax values. Those that were shorted are plotted as "all 0's" by the Vision software.

6-B1

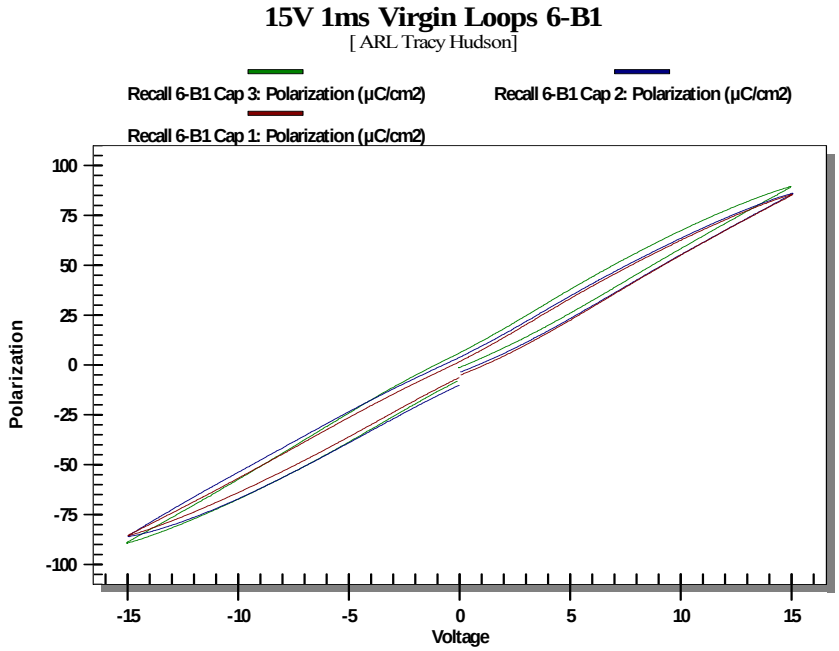

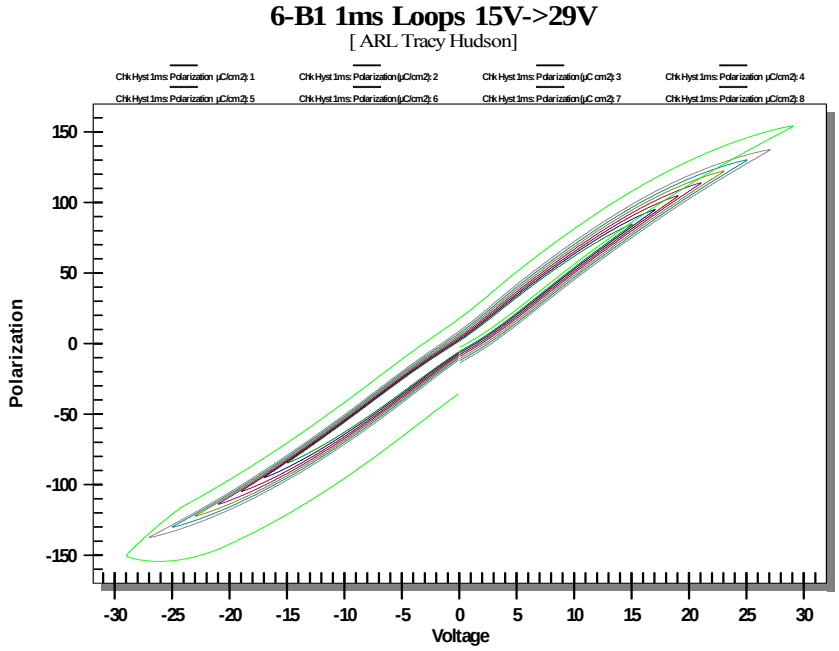

Hysteresis vs Volts at 1ms

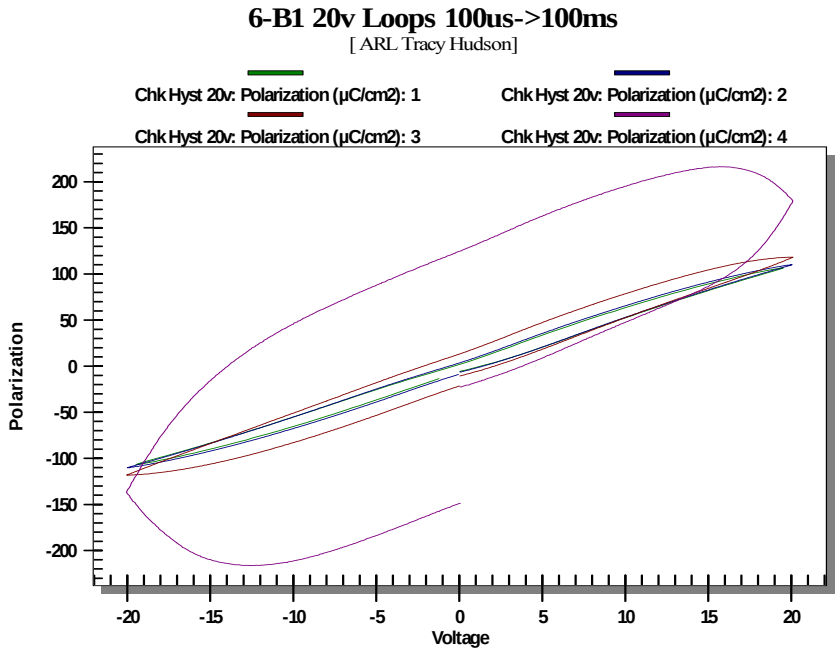

Hysteresis vs Period at 20 volts

The blow-out of the 100ms loop and its shape is in indication of blocking electrode breakdown during the loop. This type of conduction is destructive if allowed to continue. I executed the Hysteresis vs Period test again at 15 volts, this time letting it proceed to the 1 second period and the capacitor shorted during the 1 second test. I then executed the following recovery procedure on the remaining capacitors of 6-B1:

1) 15V 1ms Hysteresis
2) 15V 10Hz (10ms) Sine wave for 100 seconds
3) 15V 1ms Hysteresis

On both capacitors, the hysteresis after the sine wave recovery showed a short circuit.

6-D1

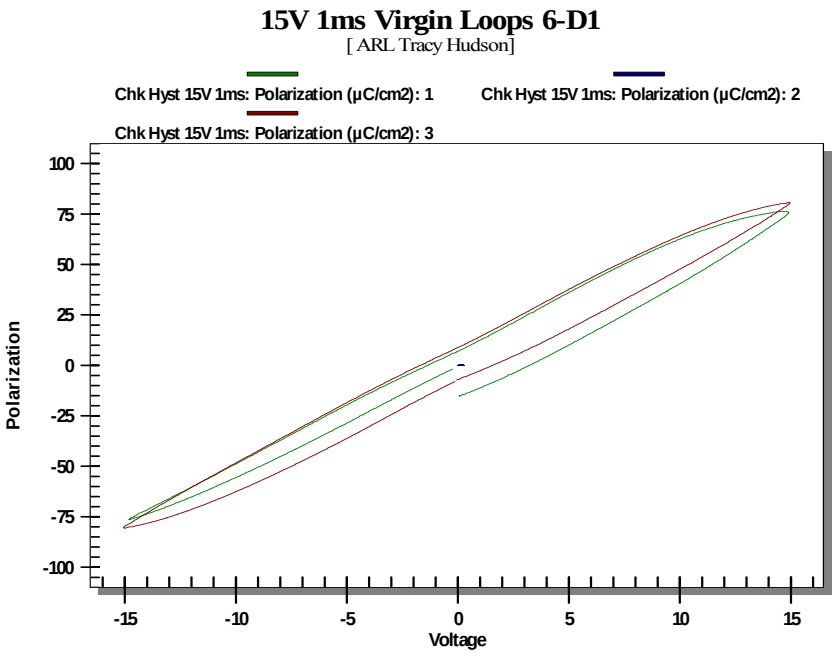
15V 1ms Virgin Loops 6-D1
[ARL Tracy Hudson]
Chk Hyst 15V 1ms: Polarization (µC/cm2): 1
Chk Hyst 15V 1ms: Polarization (µC/cm2): 2
Chk Hyst 15V 1ms: Polarization (µC/cm2): 3
Polarization
100
75
50
25
0
-25
-50
-75
-100
-15
-10
-5
0
5
10
15
Voltage

6-E4

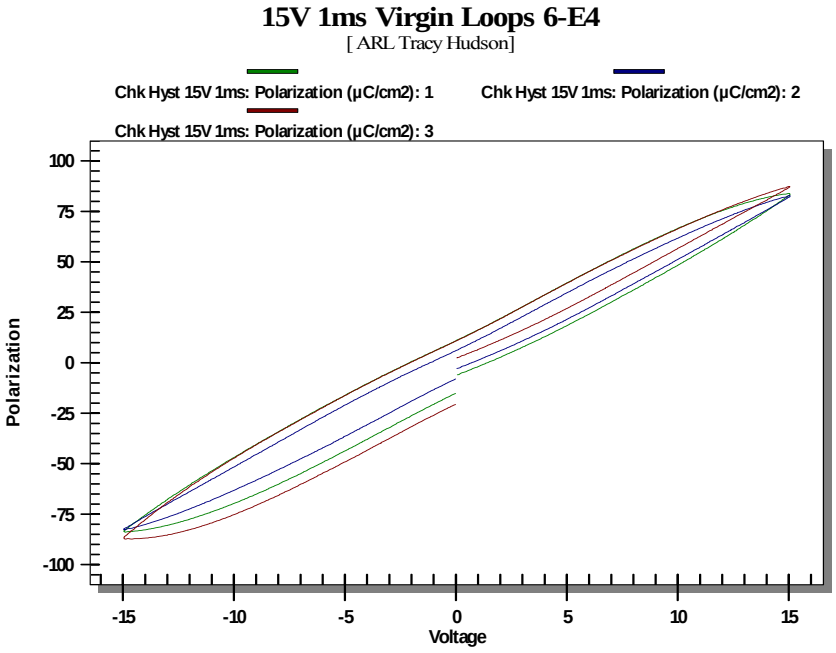
15V 1ms Virgin Loops 6-E4
[ARL Tracy Hudson]
Chk Hyst 15V 1ms: Polarization (µC/cm2): 1
Chk Hyst 15V 1ms: Polarization (µC/cm2): 2
Chk Hyst 15V 1ms: Polarization (µC/cm2): 3
Polarization
100
75
50
25
0
-25
-50
-75
-100
-15
-10
-5
0
5
10
15
Voltage

7-A5

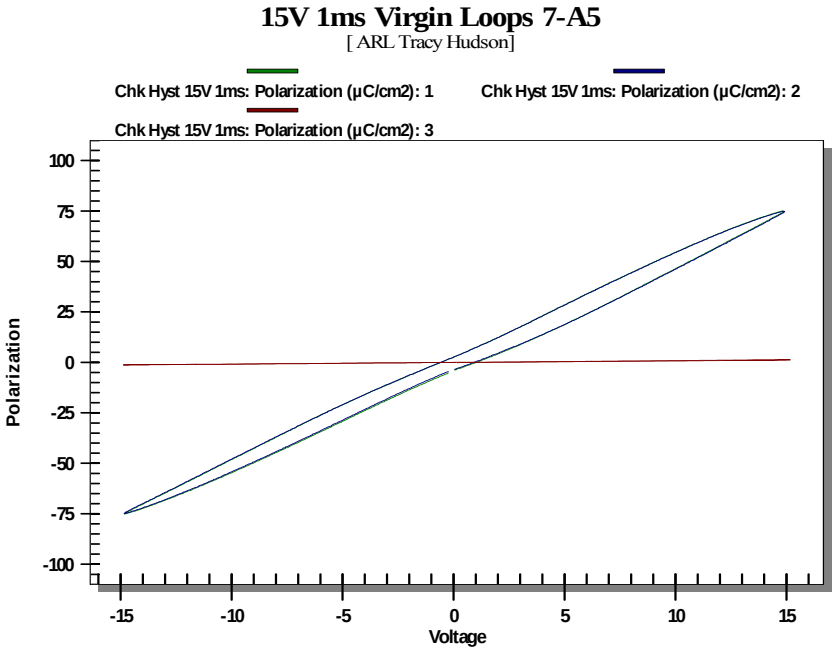
15V 1ms Virgin Loops 7-A5
[ARL Tracy Hudson]
Chk Hyst 15V 1ms: Polarization (µC/cm2): 1
Chk Hyst 15V 1ms: Polarization (µC/cm2): 2
Chk Hyst 15V 1ms: Polarization (µC/cm2): 3
Polarization
100
75
50
25
0
-25
-50
-75
-100
-15
-10
-5
0
5
10
15
Voltage

7-B1

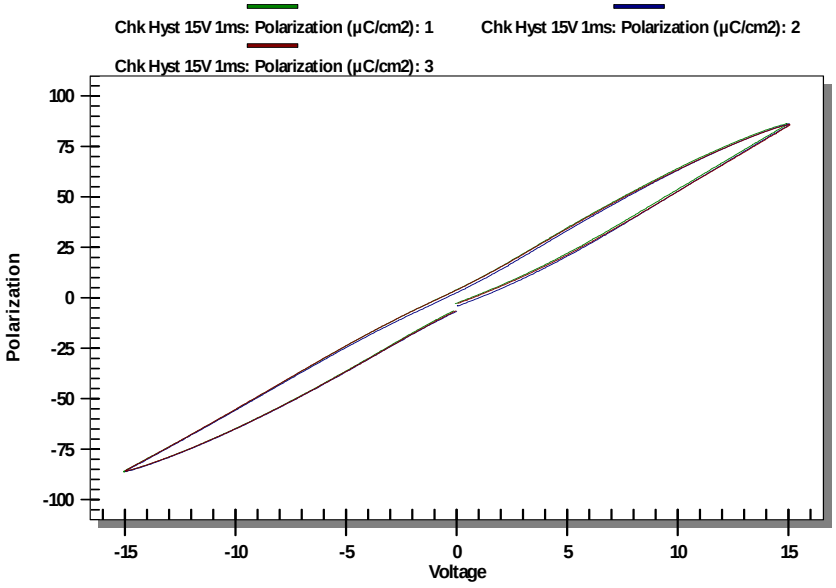
15V 1ms Virgin Loops 7-B1
[ARL Tracy Hudson]
Chk Hyst 15V 1ms: Polarization (µC/cm2): 1
Chk Hyst 15V 1ms: Polarization (µC/cm2): 2
Chk Hyst 15V 1ms: Polarization (µC/cm2): 3
Polarization
100
75
50
25
0
-25
-50
-75
-100
-15
-10
-5
0
5
10
15
Voltage

7-B5

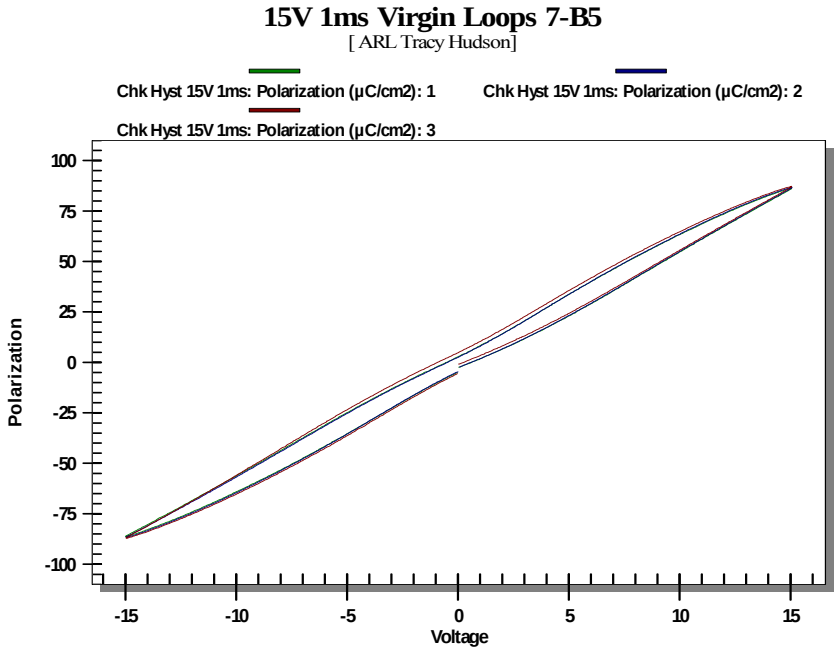
15V 1ms Virgin Loops 7-B5
[ARL Tracy Hudson]
Chk Hyst 15V 1ms: Polarization (µC/cm2): 1
Chk Hyst 15V 1ms: Polarization (µC/cm2): 2
Chk Hyst 15V 1ms: Polarization (µC/cm2): 3
Polarization
100
75
50
25
0
-25
-50
-75
-100
-15
-10
-5
0
5
10
15
Voltage

7-D1

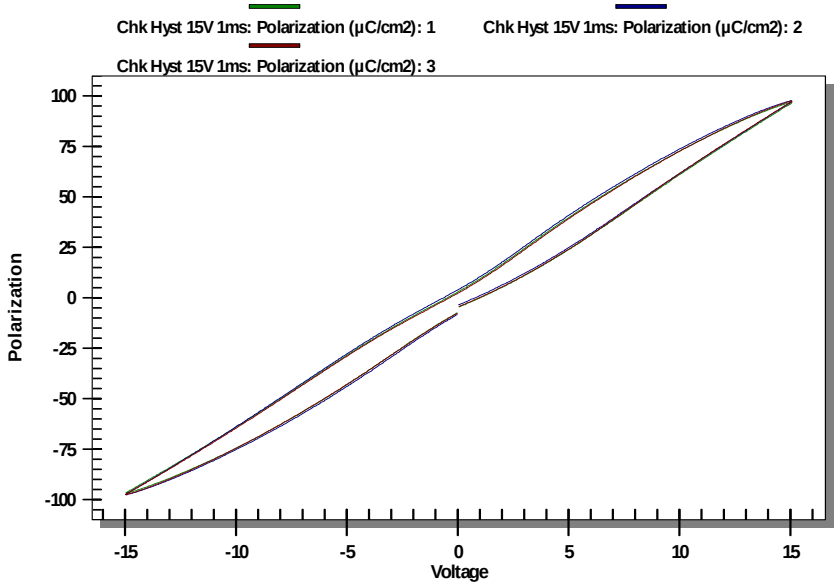
15V 1ms Virgin Loops 7-D1
[ARL Tracy Hudson]
Chk Hyst 15V 1ms: Polarization (µC/cm2): 1
Chk Hyst 15V 1ms: Polarization (µC/cm2): 2
Chk Hyst 15V 1ms: Polarization (µC/cm2): 3
Polarization
100
75
50
25
0
-25
-50
-75
-100
-15
-10
-5
0
5
10
15
Voltage

7-D4

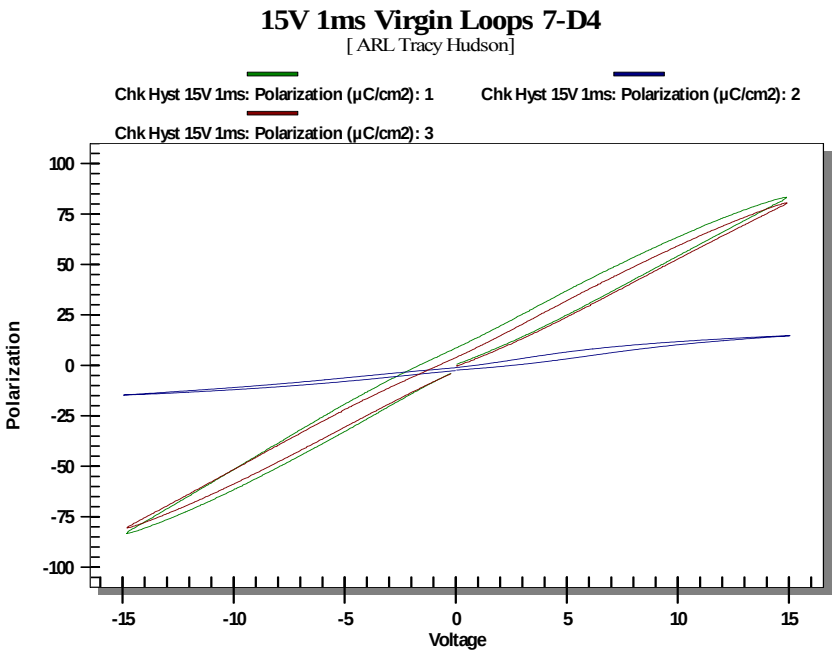
15V 1ms Virgin Loops 7-D4
[ARL Tracy Hudson]
Chk Hyst 15V 1ms: Polarization (µC/cm2): 1
Chk Hyst 15V 1ms: Polarization (µC/cm2): 2
Chk Hyst 15V 1ms: Polarization (µC/cm2): 3
Polarization
100
75
50
25
0
-25
-50
-75
-100
-15
-10
-5
0
5
10
15
Voltage

7-E3

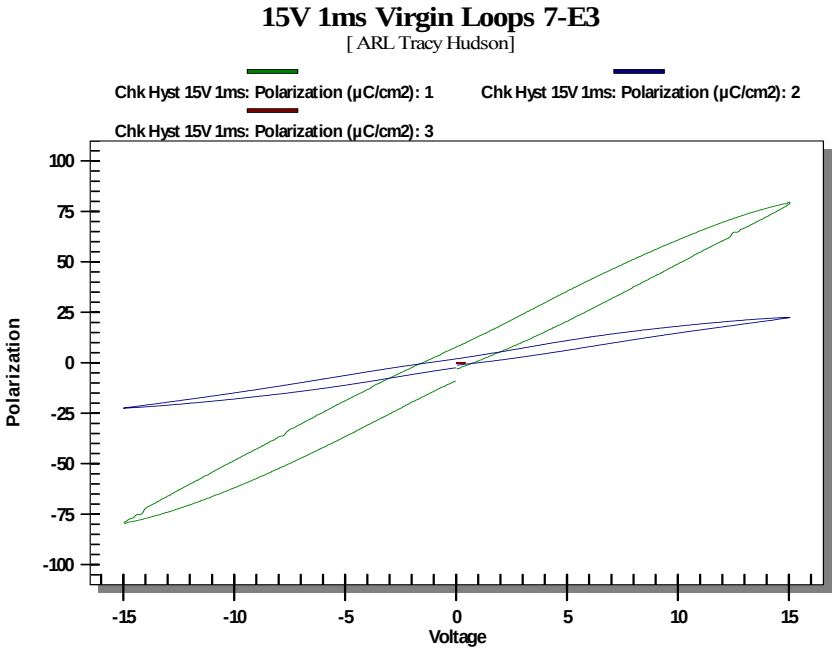
15V 1ms Virgin Loops 7-E3
[ARL Tracy Hudson]
Chk Hyst 15V 1ms: Polarization (µC/cm2): 1
Chk Hyst 15V 1ms: Polarization (µC/cm2): 2
Chk Hyst 15V 1ms: Polarization (µC/cm2): 3
Polarization
100
75
50
25
0
-25
-50
-75
-100
-15
-10
-5
0
5
10
15
Voltage

All Loops

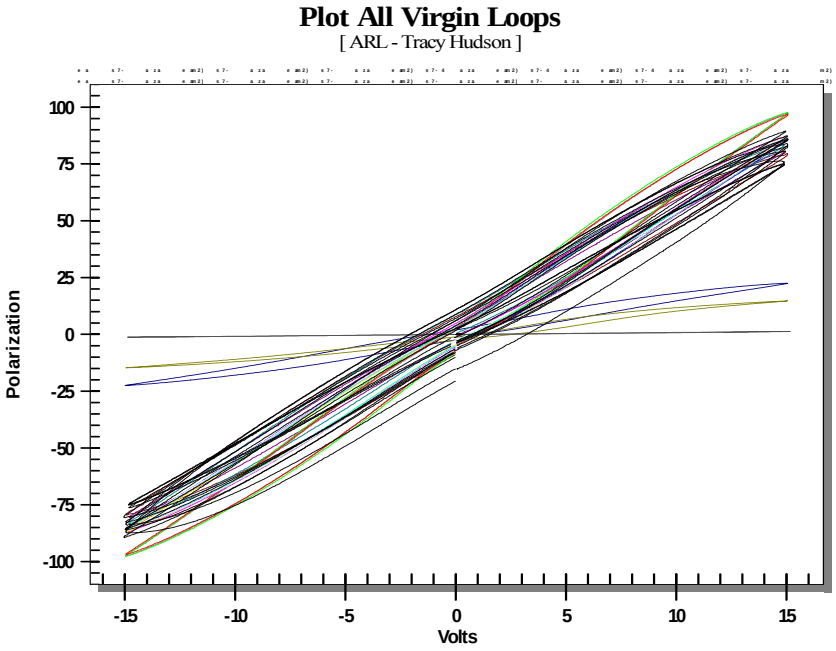

All nCVs

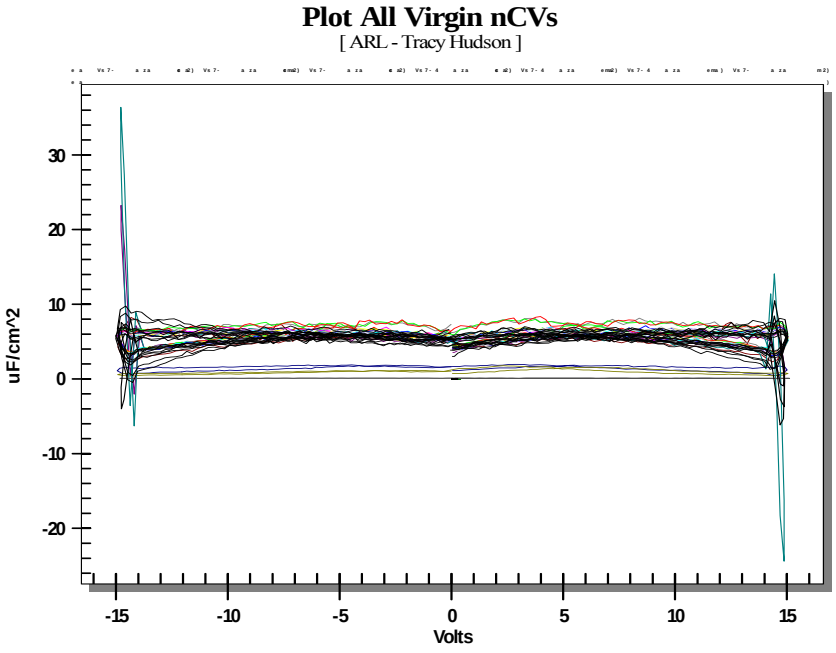

APPENDIX E
DROP TOWER CHARACTERIZATION OF CENTER-MOUNTED DEVICE ASSEMBLIES

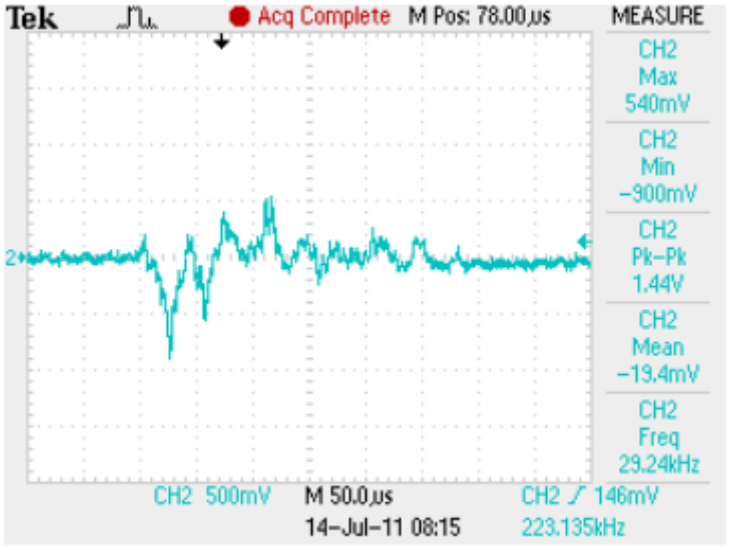

2-A2-1 DROP 1

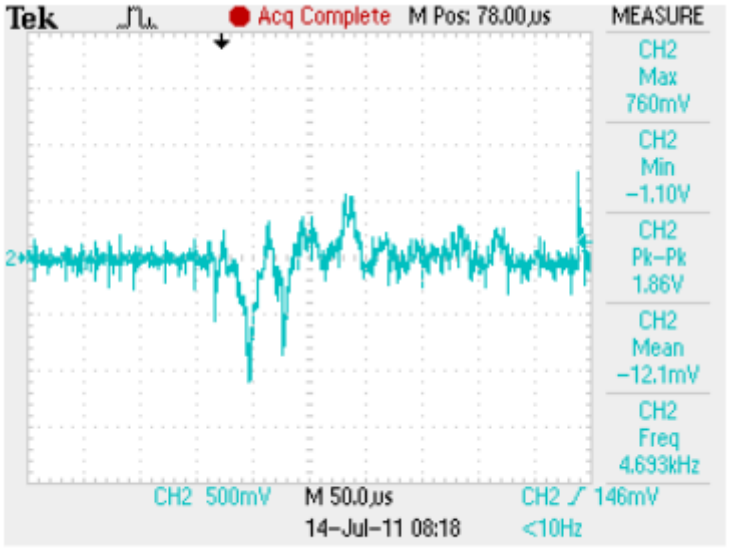

2-A2-1 DROP 2

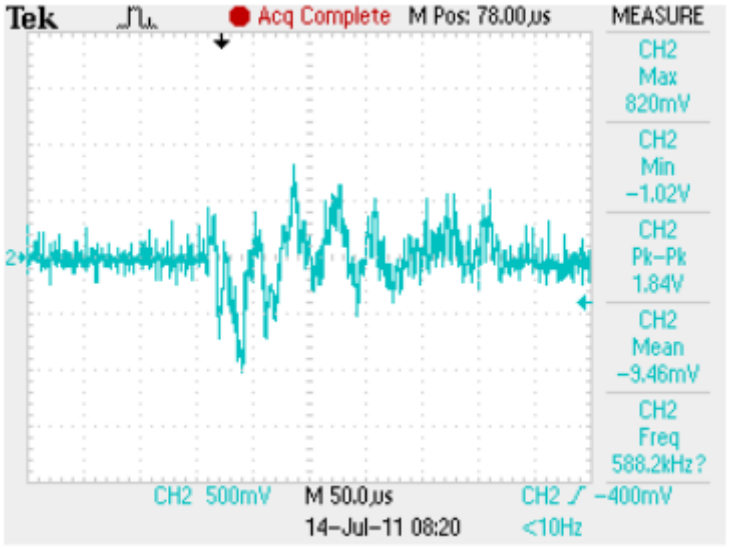

2-A2-1 DROP 3

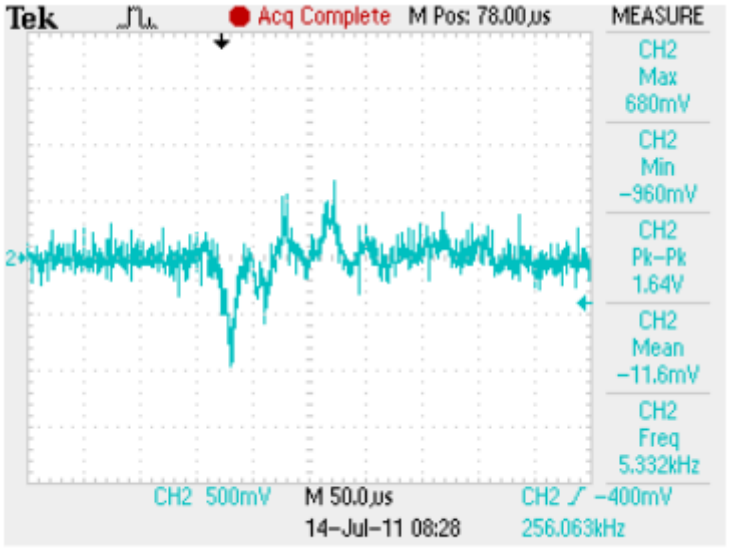

2-A2-1 DROP 4

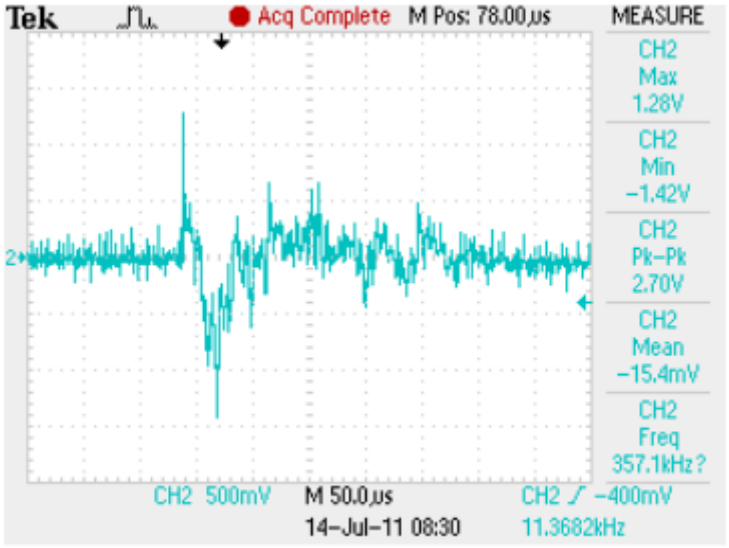

2-A2-1 DROP 5

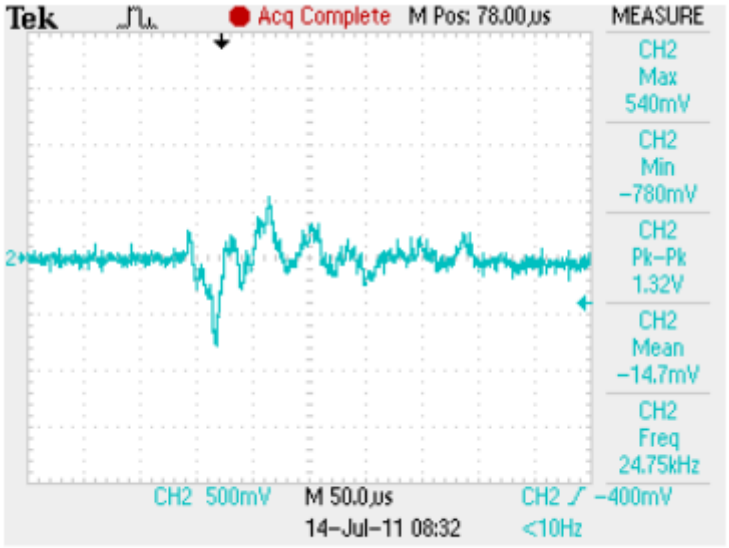

2-A2-3 DROP 1

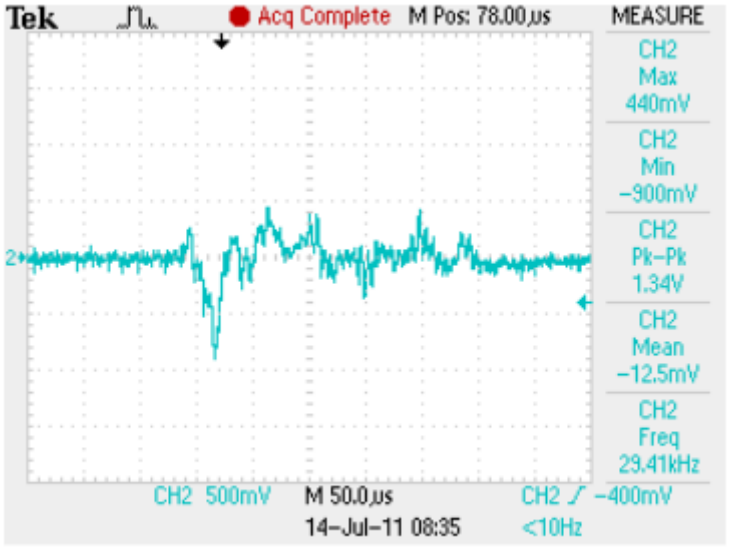

2-A2-3 DROP 2

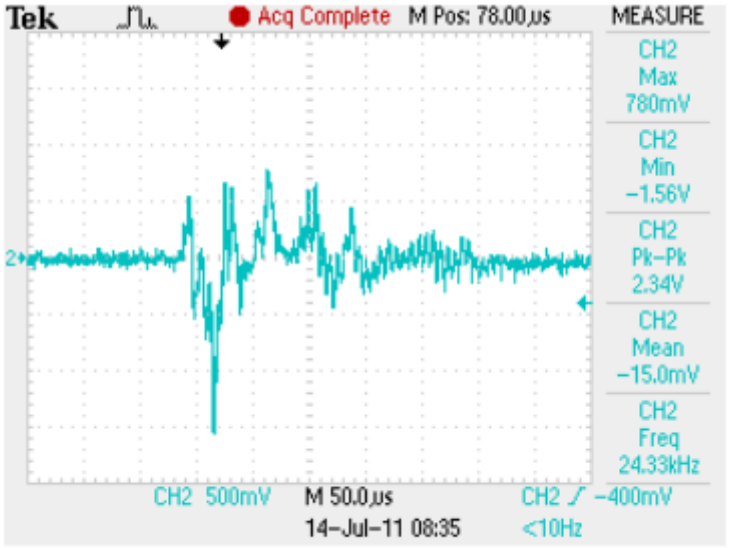

2-A2-3 DROP 3

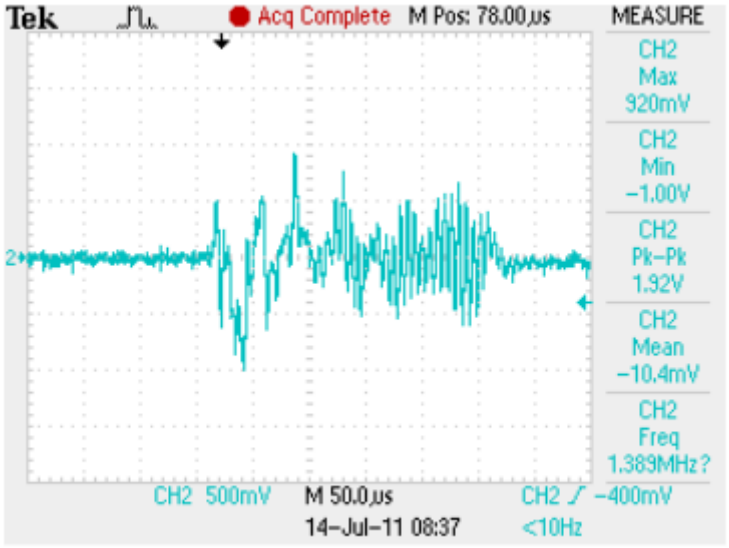

2-A2-3 DROP 4

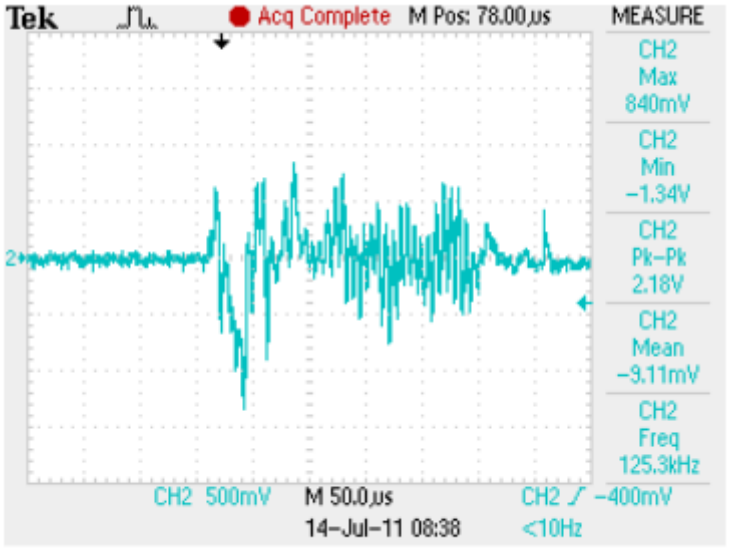

2-A2-3 DROP 5

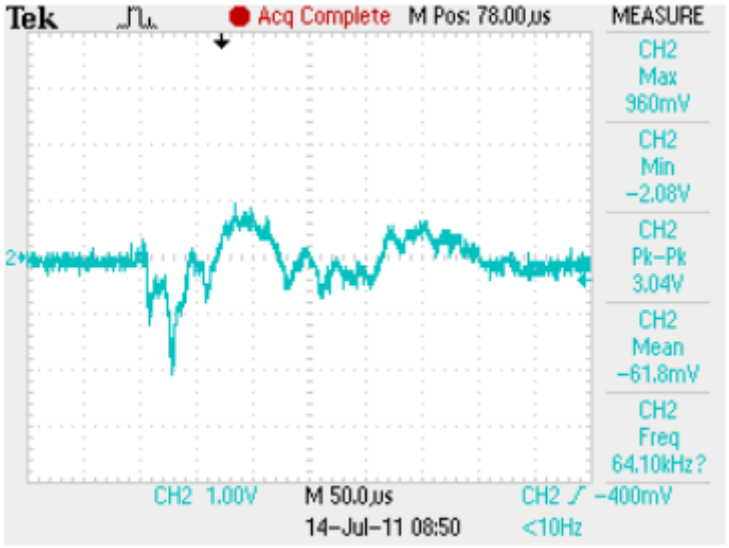

2-B5-3 DROP 1

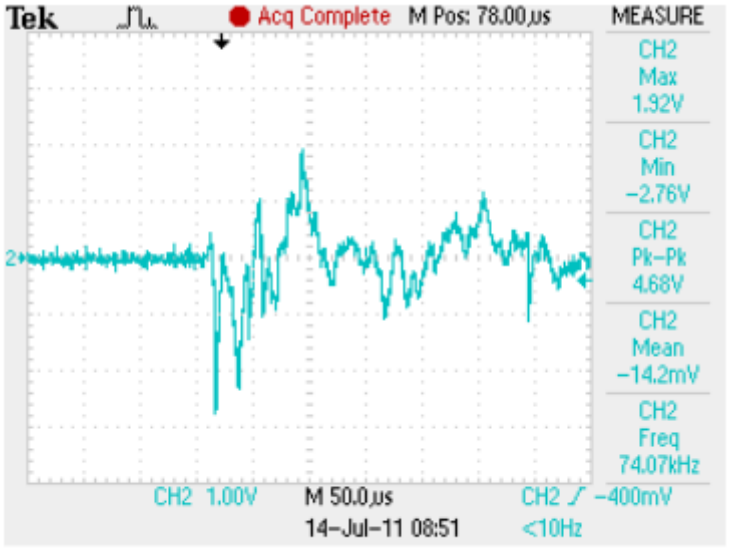

2-B5-3 DROP 2

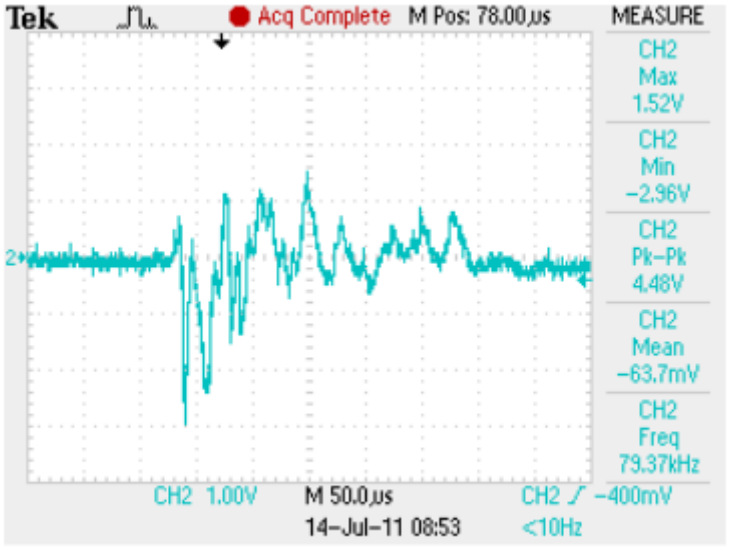

2-B5-3 DROP 3

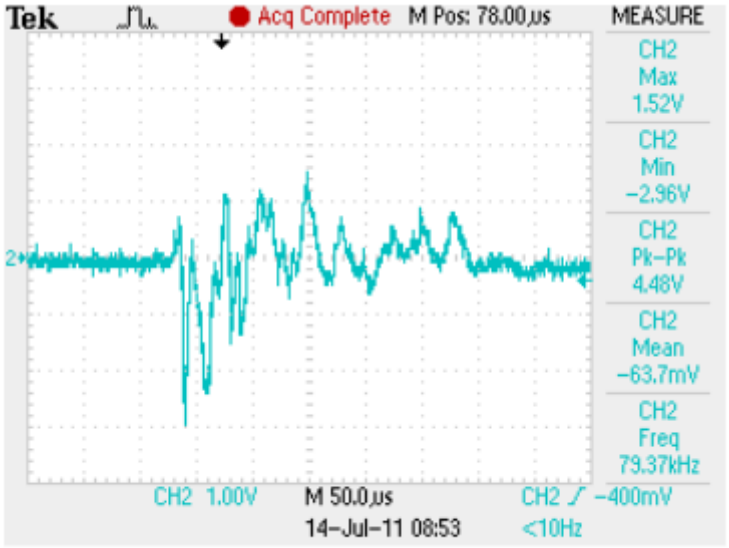

2-B5-3 DROP 4

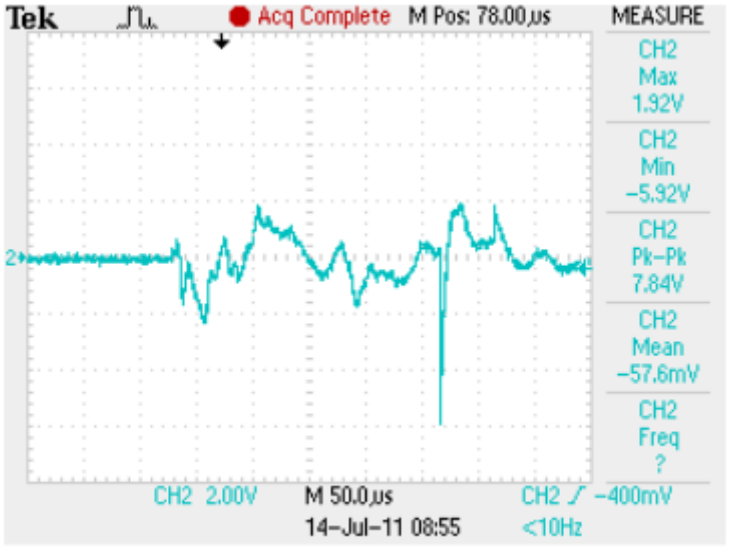

2-B5-3 DROP 5

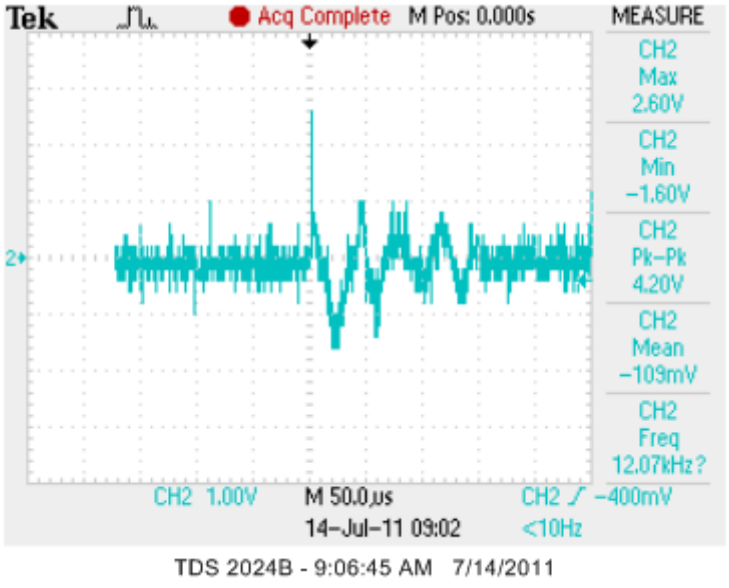

2-D1-1 DROP 1

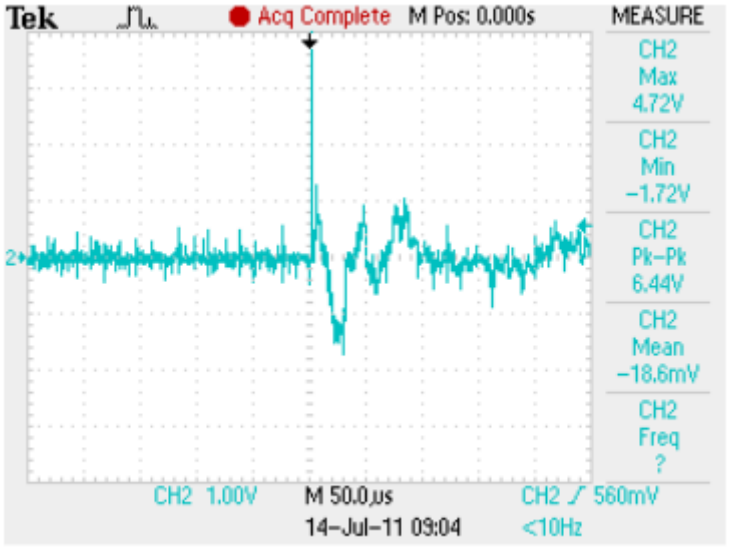

2-D1-1 DROP 2

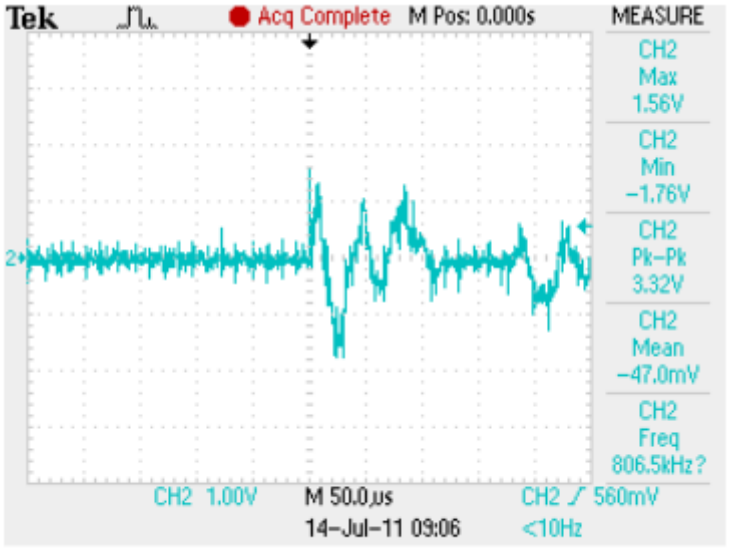

2-D1-1 DROP 3

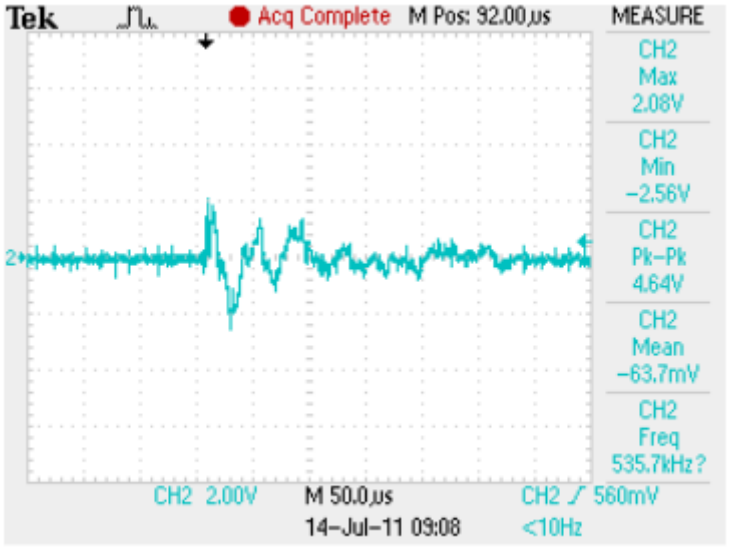

2-D1-1 DROP 4

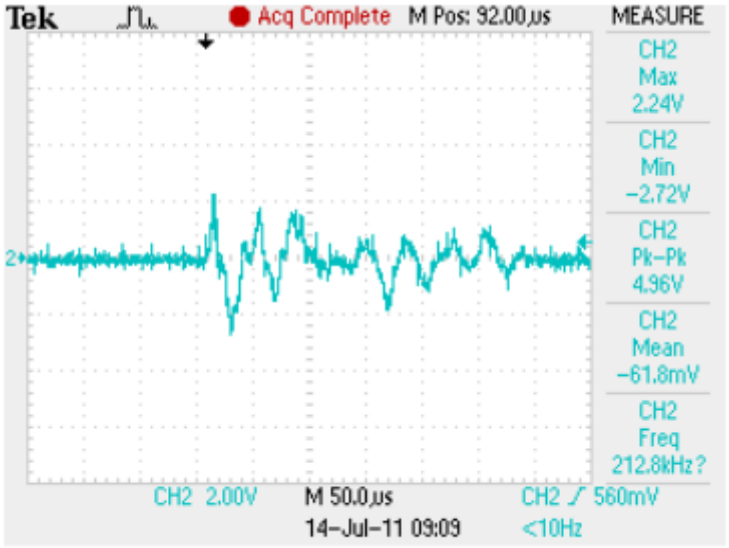

2-D1-1 DROP 5

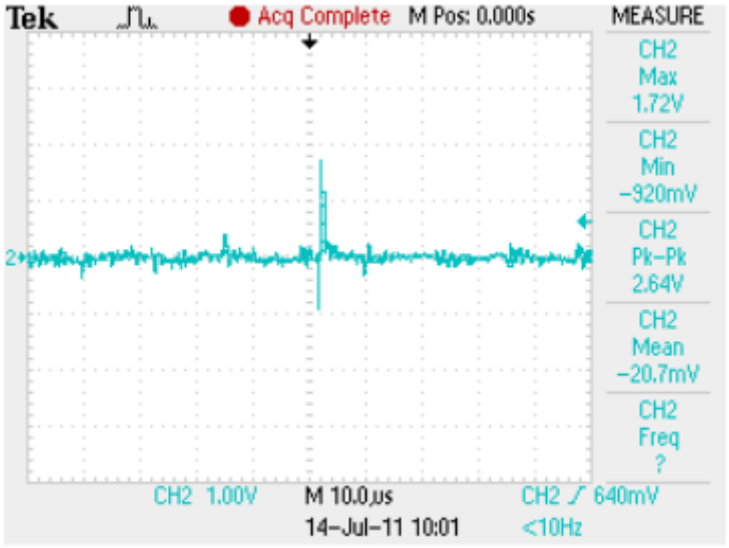

2-E1-1 DROP 1

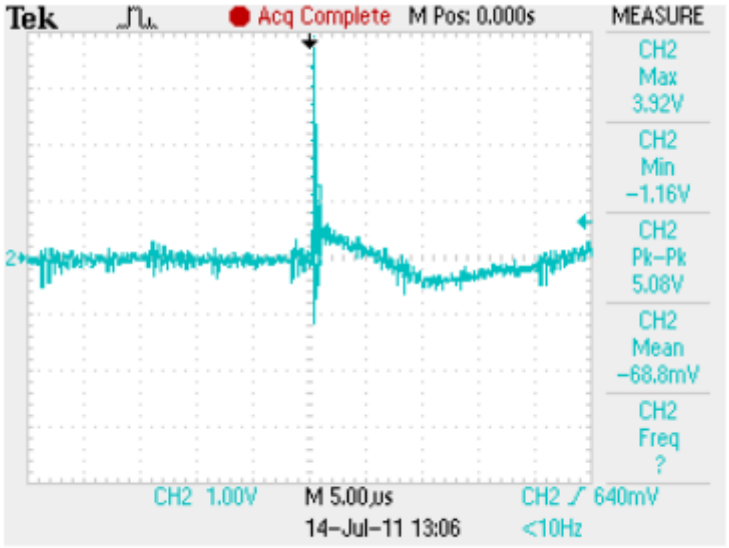

2-E1-1 DROP 2

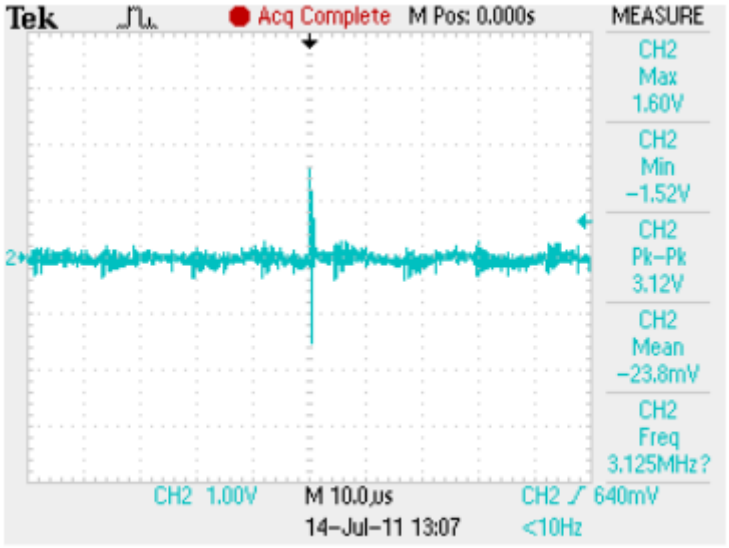

2-E1-1 DROP 3

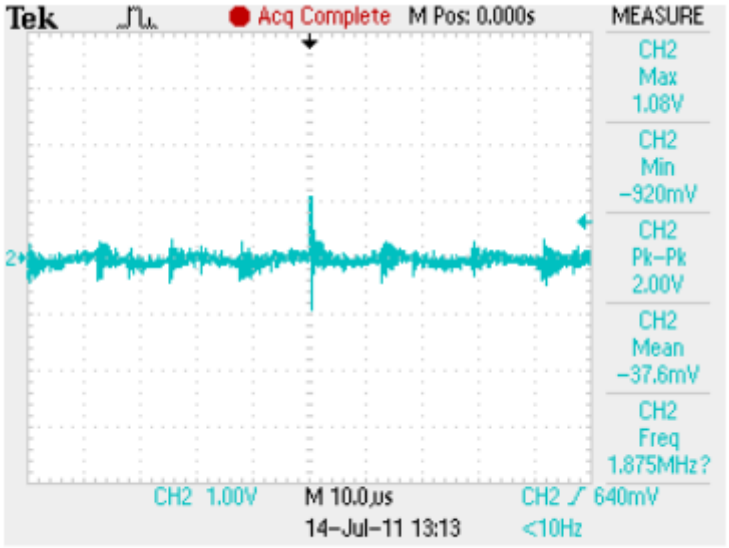

2-E1-1 DROP 4

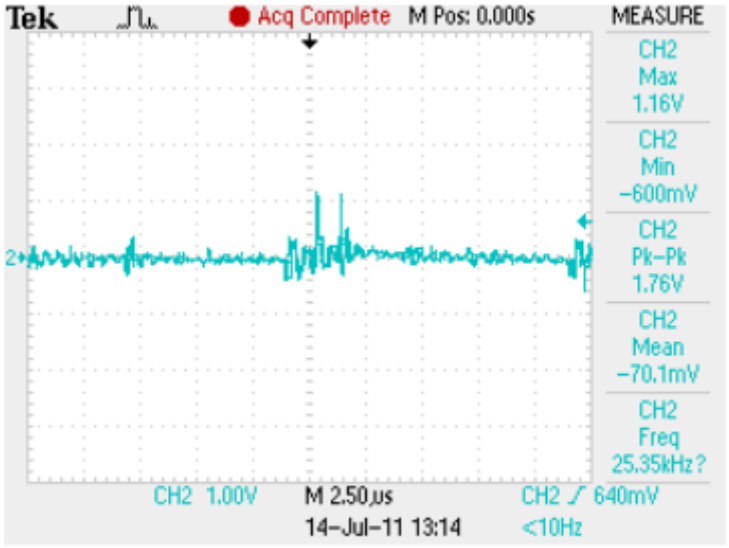

2-E1-1 DROP 5

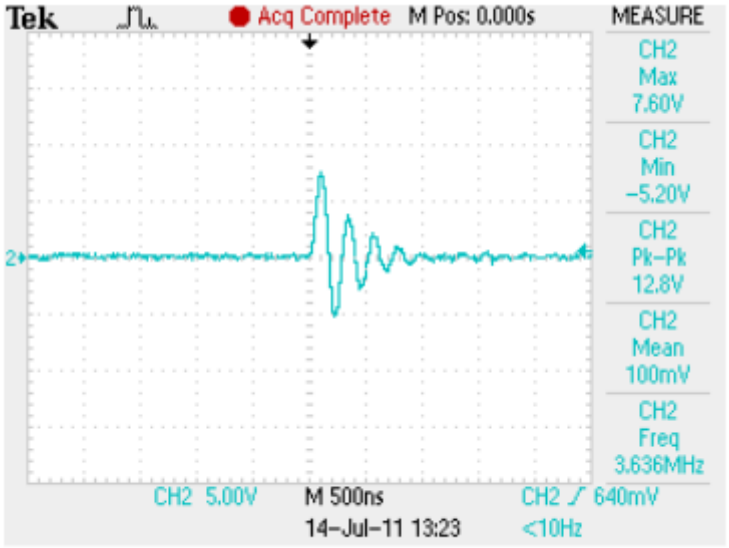

2-E1-2 DROP 1

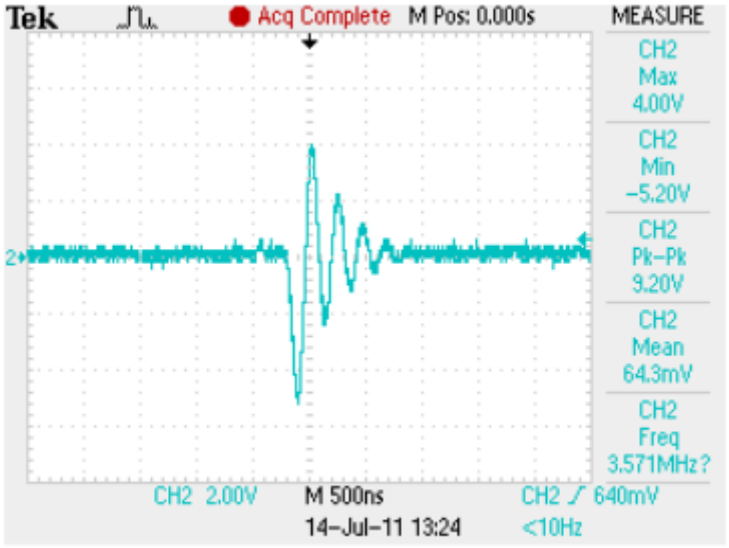

2-E1-2 DROP 2

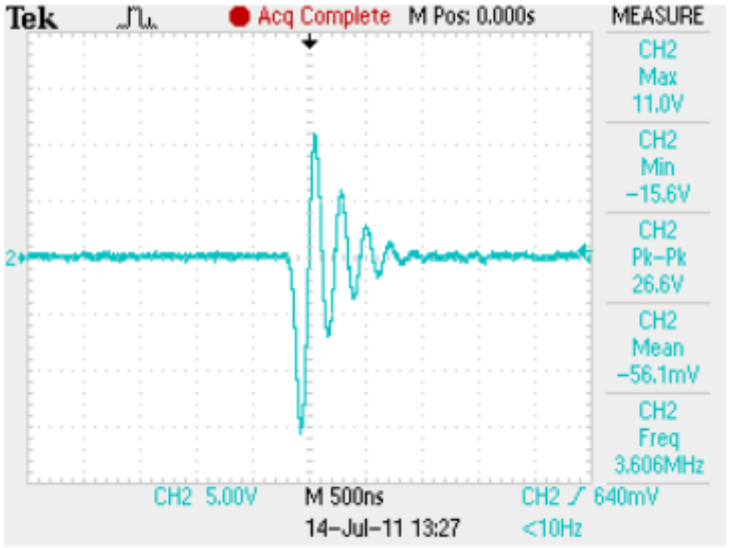

2-E1-2 DROP 3

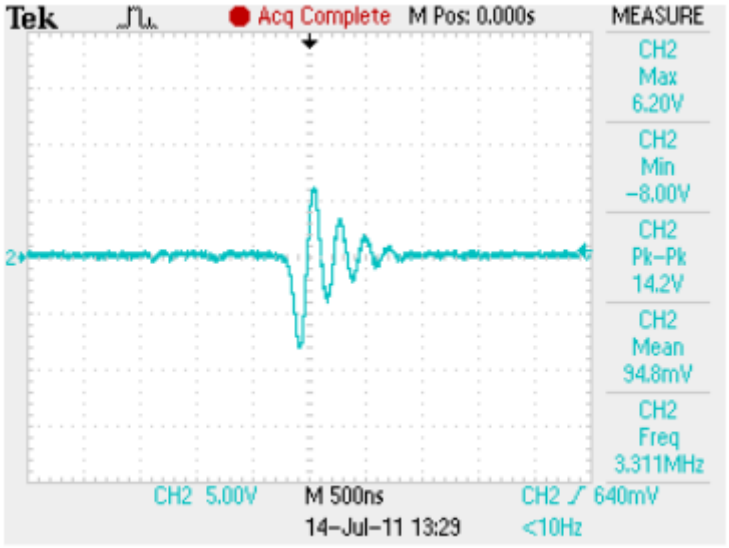

2-E1-2 DROP 4

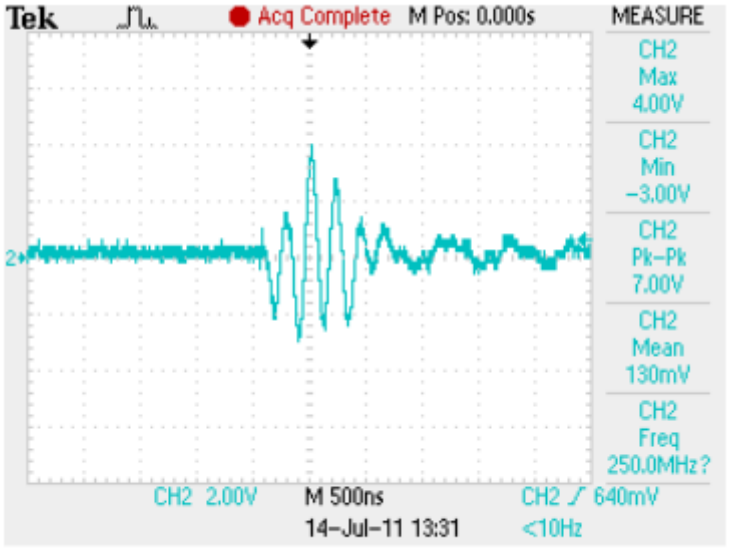

2-E1-2 DROP 5

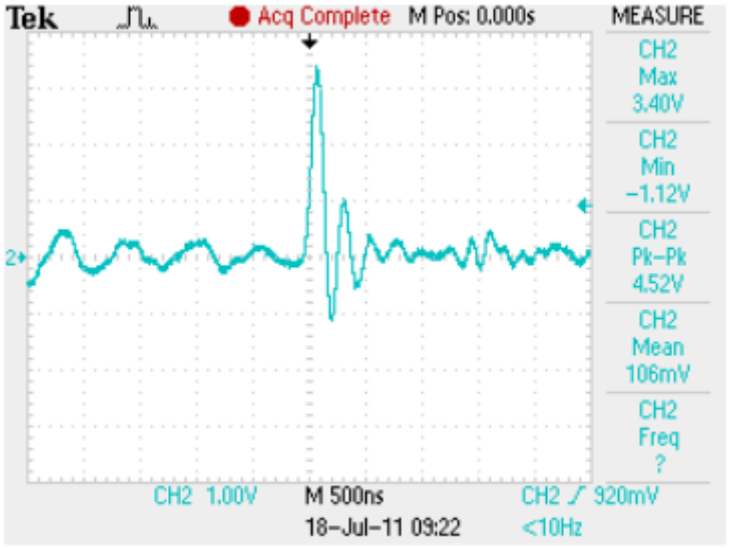

3-E1-1 DROP 1

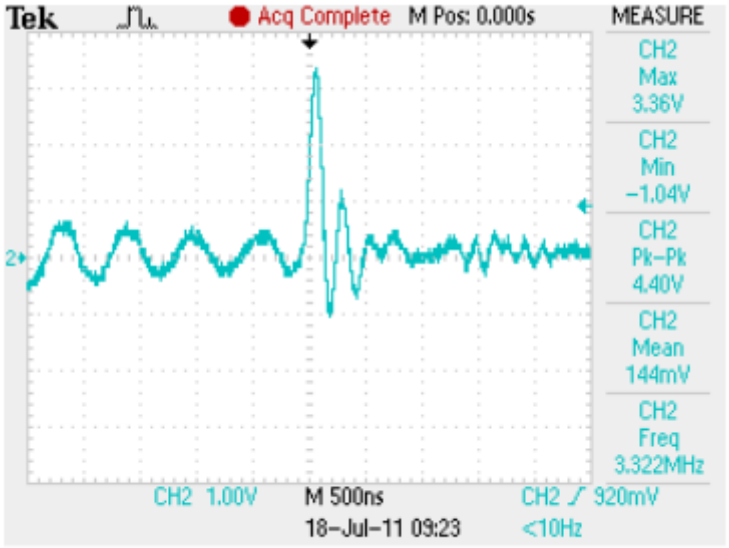

3-E1-1 DROP 2

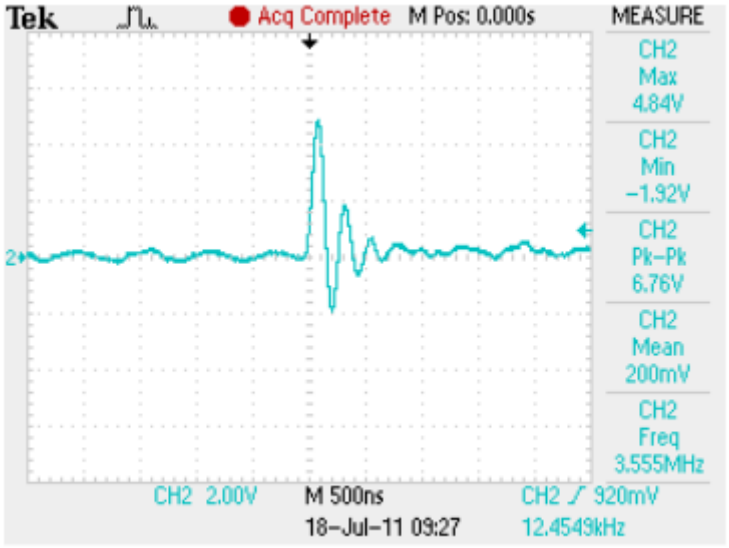

3-E1-1 DROP 3

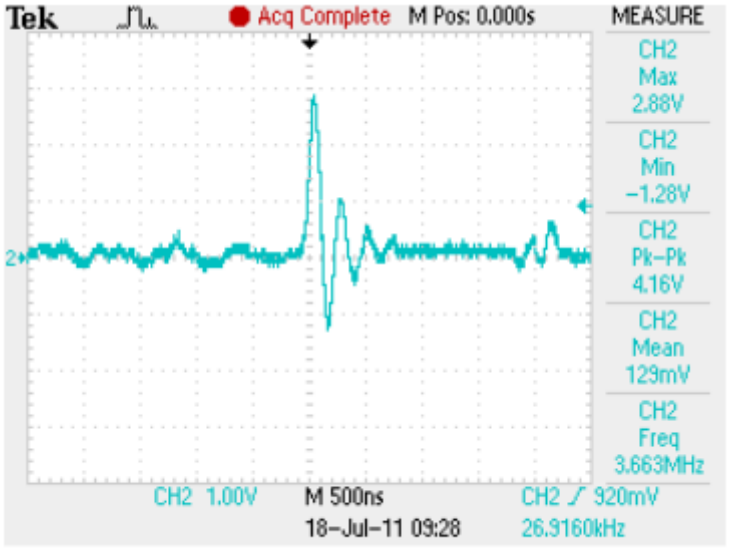

3-E1-1 DROP 4

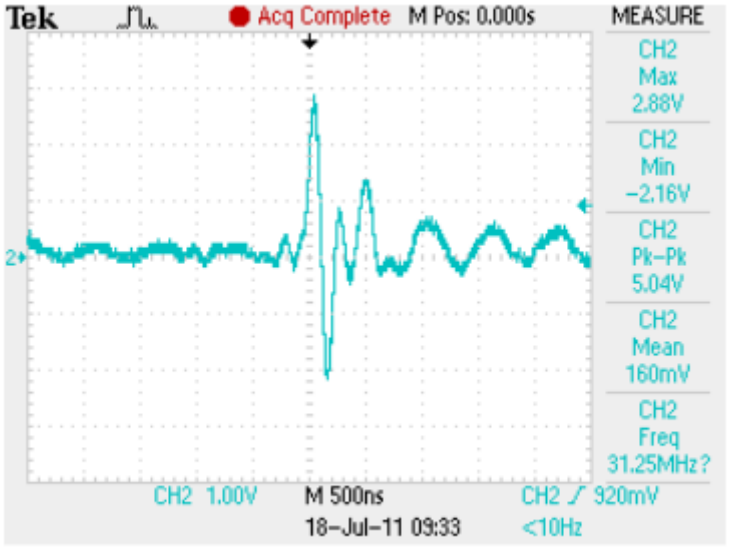

3-E1-3 DROP 1

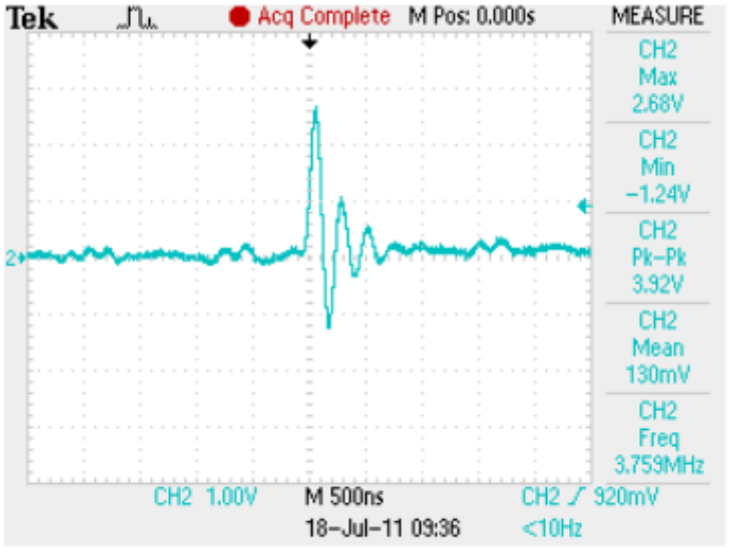

3-E1-3 DROP 2

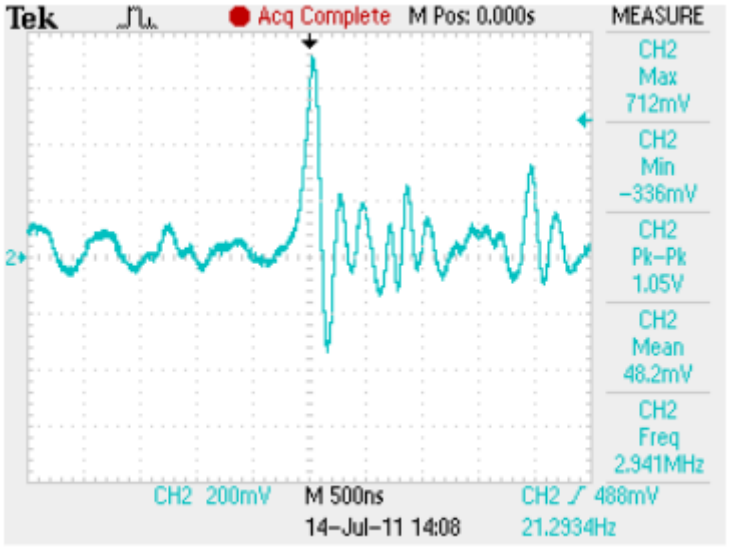

3-E3-1 DROP 1

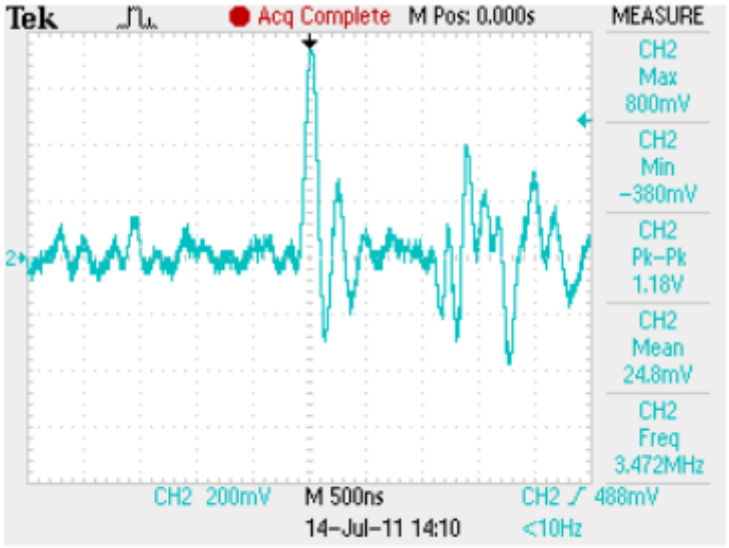

3-E3-1 DROP 2

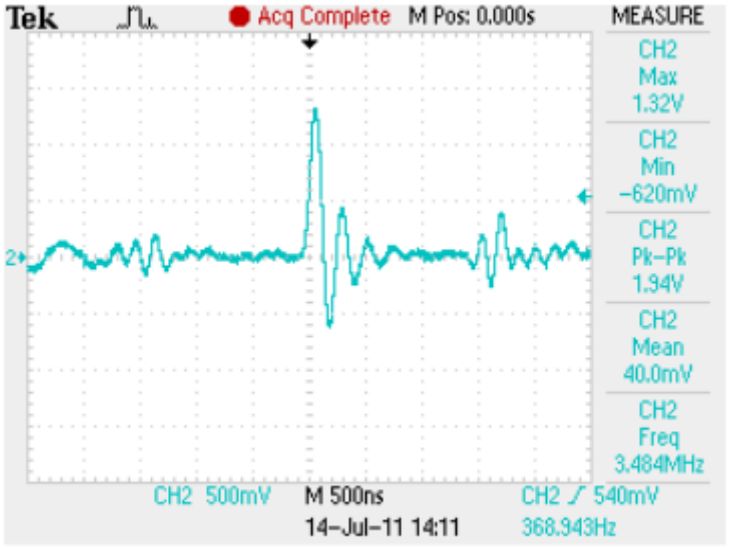

3-E3-1 DROP 3

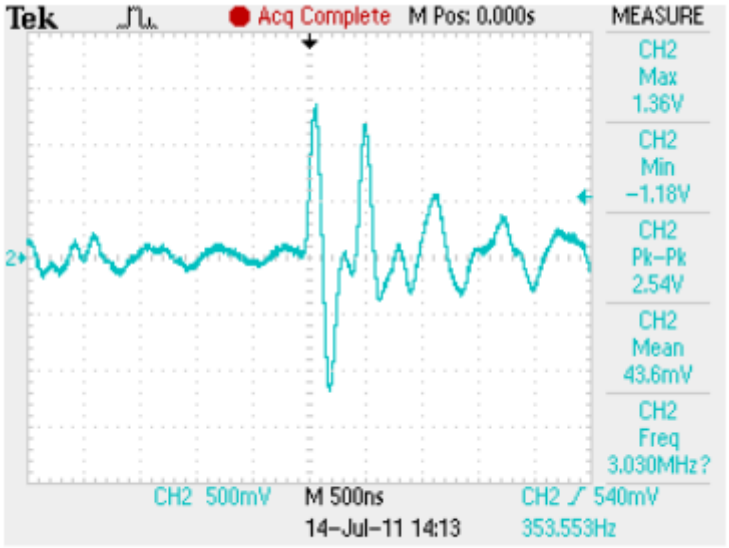

3-E3-1 DROP 4

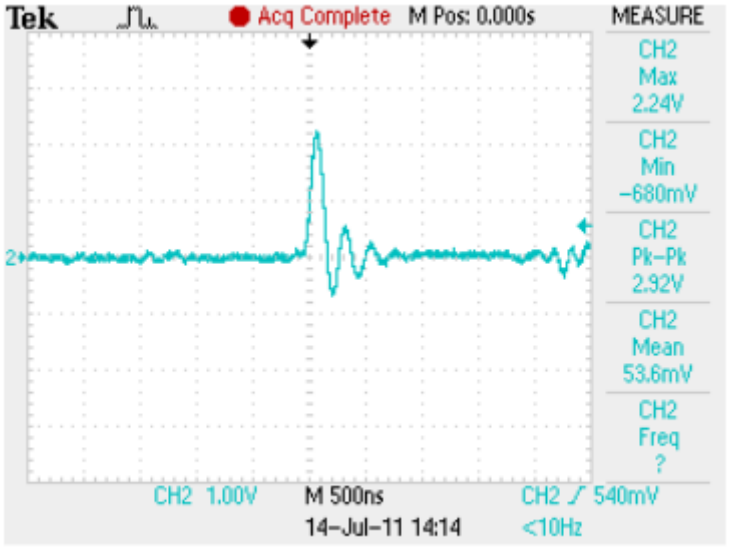

3-E3-1 DROP 5

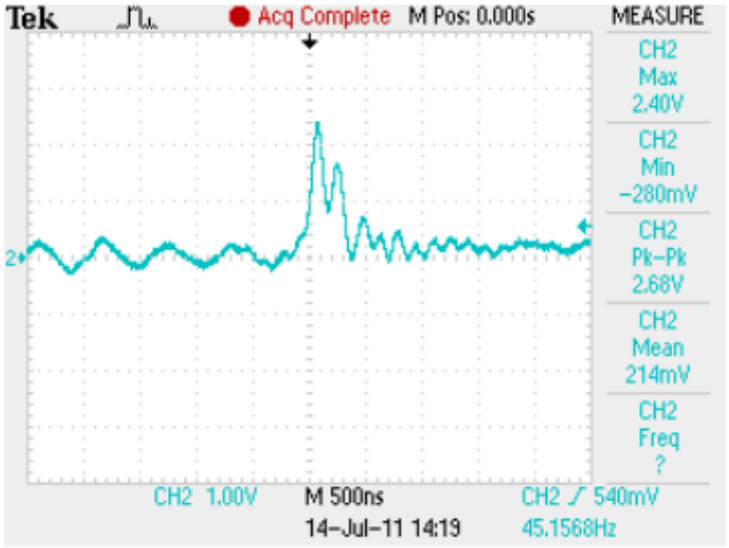

3-E3-2 DROP 1

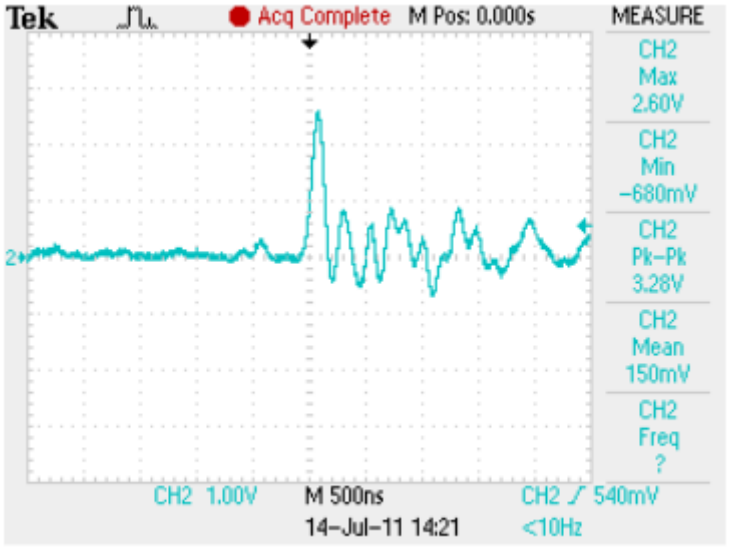

3-E3-2 DROP 2

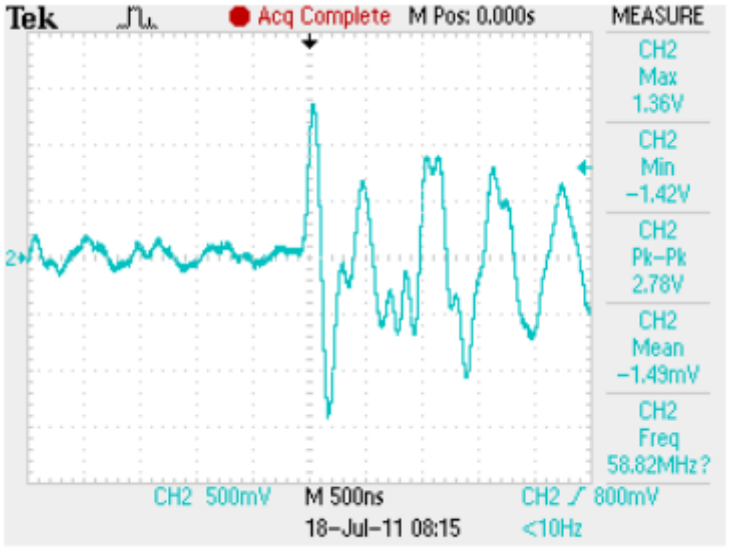

3-E3-2 DROP 3

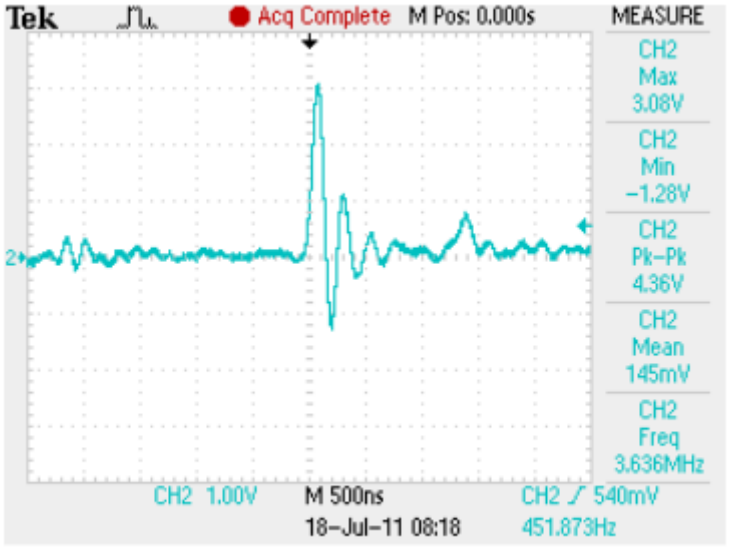

3-E3-2 DROP 4

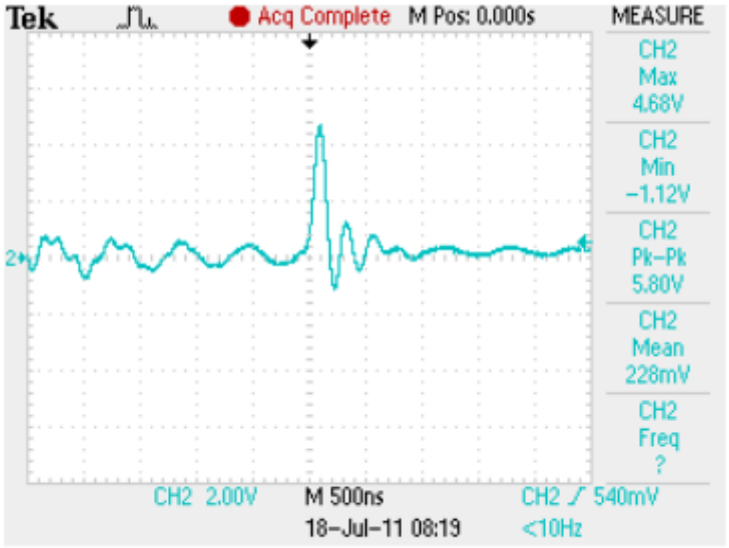

3-E3-2 DROP 5

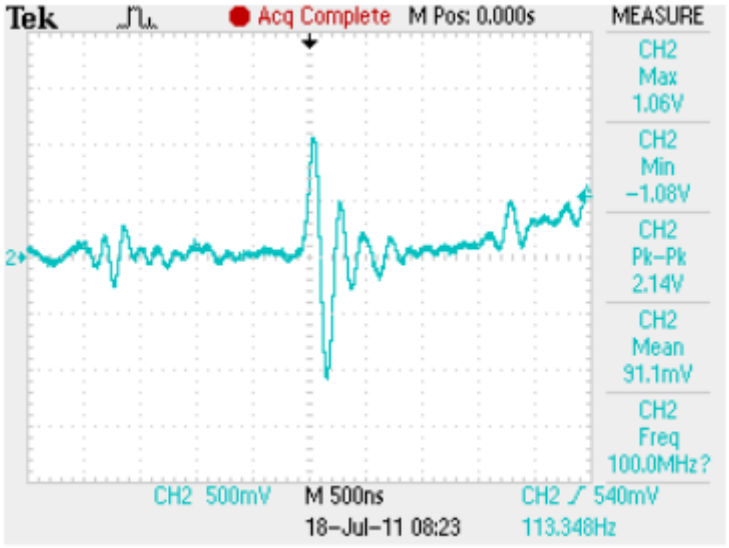

3-E3-3 DROP 1

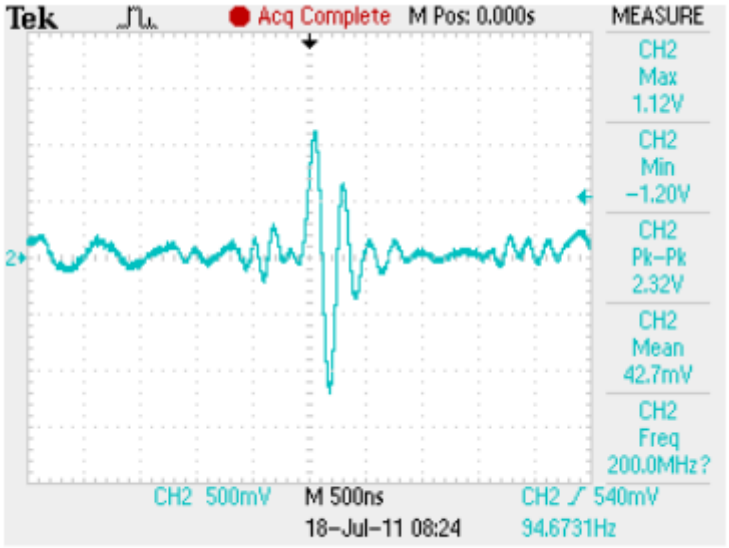

3-E3-3 DROP 2

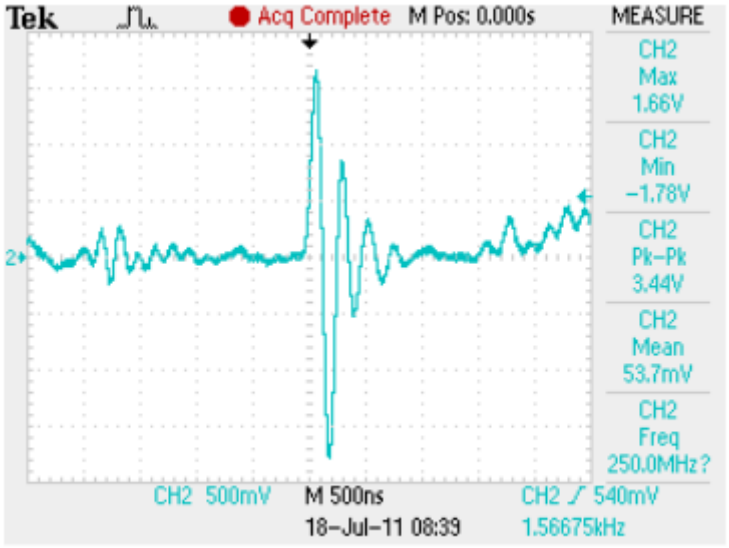

3-E3-3 DROP 3

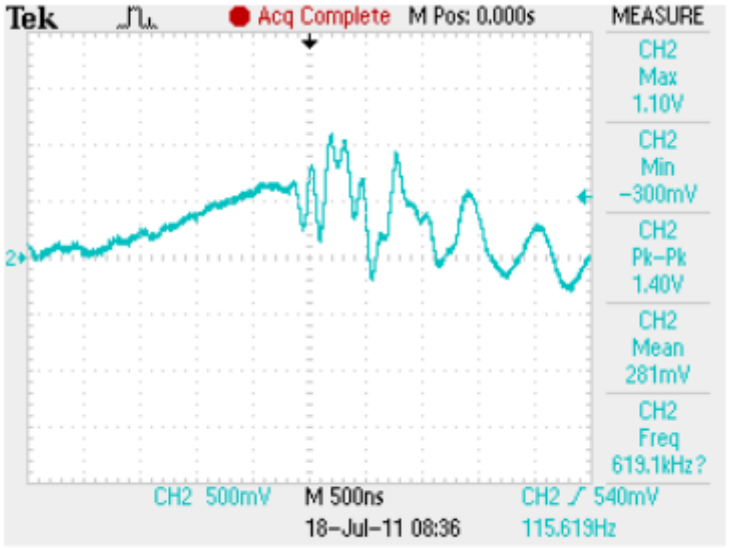

3-E3-3 DROP 4

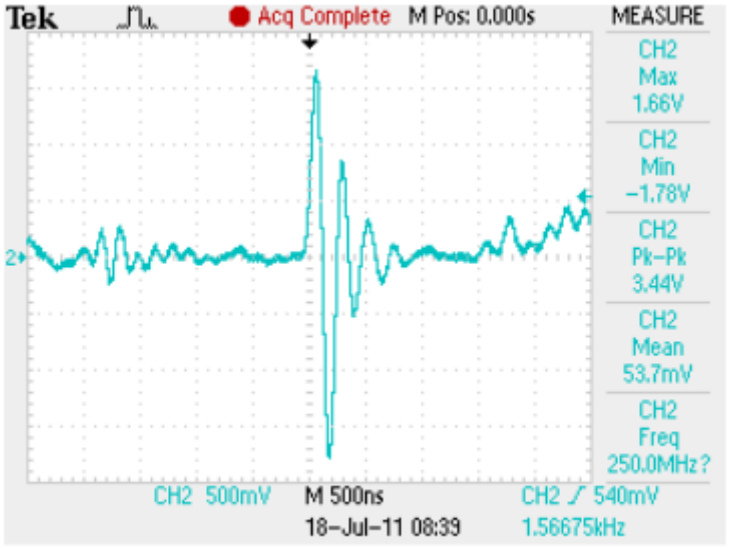

3-E3-3 DROP 5

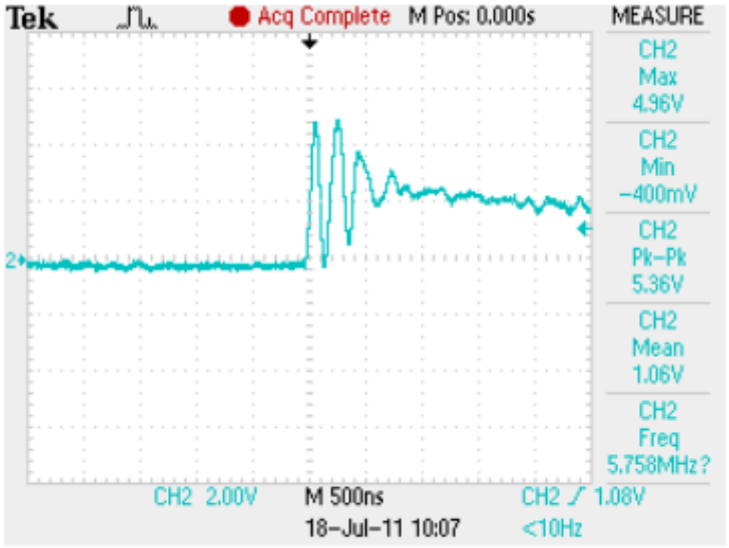

4-A2-1 DROP 1

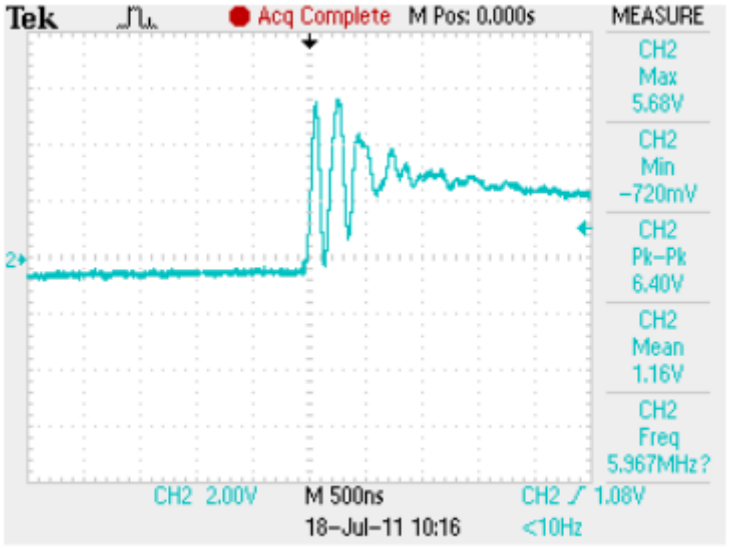

4-A2-1 DROP 2

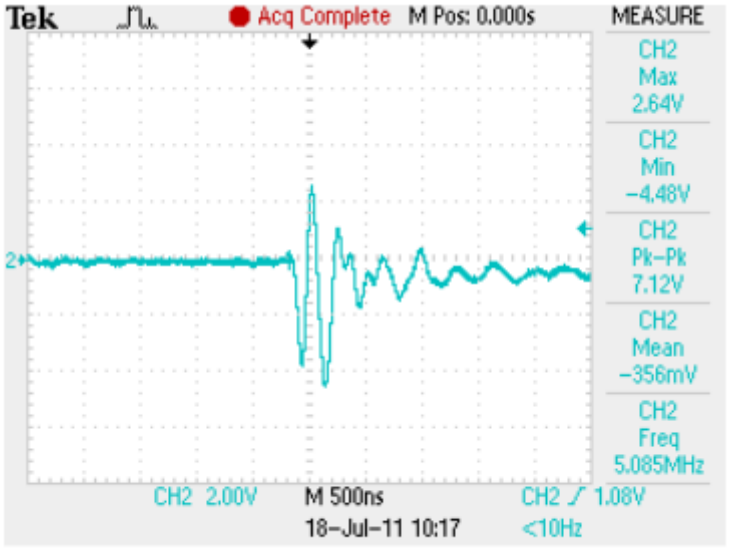

4-A2-1 DROP 3

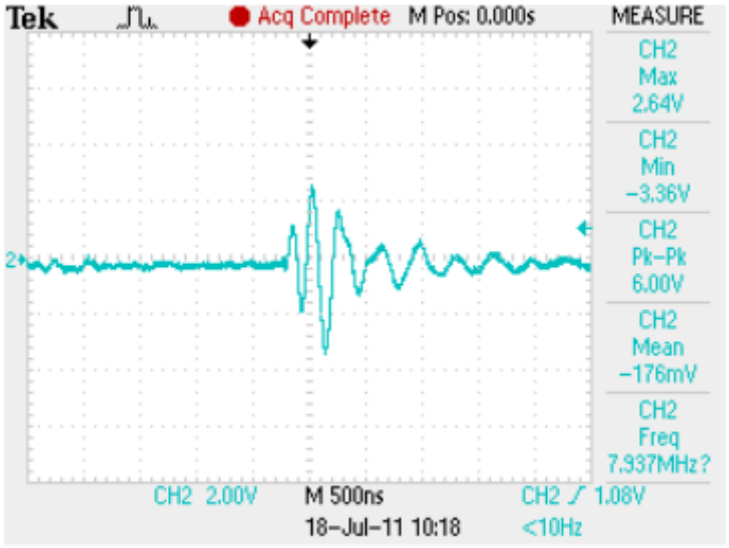

4-A2-1 DROP 4

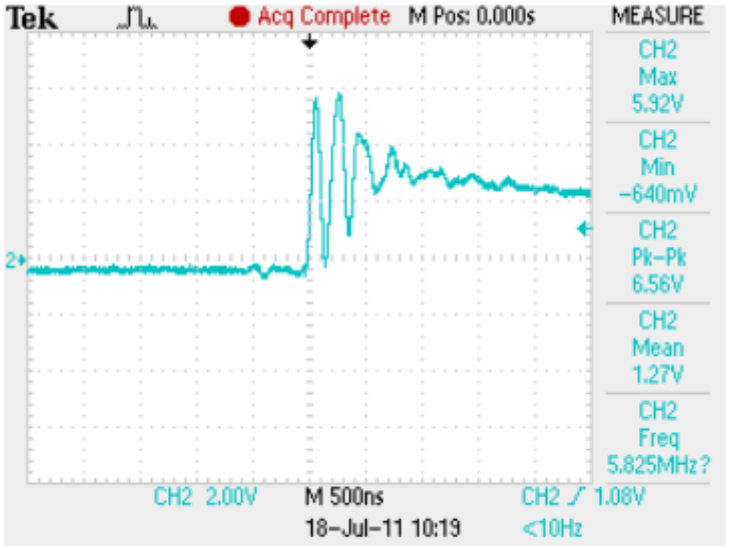

4-A2-1 DROP 5

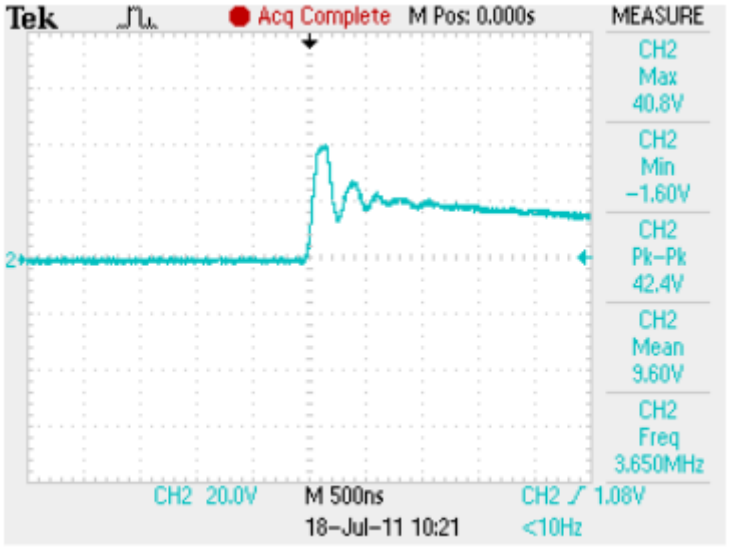

4-A2-2 DROP 1

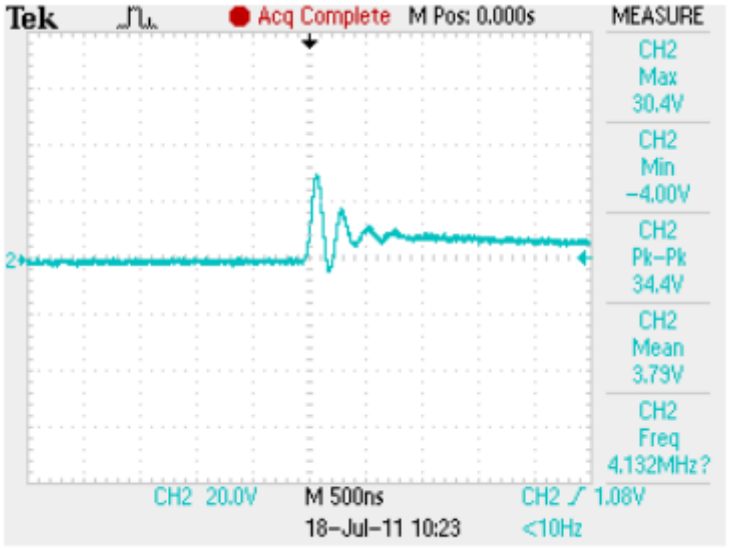

4-A2-2 DROP 2

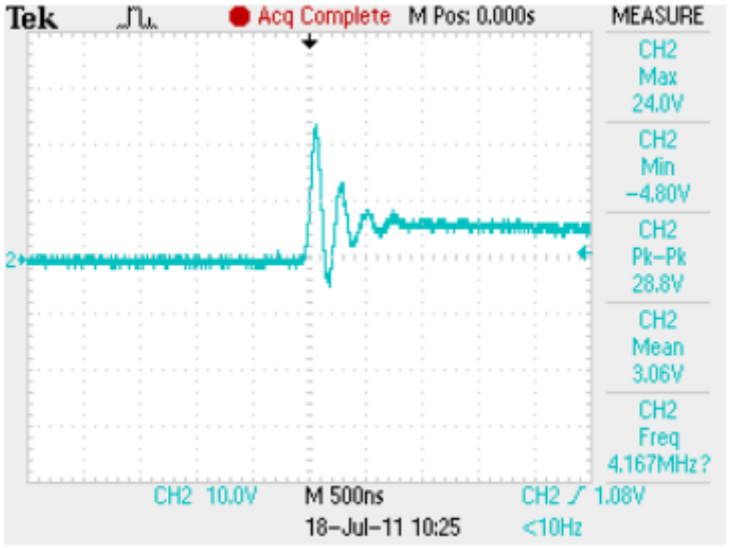

4-A2-2 DROP 3

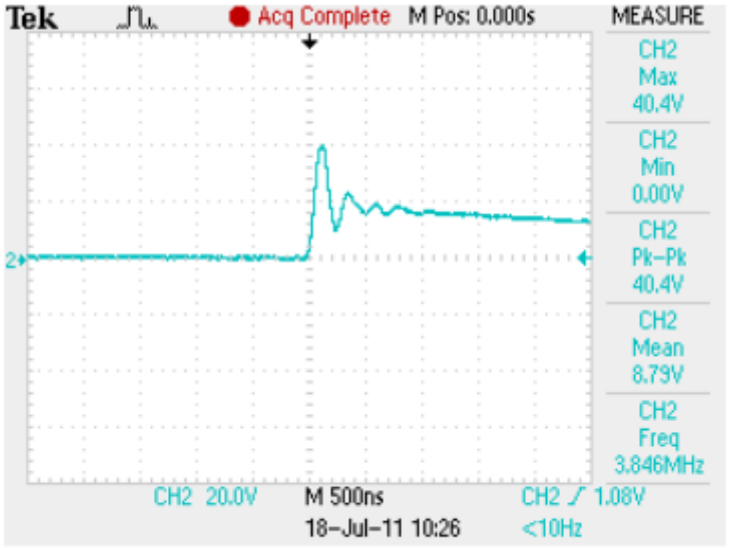

4-A2-2 DROP 4

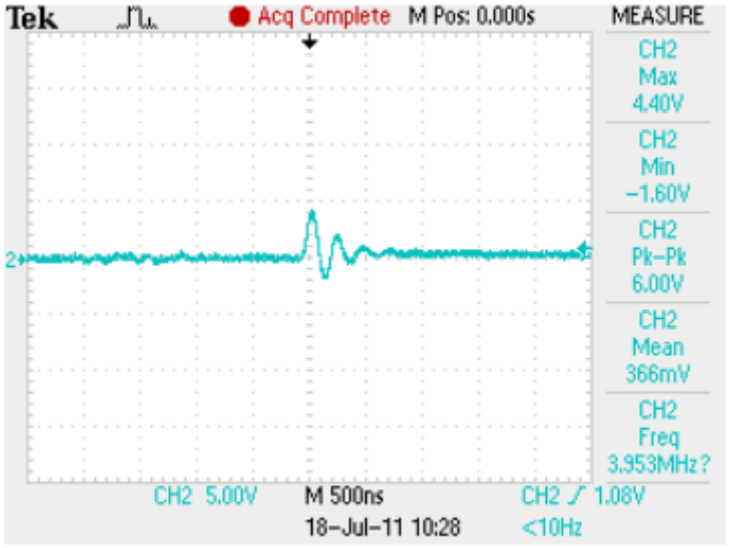

4-A2-2 DROP 5

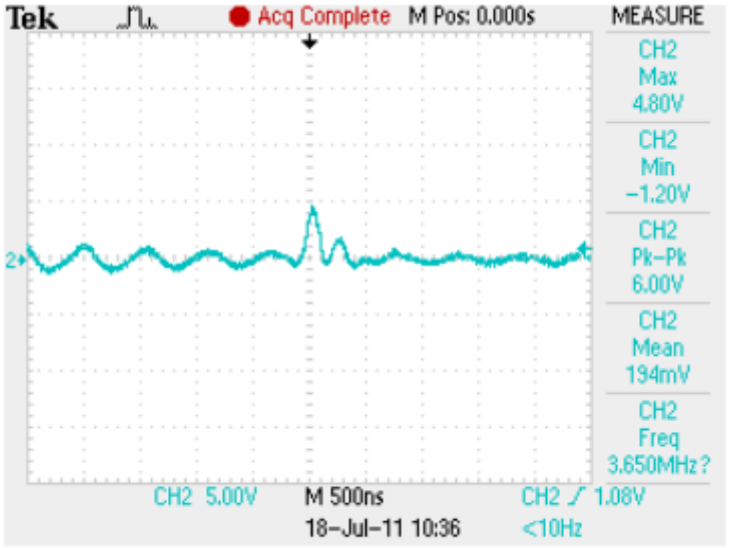

4-A2-3 DROP 1

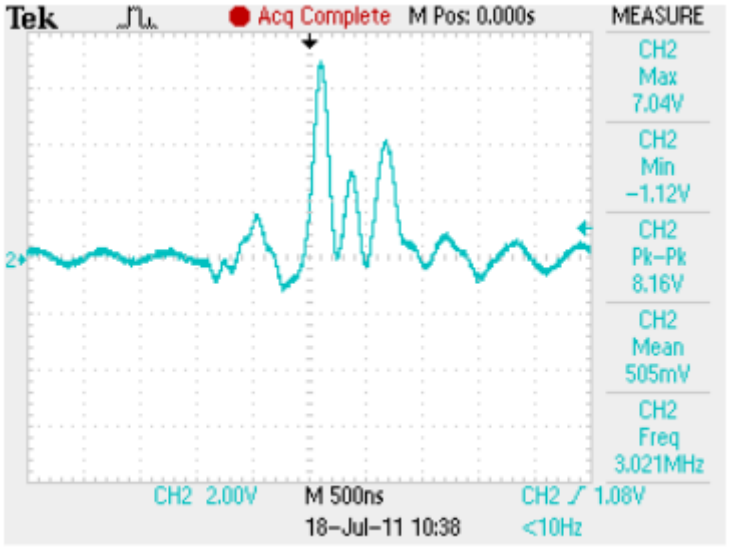

4-A2-3 DROP 2

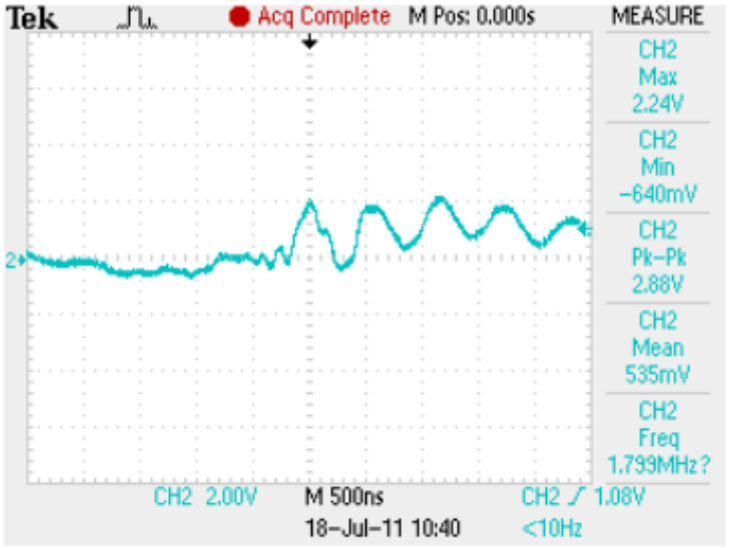

4-A2-3 DROP 3

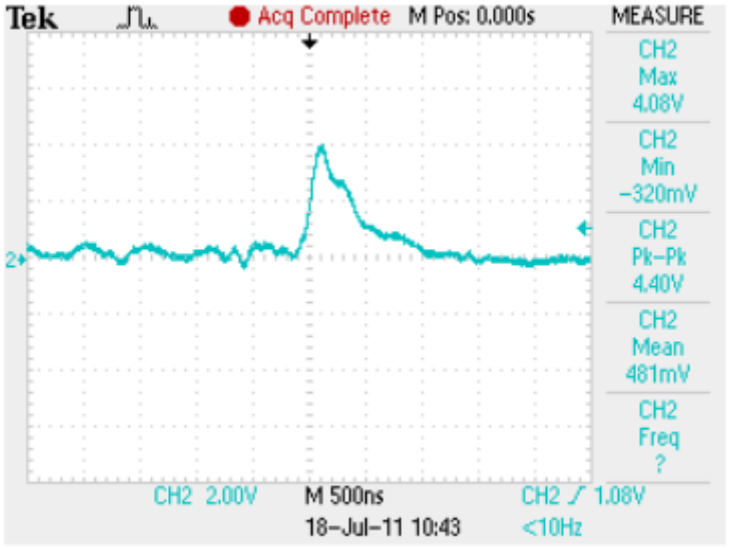

4-A2-3 DROP 4

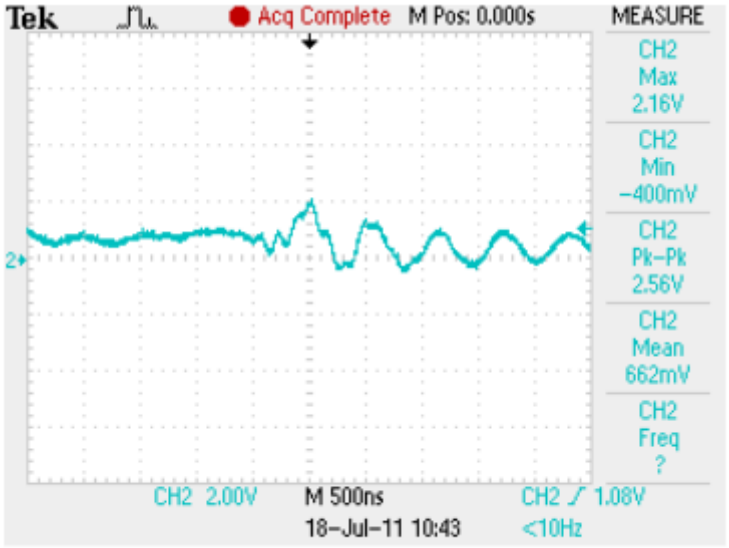

4-A2-3 DROP 5

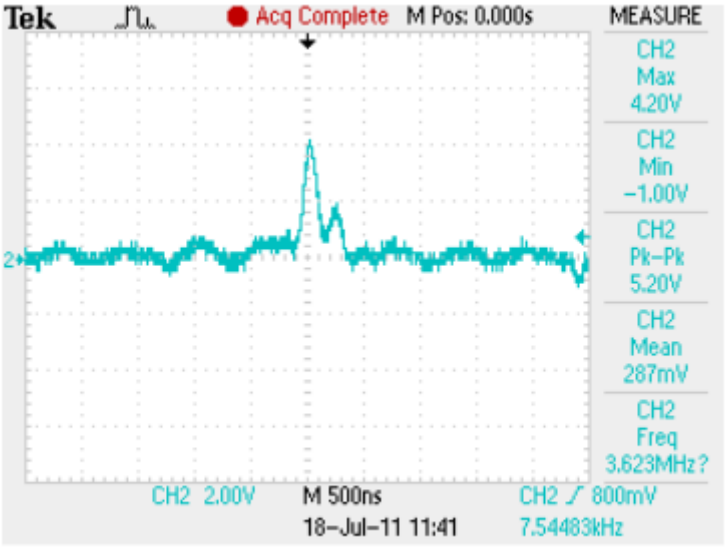

4-A4-1 DROP 1

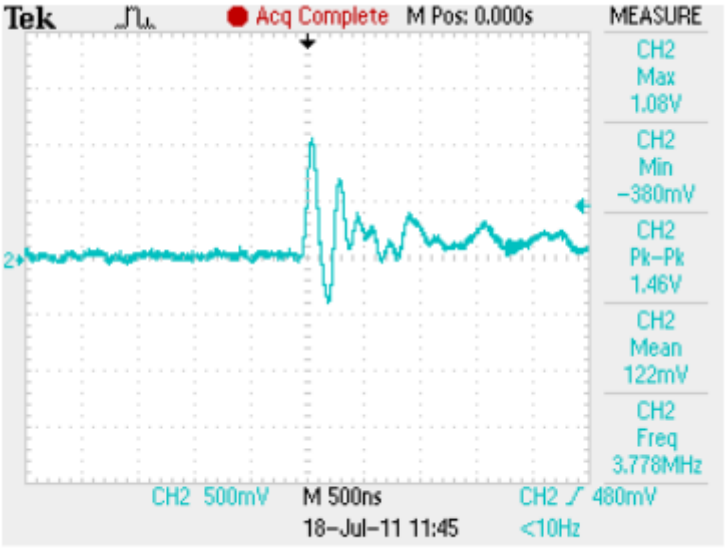

4-A4-2 DROP 1

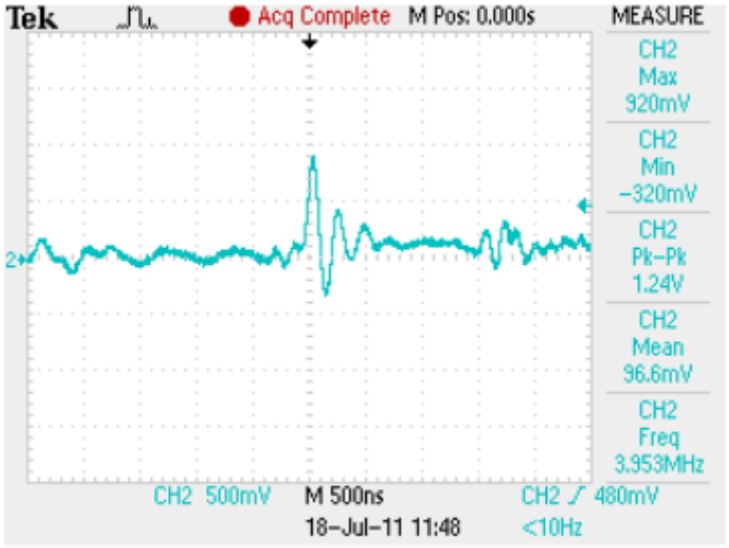

4-A4-2 DROP 2

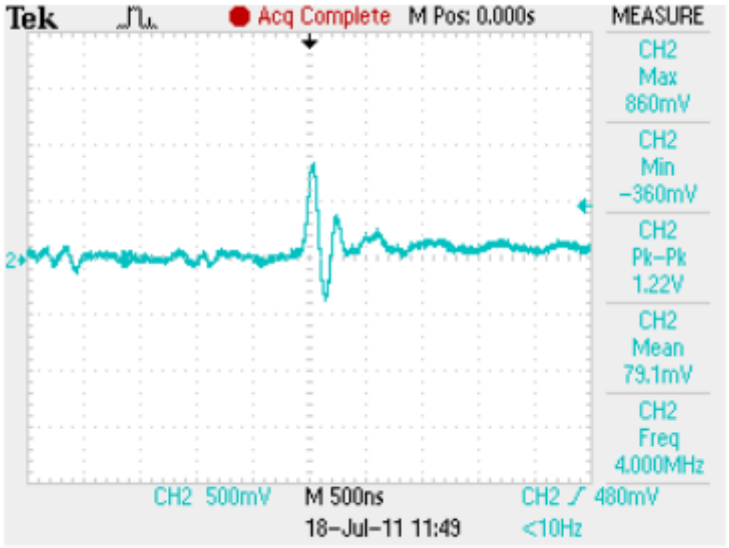

4-A4-2 DROP 3

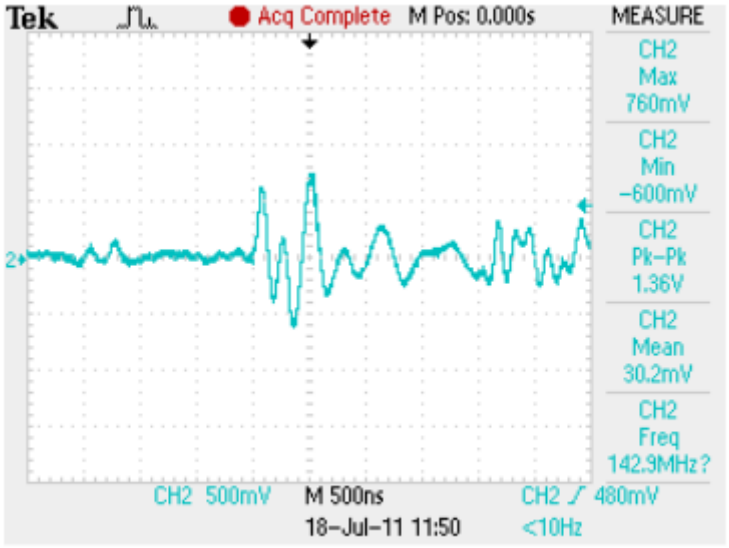

4-A4-2 DROP 4

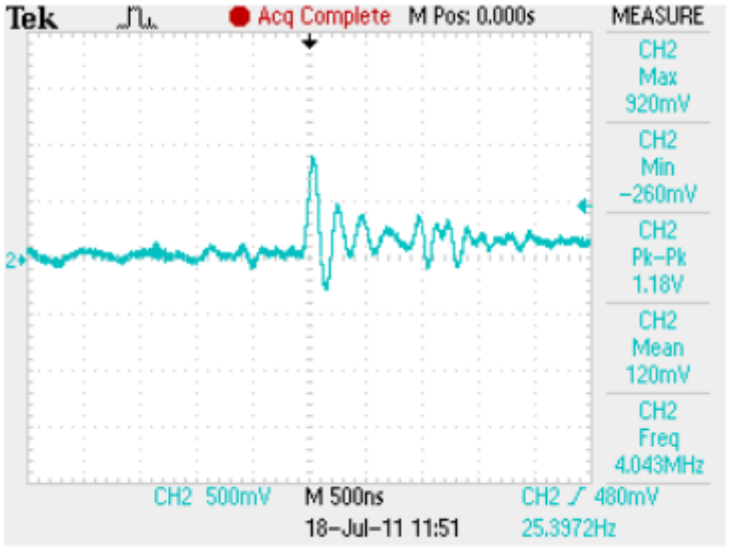

4-A4-2 DROP 5

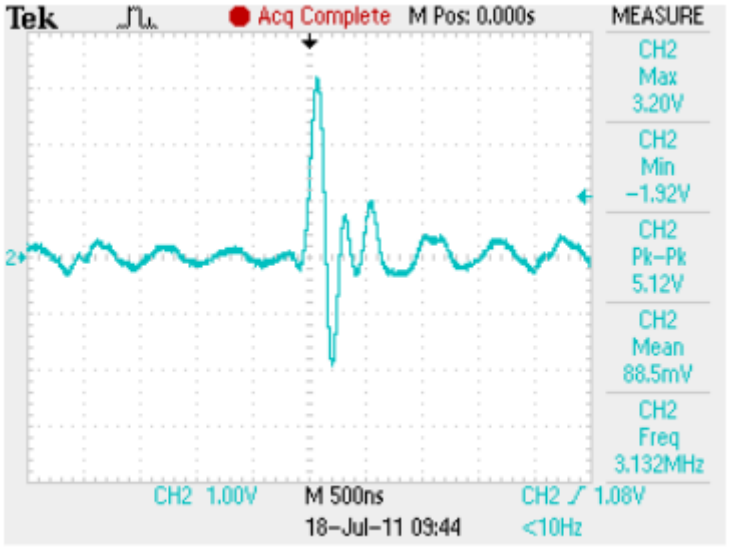

4-B1-1 DROP 1

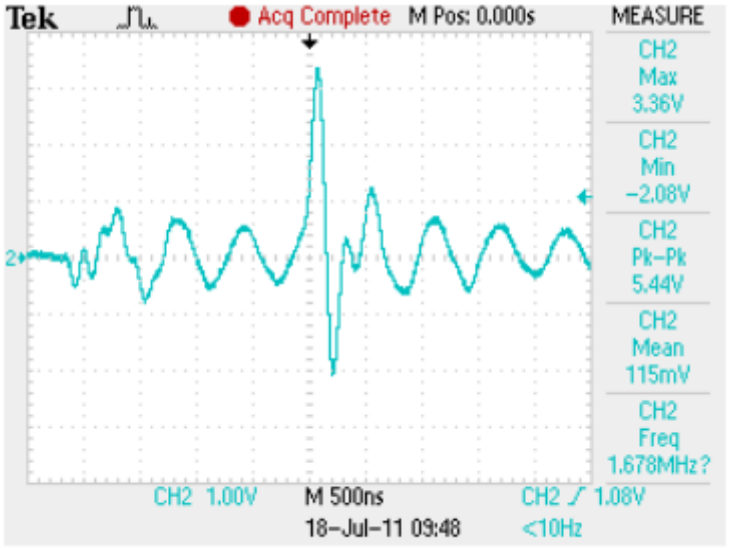

4-B1-1 DROP 2

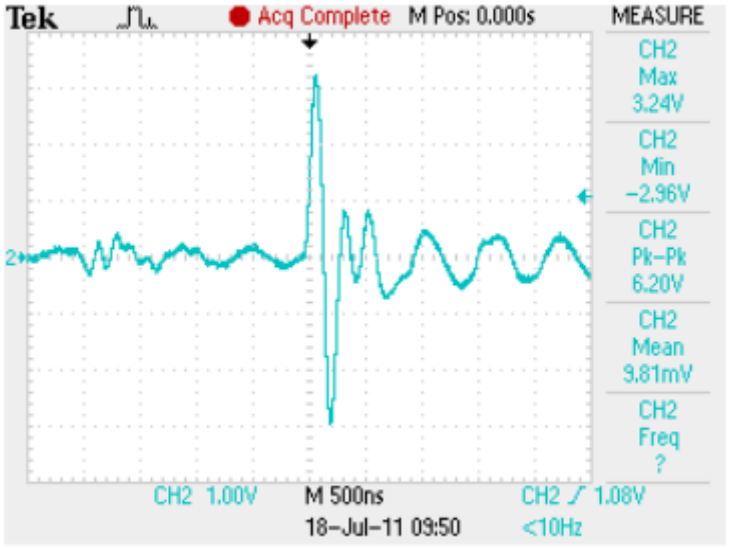

4-B1-1 DROP 3

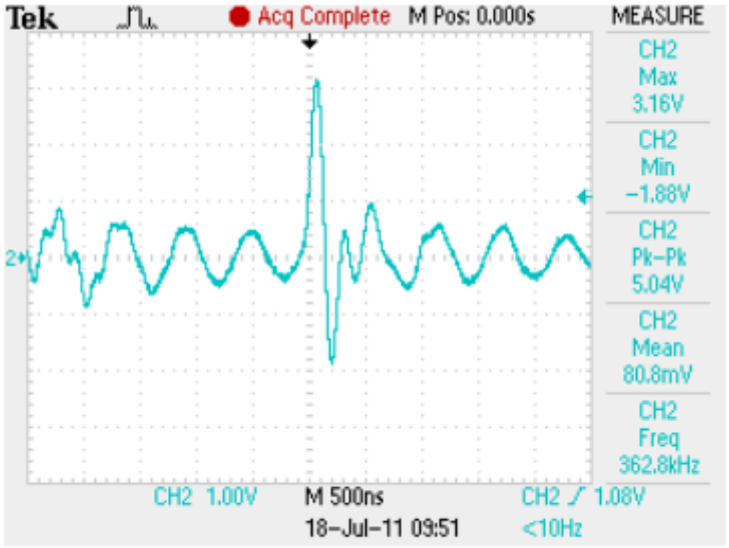

4-B1-1 DROP 4

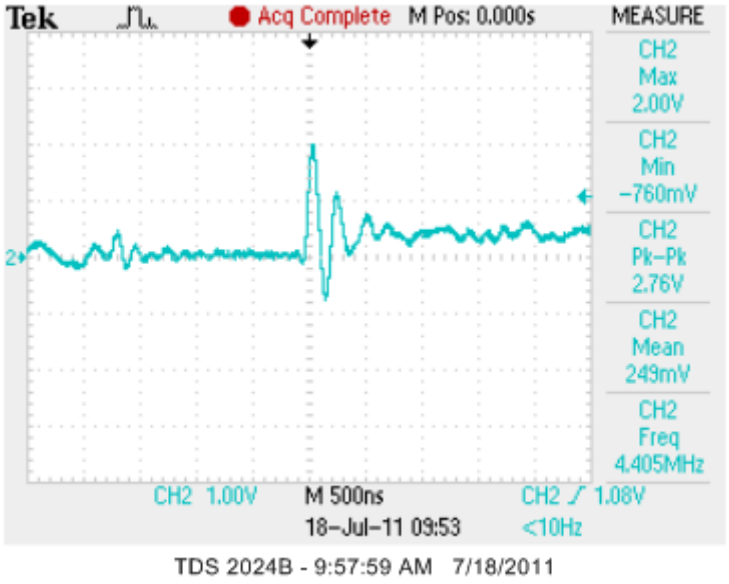
Tek
Acq Complete M Pos: 0.000s
MEASURE
CH2
Max
2.00V
CH2
Min
−760mV
CH2
Pk−Pk
2.76V
CH2
Mean
249mV
CH2
Freq
4.405MHz
CH2 1.00V
M 500ns
18−Jul−11 09:53
CH2 ⁄ 1.08V
<10Hz
TDS 2024B - 9:57:59 AM 7/18/2011

4-B1-1 DROP 5

APPENDIX F
DROP TOWER CHARACTERIZATION OF EDGE-MOUNTED DEVICE ASSEMBLIES

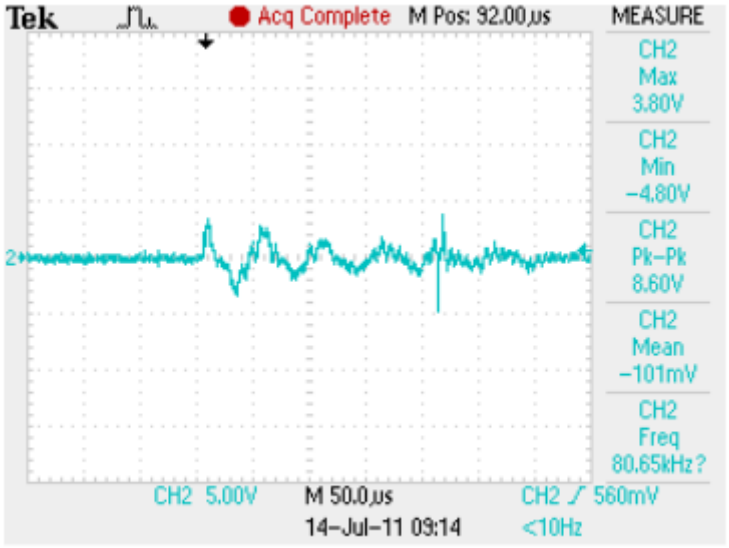

2-D1-1 DROP 2

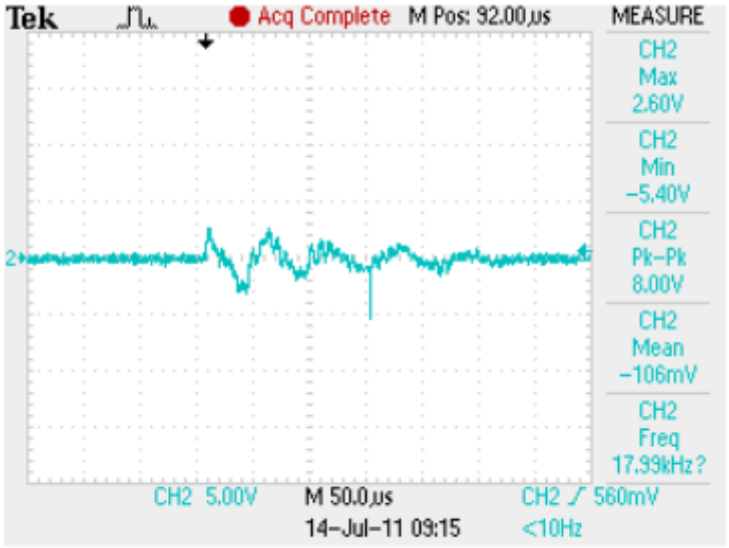

2-D1-1 DROP 3

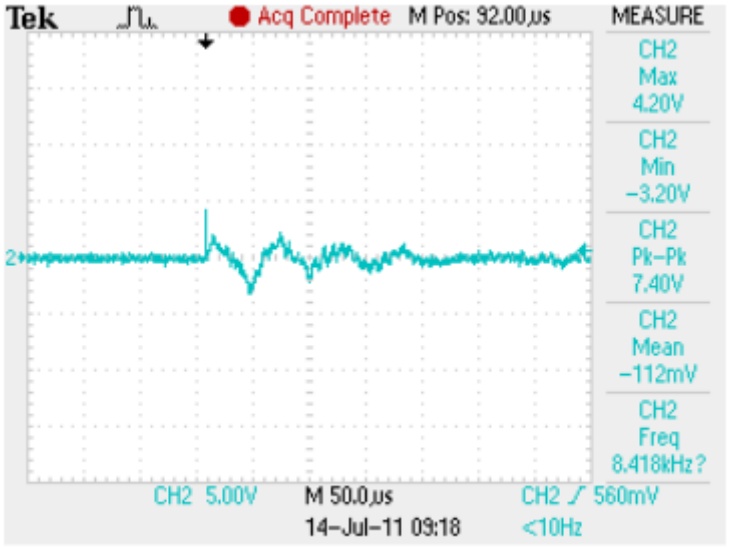

2-D1-1 DROP 4

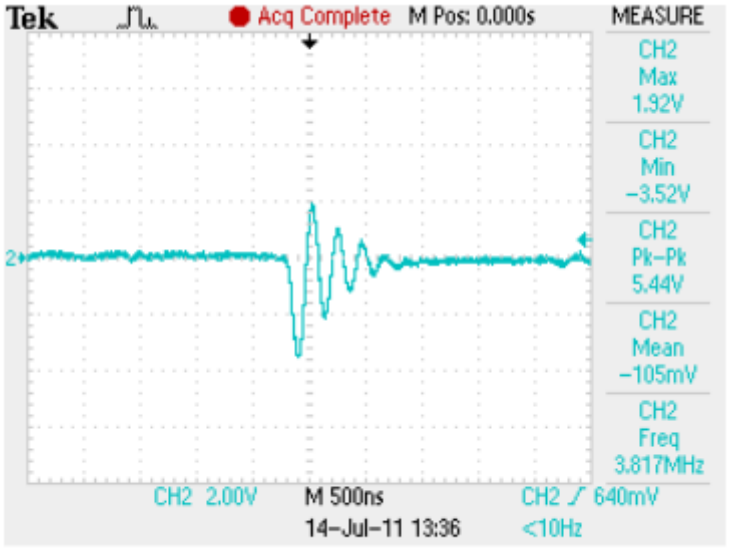

2-E1-1 DROP 1

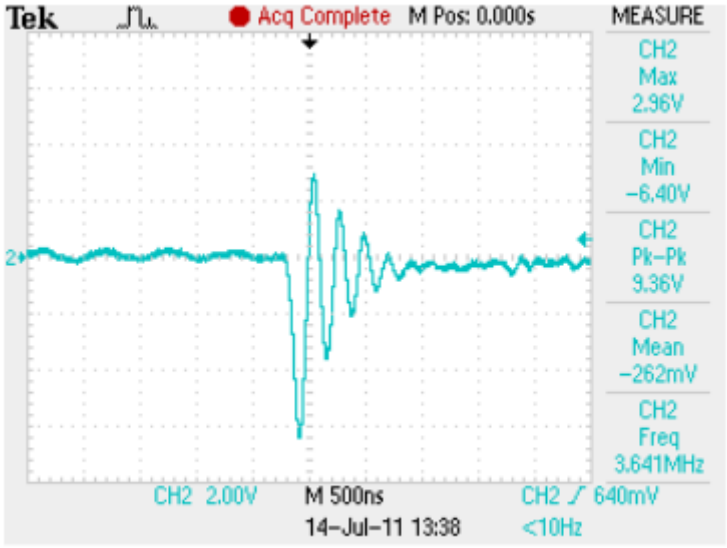

2-E1-1 DROP 2

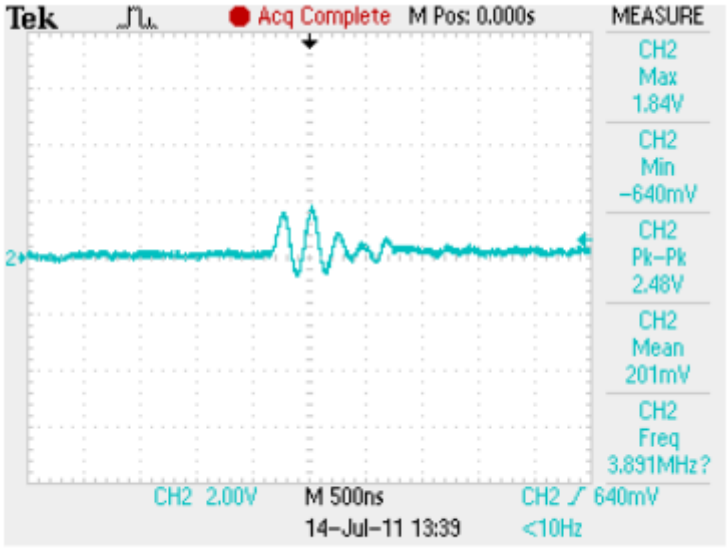

2-E1-1 DROP 3

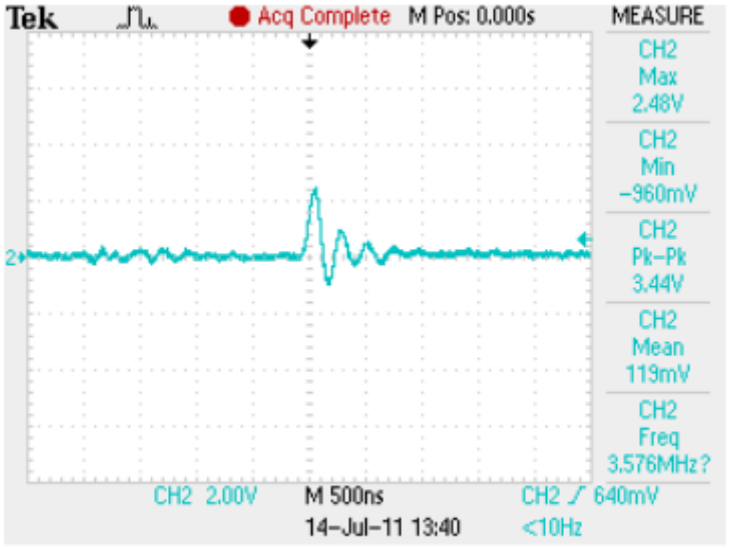

2-E1-1 DROP 4

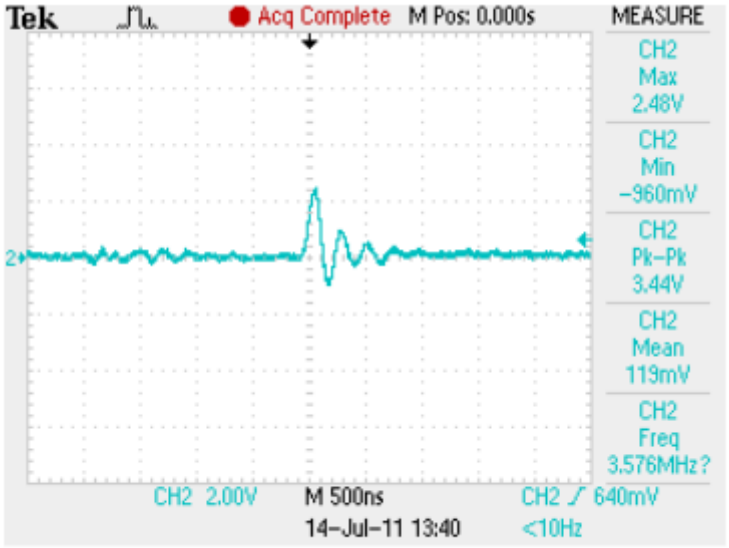

2-E1-1 DROP 5

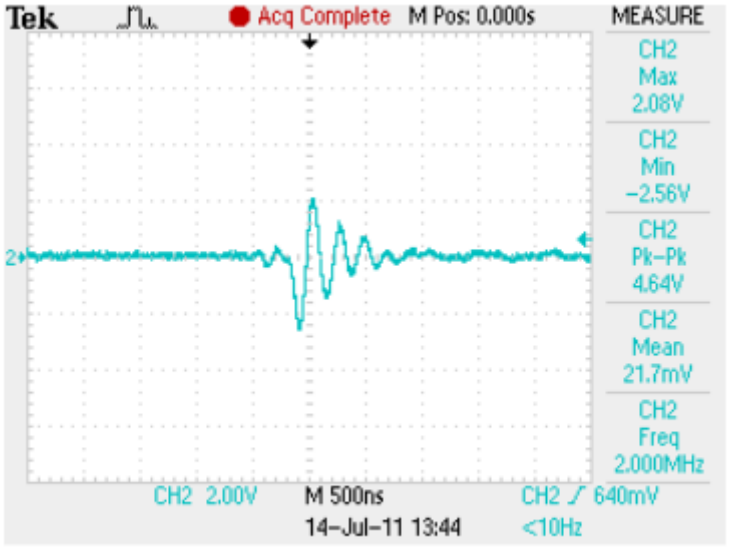

2-E1-2 DROP 1

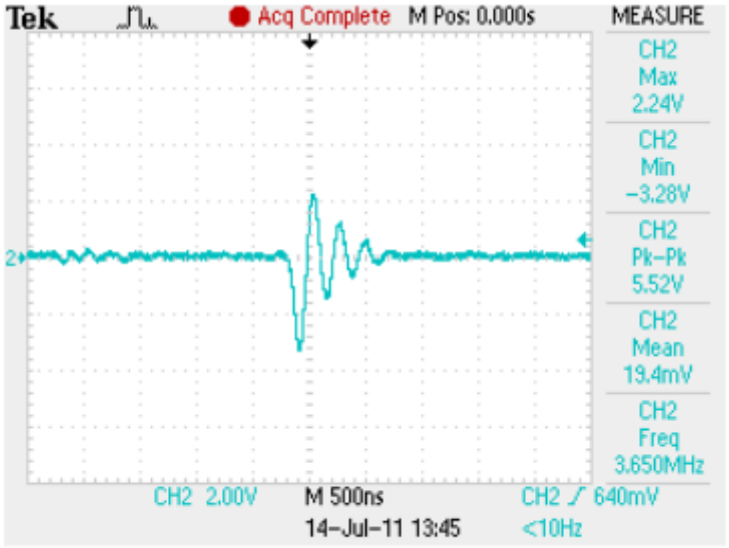

2-E1-2 DROP 2

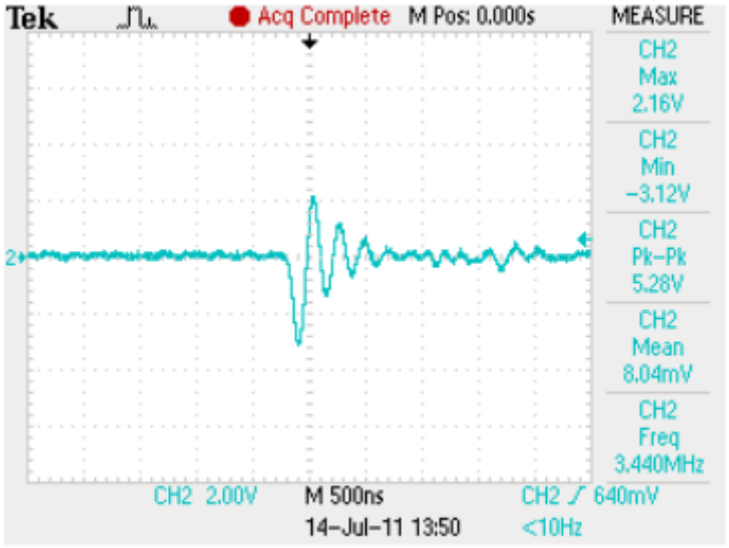

2-E1-2 DROP 3

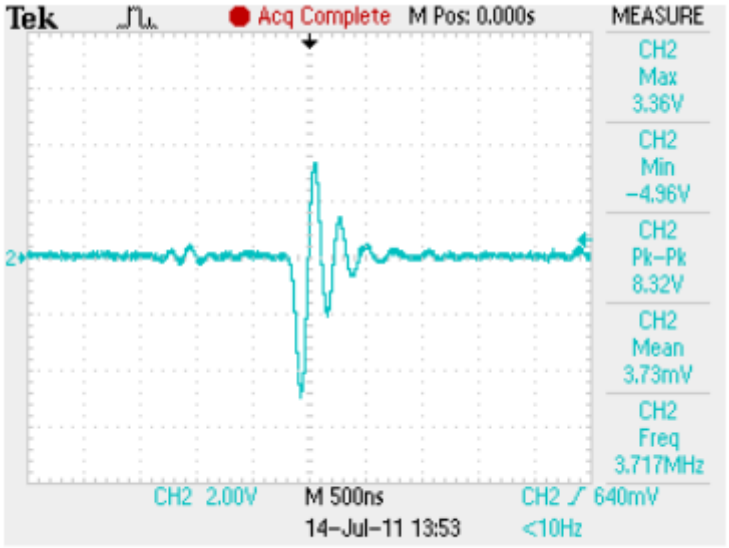

2-E1-2 DROP 4

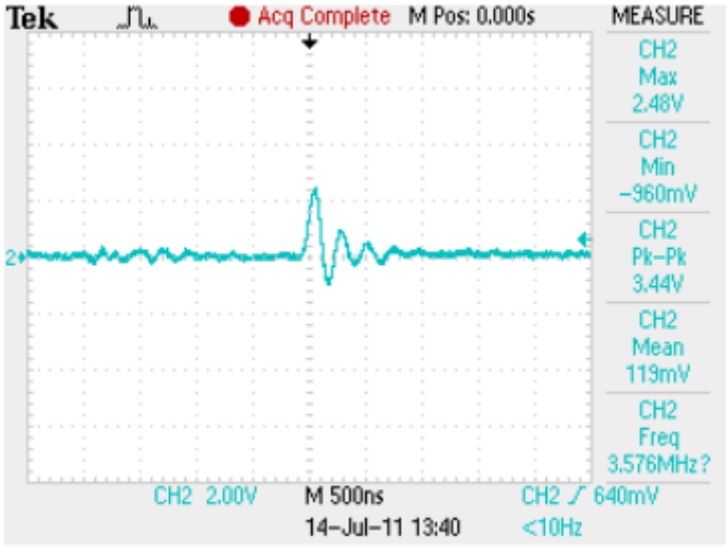

2-E1-2 DROP 5

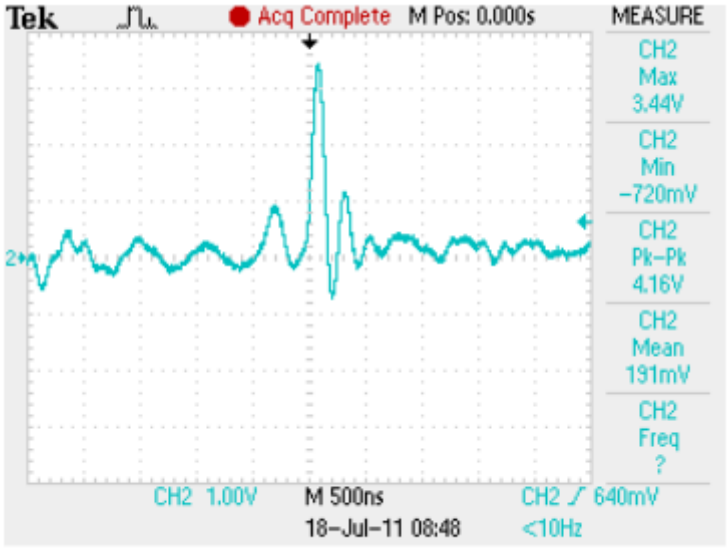

3-E3-1 DROP 1

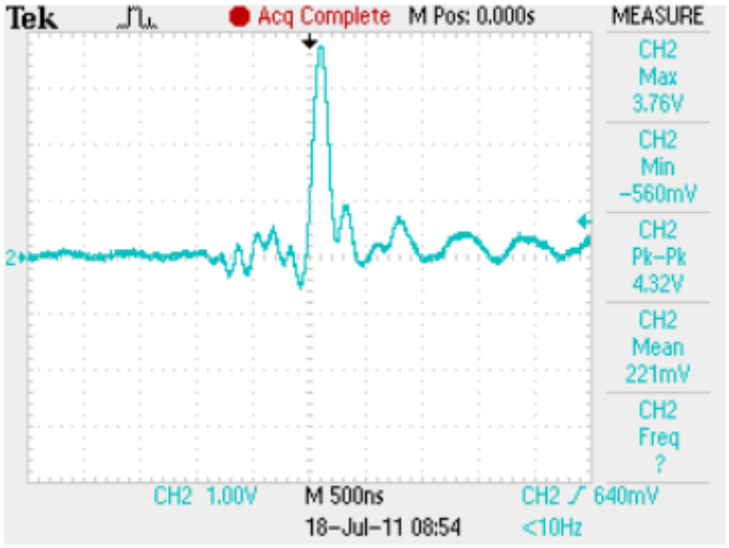

3-E3-1 DROP 2

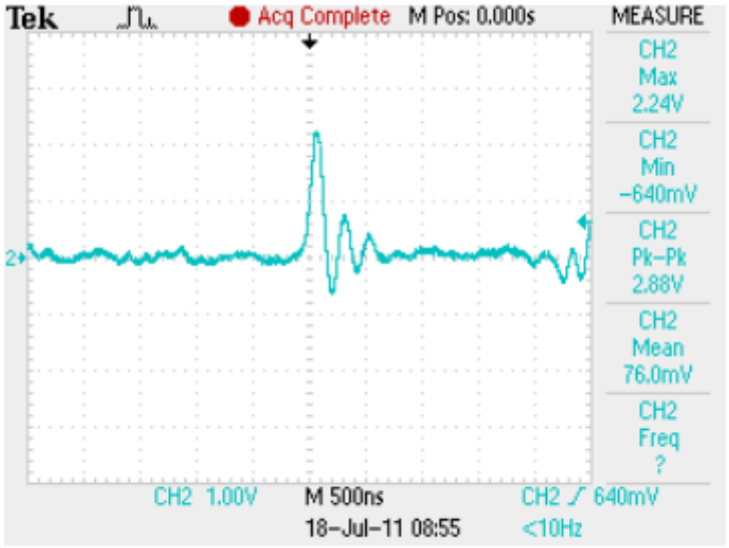

3-E3-1 DROP 3

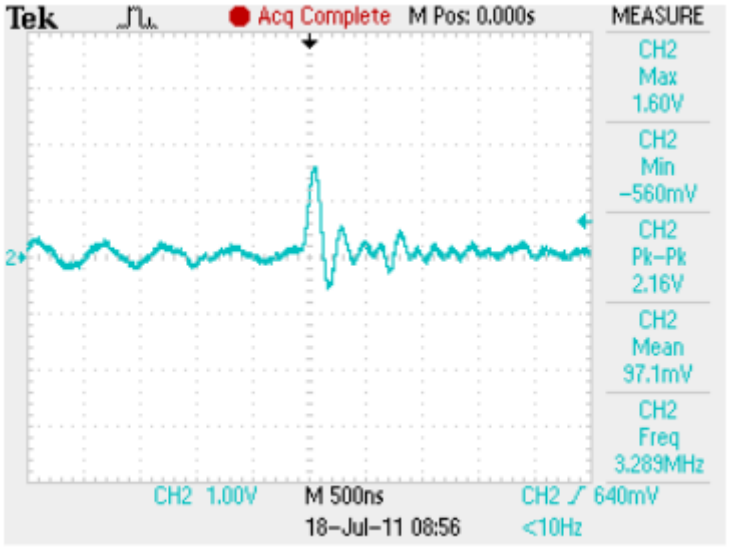

3-E3-1 DROP 4

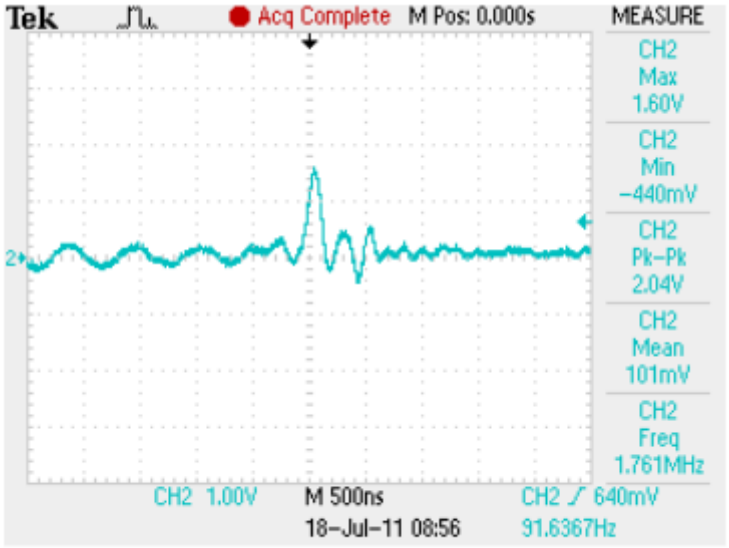

3-E3-1 DROP 5

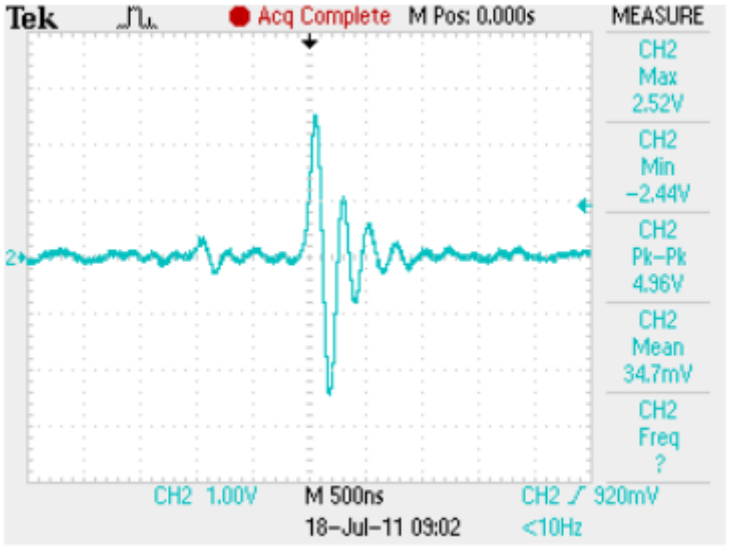

3-E3-3 DROP 1

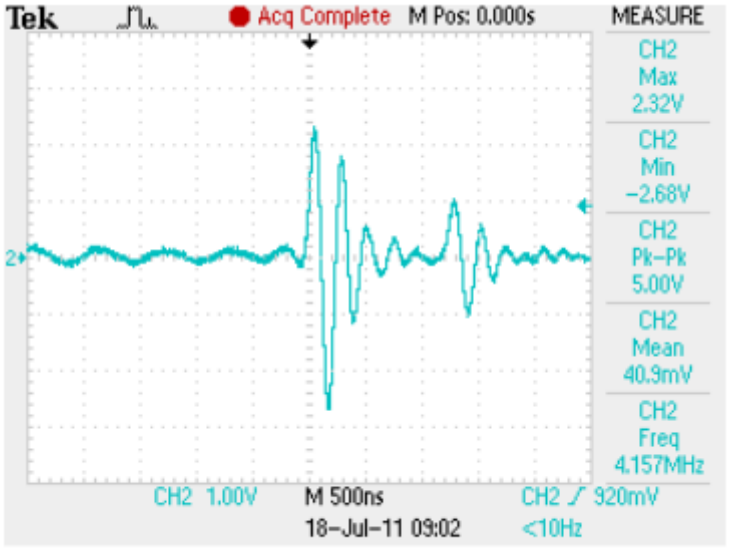

3-E3-1 DROP 2

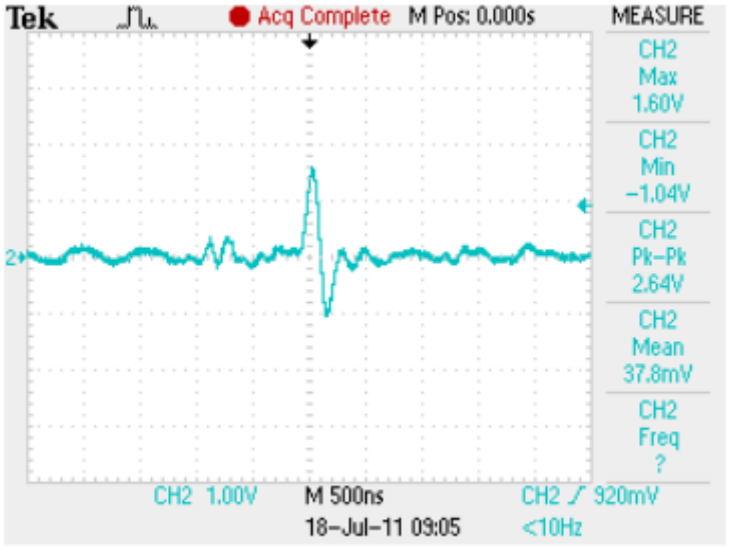

3-E3-1 DROP 3

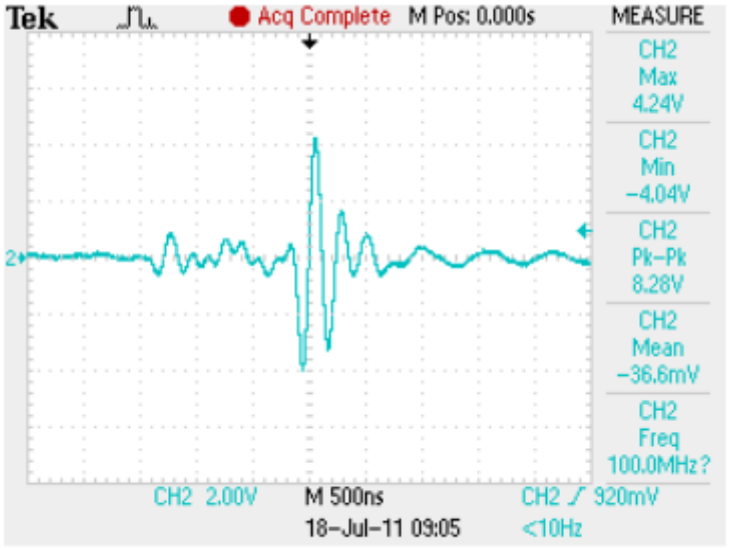

3-E3-1 DROP 4

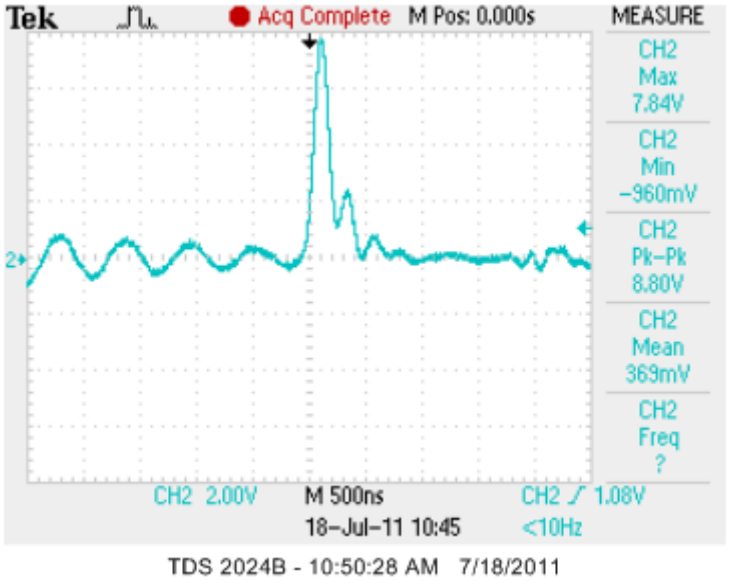
Tek
Acq Complete
M Pos: 0.000s
MEASURE
CH2
Max
7.84V
CH2
Min
−960mV
CH2
Pk−Pk
8.80V
CH2
Mean
369mV
CH2
Freq
?
CH2 2.00V
M 500ns
18−Jul−11 10:45
CH2 ⁄ 1.08V
<10Hz
TDS 2024B - 10:50:28 AM 7/18/2011

4-A2-3 DROP 1

INITIAL DISTRIBUTION LIST

		Copies
Weapon Systems Technology Information Analysis Center Alion Science and Technology 201 Mill Street Rome, NY 13440	Ms. Gina Nash gnash@alionscience.com	Electronic
Defense Technical Information Center 8725 John J. Kingman Road, Suite 0944 Fort Belvoir, VA 22060-6218	Mr. Jack L. Rike jrike@dtic.mil	Electronic
AMSAM-L	Ms. Anne C. Lanteigne anne.lanteigne@us.army.mil	Electronic
	Mr. Michael K. Gray michael.k.gray@us.army.mil	Electronic
RDMR	Mr. C. Stephen Cornelius steve.cornelius@us.army.mil	Electronic
RDMR-CSI		Electronic
RDMR-ASP	Mr. Ron Schmalbach ron.schmalbach@us.army.mil	Electronic
RDMR-WSI	Mr. Wayne Davenport wayne.davenport@us.army.mil	Electronic
	Dr. Tracy D. Hudson tracy.hudson@us.army.mil	Electronic/Hardcopy
RDMR-WDR	Dr. Paul Ruffin paul.ruffin@us.army.mil	Electronic
RDMR-SER-L 2800 Powder Mill Road Adelphi, MD 20783	Dr. Ron Polcawich ronald.g.polcawich.civ@mail.mil	Electronic
Miltec Corporation 678 Discovery Drive NW Huntsville, AL 35806-2802	Mr. Michael Allen mike.shane.allen@us.army.mil	Electronic